Matter in strong magnetic fields

Dong Lai*

Center for Radiophysics and Space Research, Department of Astronomy, Cornell University, Ithaca, New York 14853

(Published 29 August 2001)

The properties of matter are drastically modified by strong magnetic fields, $B \gg m_e^2 e^3 c/\hbar^3 = 2.35 \times 10^9$ G ($1\ \mathrm{G} = 10^{-4}$ T), as are typically found on the surfaces of neutron stars. In such strong magnetic fields, the Coulomb force on an electron acts as a small perturbation compared to the magnetic force. The strong-field condition can also be mimicked in laboratory semiconductors. Because of the strong magnetic confinement of electrons perpendicular to the field, atoms attain a much greater binding energy compared to the zero-field case, and various other bound states become possible, including molecular chains and three-dimensional condensed matter. This article reviews the electronic structure of atoms, molecules, and bulk matter, as well as the thermodynamic properties of dense plasma, in strong magnetic fields, $10^9\ \mathrm{G} \ll B \lesssim 10^{16}$ G. The focus is on the basic physical pictures and approximate scaling relations, although various theoretical approaches and numerical results are also discussed. For a neutron star surface composed of light elements such as hydrogen or helium, the outermost layer constitutes a nondegenerate, partially ionized Coulomb plasma if $B \lesssim 10^{15}$ G (at temperature $T \gtrsim 10^6$ K), and may be in the form of a condensed liquid if the magnetic field is stronger (and $T \gtrsim 10^6$ K). For an iron surface, the outermost layer of the neutron star can be in a gaseous or a condensed phase, depending on the cohesive property of the iron condensate.

CONTENTS

*Electronic address: dong@astro.cornell.edu

I. INTRODUCTION

An electron in a uniform magnetic field B gyrates in a circular orbit with radius $\rho = m_e c v/(eB)$ at the cyclotron frequency $\omega_{ce} = eB/(m_e c)$, where v is the velocity perpendicular to the magnetic field. In quantum mechanics, this transverse motion is quantized into Landau levels. The cyclotron energy (the Landau-level spacing) of the electron is

$$\hbar\omega_{ce} = \hbar \frac{eB}{m_e c} = 11.577\, B_{12}\ \mathrm{keV}, \tag{1.1}$$

and the cyclotron radius (the characteristic size of the wave packet) becomes

$$\rho_0 = \left(\frac{\hbar c}{eB}\right)^{1/2} = 2.5656 \times 10^{-10} B_{12}^{-1/2}\ \mathrm{cm}, \tag{1.2}$$

where $B_{12} = B/(10^{12}\,\mathrm{G})$ is the magnetic-field strength in units of 10^{12} G, a typical field found on the surfaces of neutron stars (see Sec. I.A). When studying matter in magnetic fields, the natural (atomic) unit for the field strength, B_0, is set by $\hbar\omega_{ce} = e^2/a_0$, or equivalently by $\rho_0 = a_0$, where a_0 is the Bohr radius. Thus it is convenient to define a dimensionless magnetic-field strength b via

$$b \equiv \frac{B}{B_0}; \quad B_0 = \frac{m_e^2 e^3 c}{\hbar^3} = 2.3505 \times 10^9\ \mathrm{G}. \tag{1.3}$$

For $b \gg 1$, the electron cyclotron energy $\hbar\omega_{ce}$ is much larger than the typical Coulomb energy, so that the

properties of atoms, molecules, and condensed matter are qualitatively changed by the magnetic field.[1] In such a strong-field regime, the usual perturbative treatment of the magnetic effects (e.g., Zeeman splitting of atomic energy levels) does not apply (see Garstang, 1977, for a review of atomic physics at $b \lesssim 1$). Instead, the Coulomb forces act as a perturbation to the magnetic forces, and the electrons in an atom settle into the ground Landau level. Because of the extreme confinement ($\rho_0 \ll a_0$) of the electrons in the transverse direction (perpendicular to the field), the Coulomb force becomes much more effective in binding the electrons along the magnetic-field direction. The atom attains a cylindrical structure. Moreover, it is possible for these elongated atoms to form molecular chains by covalent bonding along the field direction. Interactions between the linear chains can then lead to the formation of three-dimensional condensates. The properties of atoms, molecules, and bulk matter in strong magnetic fields of $b \gg 1$ are the subject of this review.

A. Astrophysics motivation

Strong magnetic fields with $b \gg 1$ exist on the surfaces of neutron stars. Most radio pulsars and accreting neutron stars in x-ray binaries have surface fields in the range of $10^{12}-10^{13}$ G; even recycled millisecond pulsars and old neutron stars in low-mass x-ray binaries have fields $B = 10^8-10^9$ G (see, for example, Lewin *et al.*, 1995; Lyne and Graham-Smith, 1998). The physical upper limit to the neutron star magnetic-field strength follows from the virial theorem of magnetohydrostatic equilibrium (Chandrasekhar and Fermi, 1953; see Shapiro and Teukolsky, 1983). The magnetic energy of the neutron star (mass $M_{\rm NS}$, radius $R_{\rm NS}$), $(4\pi R_{\rm NS}^3/3)(B^2/8\pi)$, can never exceed its gravitational binding energy, $\sim GM_{\rm NS}^2/R_{\rm NS}$; this gives

$$B \lesssim 10^{18}\left(\frac{M_{\rm NS}}{1.4M_\odot}\right)\left(\frac{R_{\rm NS}}{10\,{\rm km}}\right)^{-2}\ {\rm G}. \tag{1.4}$$

It has been suggested that magnetic fields of order 10^{15} G or stronger can be generated by dynamo processes in proto-neutron stars (Thompson and Duncan, 1993), and recent observations (e.g., Vasisht and Gotthelf, 1997; Kouveliotou *et al.*, 1998, 1999; Hurley *et al.*, 1999; Kaspi *et al.*, 1999; Mereghetti, 2000) have lent support to the idea that soft-gamma-ray repeaters and slowly spinning (with periods of a few seconds) "anomalous" x-ray pulsars in supernova remnants are neutron stars endowed with superstrong magnetic fields $B \gtrsim 10^{14}$ G, the so-called "magnetars" (Duncan and Thompson, 1992; Paczyński, 1992; Thompson and Duncan, 1995, 1996). Finally, magnetism has been detected in a few dozen white dwarfs (out of a total of about 2000) in the range from 10^5 to 10^9 G (see, for example, Koester and Chanmugan, 1990; Jordan, 1998; Wickramasinghe and Ferrario, 2000).

The main astrophysical motivation for studying matter in strong magnetic fields arises from the importance of understanding neutron star surface layers, which play a key role in many neutron star processes and observed phenomena. Theoretical models of pulsar and magnetar magnetospheres depend on the cohesive properties of the surface matter in strong magnetic fields (see, for example, Ruderman and Sutherland, 1975; Michel, 1991; Usov and Melrose, 1996; Zhang and Harding, 2000). More importantly, the surface layer directly mediates the thermal radiation from the neutron star. It has long been recognized that neutron stars are sources of soft x rays during the $\sim 10^5-10^6$ years of the cooling phase after their birth in supernova explosions (Chiu and Salpeter, 1964; Tsuruta, 1964; Bahcall and Wolf, 1965). The cooling history of the neutron star depends on poorly constrained interior physics, such as nuclear equation of state, superfluidity, and internal magnetic fields (see, for example, Pethick, 1992; Page, 1998; Tsuruta, 1998; Prakash *et al.*, 2000; Yakovlev *et al.*, 2001 for review). The advent of imaging x-ray telescopes in recent years has now made it possible to observe isolated neutron stars directly by their surface radiation. In particular, recent x-ray observatories such as ROSAT have detected pulsed x-ray thermal emission from a number of radio pulsars (see Becker and Trümper, 1997; Becker, 2000; Becker and Pavlov, 2001 for review). Some of the observed x rays are likely to be produced by nonthermal magnetospheric emission, but at least three pulsars (PSR B1055-52, B0656+14, Geminga) show emission dominated by a thermal component emitted from the whole neutron star surface, with temperatures in the range of $(2-10)\times 10^5$ K. A few of the x-ray-emitting radio pulsars show thermal-like radiation of higher temperatures, in the range $(1-5)\times 10^6$ K, from an area much smaller than that of the stellar surface, indicating a hot polar cap on the neutron star surface. Several nearby pulsars have also been detected in the extreme ultraviolet (Edelstein, Foster, and Bowyer, 1995; Korpela and Bowyer, 1998) and in the optical band (Pavlov *et al.*, 1997; Caraveo *et al.*, 2000) with spectra consistent with thermal radiation from neutron star surfaces. On the other hand, old isolated neutron stars (10^8-10^9 of which are thought to exist in the Galaxy), heated through accretion from interstellar material, are also expected to be common sources of soft-x-ray/extreme-ultraviolet emission (see, for example, Treves and Colpi, 1991; Blaes and Madau, 1993; Treves *et al.* 2000). Several radio-quiet isolated accreting neutron stars have been detected in the x-ray and optical bands (for example, Caraveo, Bignami, and Trümper, 1996; Walter, Wolk, and Neuhäuser, 1996; Walter and Matthews, 1997). Finally, the quiescent x-ray emissions from soft-gamma-ray repeaters and anomalous x-ray pulsars may be powered by the internal heating associated with decaying mag-

[1]Note that this statement applies to individual atoms, molecules, and zero-pressure condensed matter. In a medium, when the density or temperature is sufficiently high, the magnetic effects can be smeared out even for $b \gg 1$; see Sec. VI. The strong-field condition is also modified by the ion charge; see Sec. III.C.

netic fields (Thompson and Duncan, 1996). The x rays originate near the stellar surface and therefore allow one to probe radiative transport in the superstrong-field regime. Observations indicate that some of the magnetars (particularly anomalous x-ray pulsars) have a thermal component in their x-ray spectra (see Mereghetti, 2000). Overall, the detections of surface emission from neutron stars can provide invaluable information on the structure and evolution of neutron stars and enable one to put constraints on the nuclear equation of state, various heating/accretion processes, magnetic-field structure, and surface chemical composition. The recently launched x-ray telescopes, including Chandra X-ray Observatory and XMM-Newton Observatory, have much improved sensitivity and spectral resolution in the soft-x-ray band, making it promising for spectroscopic studies of isolated or slowly accreting neutron stars. Since the surface layer/atmosphere directly determines the characteristics of the thermal emission, proper interpretations of the observations require a detailed understanding of the physical properties of the neutron star envelope in the presence of intense magnetic fields ($B \gtrsim 10^{12}$ G).

B. Laboratory physics motivation

The highest static magnetic field currently produced in a terrestrial laboratory is 45 T (4.5×10^5 G), far below B_0; a stronger transient field of order 10^3 T can be produced using explosive flux compression techniques, but this is still below B_0 (see, for example, Crow *et al.*, 1998). However, high-magnetic-field conditions can be mimicked in some semiconductors where a small effective electron mass m_* and a large dielectric constant ε reduce the Coulomb force relative to the magnetic force. For hydrogenlike excitons in semiconductors, the atomic unit of length is $a_{0*}=\varepsilon\hbar^2/(m_*e^2)$, and the corresponding natural unit for a magnetic field is $B_{0*}=m_*^2e^3c/(\varepsilon^2\hbar^3)$. For example, in GaAs, the dielectric constant is $\varepsilon=12.56$ and the electron bound to a positively charged donor has an effective mass $m_*=0.006\,65m_e$, thus $B_{0*}=6.57$ T. The critical field B_{0*} can be as small as 0.2 T for InSb. Such a low value of B_{0*} implies that the structure of excitons, biexcitonic molecules, and quantum dots (which resemble multielectron atoms; see Kastner, 1992) in semiconductors must experience significant changes already in laboratory magnetic fields (see, for example, Lieb *et al.*, 1995; Timofeev and Chernenko, 1995; Klaassen *et al.*, 1998). Some of the earliest studies of atoms in superstrong magnetic fields (Elliot and Loudon, 1960; Hasegawa and Howard, 1961) were motivated by applications in semiconductor physics.

C. Plan of this paper

In this paper we review the properties of different forms of matter (atoms, molecules, and bulk condensed matter) in strong magnetic fields. We also discuss astrophysical situations in which magnetized matter plays an important role. We shall focus on magnetic-field strengths in the range of $B\gg10^9$ G so that $b\gg1$ is well satisfied, although in several places (Secs. III.D and IV.E) we shall also touch upon issues for b only somewhat larger than 1. Throughout the paper, our emphasis is on physical understanding and analytic approximate relations (whenever they exist), rather than on computational techniques for the electronic structure calculations, although we shall discuss the latter aspects and provide references to the literature.

This paper is organized as follows. After a brief summary of the basics of electron Landau levels in Sec. II, we discuss the physics of various bound states in strong magnetic fields in Sec. III (atoms), Sec. IV (molecules), and Sec. V (condensed matter). Section VI summarizes the thermodynamic properties of free-electron gas (at finite density and temperature). In Sec. VII we review the physical properties of the envelope of a strongly magnetized neutron star.

Throughout the paper we shall use real physical units and atomic units (a.u.) interchangeably, whichever is more convenient. Recall that in atomic units, mass and length are expressed in units of the electron mass m_e and the Bohr radius $a_0=0.529\times10^{-8}$ cm, energy in units of 2 Ry$=e^2/a_0=2\times13.6$ eV, field strength in units of B_0 [Eq. (1.3)], temperature in units of 3.16×10^5 K, and pressure in units of $e^2/a_0^4=2.94\times10^{11}$ newtons/m^2.

D. Bibliographic notes

Theoretical research on matter in superstrong magnetic fields started in the early 1960s. A large number of papers have been written on the subject over the years and they are scattered through the literatures of astrophysics, atomic/molecular physics, and condensed-matter physics. Although we have tried to identify original key papers whenever possible, our references put more emphasis on recent works from which earlier papers can be found. We apologize to the authors of the relevant papers that are not mentioned here.

In recent years there has been no general review article that covers the broad subject of matter in strong magnetic fields, although good review articles exist on aspects of the problem. An extensive review of atoms (especially for H and He) in strong magnetic fields, including tabulations of numerical results, can be found in the monograph *Atoms in Strong Magnetic Fields* by Ruder *et al.* (1994). A recent reference is the conference proceedings on *Atoms and Molecules in Strong External Fields* edited by Schmelcher and Schweizer (1998). An insightful, short review of earlier works is that of Ruderman (1974). Other reviews on general physics in strong magnetic fields include the article by Canuto and Ventura (1977) and the monograph by Mészáros (1992).

II. BASICS ON LANDAU LEVELS

The quantum mechanics of a charged particle in a magnetic field is presented in many texts (e.g., Sokolov and Ternov, 1968; Canuto and Ventura, 1977; Landau

and Lifshitz, 1977; Mészáros, 1992). Here we summarize the basics needed for our later discussion.

For a free particle of charge e_i and mass m_i in a constant magnetic field (assumed to be along the z axis), the kinetic energy of transverse motion is quantized into Landau levels

$$E_\perp=\frac{1}{2}m_i\mathbf{v}_\perp^2=\frac{1}{2m_i}\mathbf{\Pi}_\perp^2\rightarrow\left(n_L+\frac{1}{2}\right)\hbar\omega_c,$$
$$n_L=0,1,2,\ldots, \tag{2.1}$$

where $\omega_c=|e_i|B/(m_ic)$ is the cyclotron (angular) frequency, $\mathbf{\Pi}=\mathbf{P}-(e_i/c)\mathbf{A}=m_i\mathbf{v}$ is the mechanical momentum, $\mathbf{P}=-i\hbar\nabla$ is the canonical momentum, and $\mathbf{A}$ is the vector potential of the magnetic field.

A Landau level is degenerate, reflecting the fact that the energy is independent of the location of the guiding center of gyration. To count the degeneracy, it is useful to define the *pseudomentum* (or the generalized momentum)

$$\mathbf{K}=\mathbf{\Pi}+(e_i/c)\mathbf{B}\times\mathbf{r}. \tag{2.2}$$

That $\mathbf{K}$ is a constant of motion (i.e., commuting with the Hamiltonian) can be easily seen from the classical equation of motion for the particle, $d\mathbf{\Pi}/dt=(e_i/c)(d\mathbf{r}/dt)\times\mathbf{B}$. Mathematically, the conservation of $\mathbf{K}$ is the result of the invariance of the Hamiltonian under a spatial translation plus a gauge transformation (Avron *et al.*, 1978). The parallel component K_z is simply the linear momentum, while the constancy of the perpendicular component $\mathbf{K}_\perp$ is the result of the fact that the guiding center of the gyromotion does not change with time. The position vector $\mathbf{R}_c$ of this guiding center is related to $\mathbf{K}_\perp$ by

$$\mathbf{R}_c=\frac{c\mathbf{K}_\perp\times\mathbf{B}}{e_iB^2}=\frac{c}{e_iB}\mathbf{\Pi}_\perp\times\hat{\mathbf{B}}+\mathbf{r}_\perp, \tag{2.3}$$

where $\hat{\mathbf{B}}$ is the unit vector along $\mathbf{B}$. Clearly, the radius of gyration, $\rho=m_icv_\perp/(|e_i|B)$, is quantized according to

$$|\mathbf{r}_\perp-\mathbf{R}_c|=\frac{c}{|e_i|B}|\mathbf{\Pi}_\perp|\rightarrow(2n_L+1)^{1/2}\rho_0, \tag{2.4}$$

where

$$\rho_0=\left(\frac{\hbar c}{|e_i|B}\right)^{1/2}=b^{-1/2}a_0 \tag{2.5}$$

is the cyclotron radius (or the magnetic length). We can use $\mathbf{K}$ to classify the eigenstates. However, since the two components of $\mathbf{K}_\perp$ do not commute, $[K_x,K_y]=-i\hbar(e_i/c)B$, only one of the components can be diagonalized for stationary states. This means that the guiding center of the particle cannot be specified. If we use K_x to classify the states, then the wave function has the well-known form $e^{iK_xx/\hbar}\phi(y)$ (Landau and Lifshitz, 1977), where the function $\phi(y)$ is centered at $y_c=-cK_x/(e_iB)$ [see Eq. (2.3)]. The Landau degeneracy in an area $\mathcal{A}_g=L_g^2$ is thus given by

$$\frac{L_g}{h}\int dK_x=\frac{L_g}{h}|K_{x,g}|=\mathcal{A}_g\frac{|e_i|B}{hc}=\frac{\mathcal{A}_g}{2\pi\rho_0^2}, \tag{2.6}$$

where we have used $K_{x,g}=-e_iBL_g/c$. On the other hand, if we choose to diagonalize $K_\perp^2=K_x^2+K_y^2$, we obtain the Landau wave function $W_{nm}(\mathbf{r}_\perp)$ in cylindrical coordinates (Landau and Lifshitz, 1977), where m is the "orbital" quantum number (denoted by s or $-s$ in some references). For the ground Landau level, this is (for $e_i=-e$)

$$W_{0m}(\mathbf{r}_\perp)\equiv W_m(\rho,\phi)$$
$$=\frac{1}{(2\pi m!)^{1/2}\rho_0}\left(\frac{\rho}{\sqrt{2}\rho_0}\right)^m\exp\left(\frac{\rho^2}{4\rho_0^2}\right)\exp(-im\phi), \tag{2.7}$$

where the normalization $\int d^2\mathbf{r}_\perp|W_m|^2=1$ is adopted. The (transverse) distance of the particle's guiding center from the origin of the coordinates is given by

$$|\mathbf{R}_c|\rightarrow\rho_m=(2m+1)^{1/2}\rho_0,\quad m=0,1,2,\ldots. \tag{2.8}$$

The corresponding value of $K_\perp$ is $K_\perp^2=(\hbar|e_i|B/c)(2m+1)$. Note that $K_\perp^2$ assumes discrete values, since m is required to be an integer in order for the wave function to be single valued. The degeneracy m_g of the Landau level in an area $\mathcal{A}_g=\pi R_g^2$ is then determined by $\rho_{m_g}\simeq(2m_g)^{1/2}\rho_0=R_g$, which again yields $m_g=\mathcal{A}_g|e_i|B/(hc)$ as in Eq. (2.6). We shall refer to different m states as different Landau orbitals. Note that despite the similarity between Eqs. (2.8) and (2.4), their physical meanings are quite different: the circle $\rho=\rho_m$ does not correspond to any gyromotion of the particle, and the energy is independent of m.

We also note that $K_\perp^2$ is related to the z projection of angular momentum J_z, as is evident from the $e^{-im\phi}$ factor in the cylindrical wave function [Eq. (2.7)]. In general, we have

$$J_z=xP_y-yP_x=\frac{1}{2e_iB}(\mathbf{K}_\perp^2-\mathbf{\Pi}_\perp^2)$$
$$=(m-n_L)\frac{|e_i|}{e_i}, \tag{2.9}$$

where we have used $\mathbf{\Pi}_\perp^2=(\hbar|e_i|/c)B(2n_L+1)$.

Including the spin energy of the electron ($e_i\rightarrow-e$, $\omega_c\rightarrow\omega_{ce}$), $E_{\sigma_z}=e\hbar/(2m_ec)\boldsymbol{\sigma}\cdot\mathbf{B}=\hbar\omega_{ce}\sigma_z/2$, the total electron energy can be written as

$$E=n_L\hbar\omega_{ce}+\frac{p_z^2}{2m_e}, \tag{2.10}$$

where the index n_L now includes the spin. For the ground Landau level ($n_L=0$), the spin degeneracy is 1 ($\sigma_z=-1$); for excited levels, the spin degeneracy is 2.

For extremely strong magnetic fields such that $\hbar\omega_{ce}\gtrsim m_ec^2$, or

$$B\gtrsim B_{\rm rel}=\frac{m_e^2c^3}{e\hbar}=\frac{B_0}{\alpha^2}=4.414\times10^{13}\ \text{G} \tag{2.11}$$

(here $\alpha=e^2/\hbar c$ is the fine-structure constant), the transverse motion of the electron becomes relativistic. Equa-

tion (2.10) for the energy of a free electron should be replaced by (Johnson and Lippmann, 1949)

$$E=[c^2p_z^2+m_e^2c^4(1+2n_L\beta)]^{1/2}, \tag{2.12}$$

where

$$\beta\equiv\frac{B}{B_{\rm rel}}=\alpha^2\,b. \tag{2.13}$$

Higher-order corrections in e^2 to Eq. (2.12) have the form $(\alpha/4\pi)m_ec^2F(\beta)$, with $F(\beta)=-\beta$ for $\beta\ll1$ and $F(\beta)=[\ln(2\beta)-(\gamma+3/2)]^2+\cdots$ for $\beta\gg1$, where $\gamma=0.5772$ is Euler's constant (Schwinger, 1988); these corrections will be neglected.

When studying bound states (atoms, molecules, and condensed matter near zero pressure) in strong magnetic fields (Secs. III–V), we shall use nonrelativistic quantum mechanics, even for $B\gtrsim B_{\rm rel}$. The nonrelativistic treatment of bound states is valid for two reasons: (i) For electrons in the ground Landau level, the free-electron energy reduces to $E\simeq m_ec^2+p_z^2/(2m_e)$; the electron remains nonrelativistic in the z direction (along the field axis) as long as the binding energy E_B is much less than m_ec^2; (ii) the shape of the Landau wave function in the relativistic theory is the same as in the nonrelativistic theory, as seen from the fact that ρ_0 is independent of the particle mass. Therefore, as long as $E_B/(m_ec^2)\ll1$, the relativistic effect on bound states is a small correction (Angelie and Deutch, 1978). For bulk matter under pressure, the relativistic correction becomes increasingly important as density increases (Sec. VI).

III. ATOMS

A. Hydrogen atom

In a strong magnetic field with $b\gg1$, the electron is confined to the ground Landau level (the *adiabatic approximation*), and the Coulomb potential can be treated as a perturbation. Assuming infinite proton mass (see Sec. III.E), the energy spectrum of the H atom is specified by two quantum numbers (m,ν), where m measures the mean transverse separation [Eq. (2.8)] between the electron and the proton, while ν specifies the number of nodes in the z wave function. We may write the electron wave function as $\Phi_{m\nu}(\mathbf{r})=W_m(\mathbf{r}_\perp)f_{m\nu}(z)$. Substituting this function into the Schrödinger equation and averaging over the transverse direction, we obtain a one-dimensional Schrödinger equation for $f_{m\nu}(z)$:

$$-\frac{\hbar^2}{2m_e\rho_0^2}f''_{m\nu}-\frac{e^2}{\rho_0}V_m(z)f_{m\nu}=E_{m\nu}f_{m\nu}$$
$$(m,\nu=0,1,2,\ldots). \tag{3.1}$$

The averaged potential is given by

$$V_m(z)=\int d^2\vec{r}_\perp|W_m(\vec{r}_\perp)|^2\frac{1}{r}. \tag{3.2}$$

Here and henceforth we shall employ ρ_0 as our length unit in all the wave functions and averaged potentials, making them dimensionless functions [thus $f''_{m\nu}=d^2f_{m\nu}(z)/dz^2$, with z in units of ρ_0].

There are two distinct types of states in the energy spectrum $E_{m\nu}$. The tightly bound states have no node in their z wave functions ($\nu=0$). The transverse size of the atom in the $(m,0)$ state is $L_\perp\sim\rho_m=[(2m+1)/b]^{1/2}$. For $\rho_m\ll1$, the atom is elongated with $L_z\gg L_\perp$. We can estimate the longitudinal size L_z by minimizing the energy given by $E\sim L_z^{-2}-L_z^{-1}\ln(L_z/L_\perp)$, in atomic units (e^2/a_0). This gives

$$L_z\sim\frac{1}{2\ln(1/\rho_m)}=l_m^{-1}\ \text{a.u.}, \tag{3.3}$$

where

$$l_m\equiv\ln\frac{b}{2m+1}. \tag{3.4}$$

The energy of the tightly bound state is then

$$E_m\simeq-0.16A\,l_m^2\ \text{a.u.}\ (\text{for}\ 2m+1\ll b). \tag{3.5}$$

For $\rho_m\gtrsim a_0$, or $2m+1\gtrsim b$ [but still $b\gg(2m+1)^{-1}$ so that the adiabatic approximation ($|E_m|\ll b$) is valid], we have $L_z\sim\rho_m^{1/2}a_0$ and the energy levels are approximated by

$$E_m\simeq-0.6\left(\frac{b}{2m+1}\right)^{1/2}\ \text{a.u.}$$
$$[\text{for}\ 2m+1\gtrsim b\gg(2m+1)^{-1}]. \tag{3.6}$$

In Eqs. (3.5) and (3.6), the numerical coefficients are obtained from numerical solutions of the Schrödinger Eq. (3.1); the coefficient A in Eq. (3.5) is close to unity for the range of b of interest ($1\ll b\lesssim10^6$) and varies slowly with b and m (e.g., $A\simeq1.01$–1.3 for $m=0$–5 when $B_{12}=1$, and $A\simeq1.02$–1.04 for $m=0$–5 when $B_{12}=10$. Note that E_m asymptotically approaches $-0.5\,l_m^2$ when $b\to\infty$; see Hasagawa and Howard, 1961 and Haines and Roberts, 1969). For the ground state, $(m,\nu)=(0,0)$, the sizes of the atomic wave function perpendicular and parallel to the field are of order $L_\perp\sim\rho_0=b^{-1/2}$ and $L_z\sim l_0^{-1}$, where $l_0\equiv\ln b$. The binding energy $|E(\mathrm{H})|$ (or the ionization energy Q_1) of the atom is given by

$$Q_1=|E(\mathrm{H})|\simeq0.16A\,l_0^2\ \text{a.u.}, \tag{3.7}$$

where A can be approximated by $A=1+1.36\times10^{-2}[\ln(1000/b)]^{2.5}$ for $b<10^3$ and $A=1+1.07\times10^{-2}[\ln(b/1000)]^{1.6}$ for $b\geq10^3$ (this is accurate to within 1% for $100\lesssim b\lesssim10^6$). Figure 1 depicts Q_1 as a function of B. Numerical values of Q_1 for selected B's are given in Table I. Numerical values of E_m for different B's can be found, for example, in Ruder *et al.* (1994). A fitting formula for E_m (accurate to within 0.1–1% at $0.1\lesssim b\lesssim10^4$) is given by Potekhin (1998):

$$E_m=-\tfrac{1}{2}\ln\{\exp[(1+m)^{-2}]+p_1[\ln(1+p_2\,b^{0.5})]^2\}$$
$$-\tfrac{1}{2}\,p_3[\ln(1+p_4\,b^{p_5})]^2\ \text{a.u.}, \tag{3.8}$$

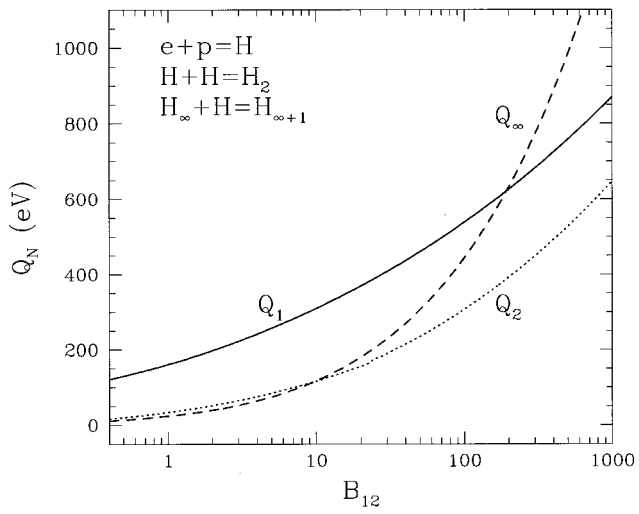

FIG. 1. Energy releases from several atomic and molecular processes as a function of the magnetic-field strength; solid line, ionization energy Q_1 of the H atom; dotted line, dissociation energy Q_2 of H_2; dashed line, cohesive energy Q_∞ of linear chain H_∞. The zero-point energy corrections have been included in Q_2 and Q_∞.

where p_1-p_5 are independent of b (for the $m=0$ state, the parameters p_1-p_5 are 15.55, 0.378, 2.727, 0.3034, and 0.438, respectively). Note that, unlike the field-free case, the excitation energy $\Delta E_m=|E(\mathrm{H})|-|E_m|$ is small compared to $|E(\mathrm{H})|$.

Another type of state of the H atom has nodes in the z wave functions ($\nu>0$). These states are weakly bound. For example, the $\nu=1$ state has about the same binding energy as the ground state of a zero-field H atom, $E\simeq-13.6$ eV, since the equation governing this odd-parity state is almost the same as the radial equation satisfied by the s state of the zero-field H atom. The energy levels of the weakly bound states are approximately given by (Haines and Roberts, 1969)

$$E_{m\nu}=-\frac{1}{2(\nu_1+\delta)^2}\ \text{a.u.}\ \ (\nu_1=1,2,3,\ldots), \tag{3.9}$$

where

$$\delta=\begin{cases}2\rho_m/a_0, & \text{for}\ \ \nu=2\nu_1-1\\ [\ln(a_0/\rho_m)]^{-1}, & \text{for}\ \ \nu=2\nu_1.\end{cases} \tag{3.10}$$

(A more accurate fitting formula for δ is given by Potekhin, 1998). The sizes of the wave functions are ρ_m perpendicular to the field and $L_z\sim\nu^2 a_0$ along the field.

The above results assume a fixed Coulomb potential produced by the proton (i.e., infinite proton mass). The use of a reduced electron mass $m_e m_p/(m_e+m_p)$ introduces a very small correction to the energy [of order $(m_e/m_p)|E_{m\nu}|$]. However, in strong magnetic fields, the effect of the center-of-mass motion on the energy spectrum is complicated. An analysis of the two-body problem in magnetic fields shows that, even for the H atom "at rest," there is a proton cyclotron correction, $m\hbar\omega_{cp}=m\,(m_e/m_p)\,b$ a.u., to the energy [see Eq. (3.40)]. We shall return to this issue in Sec. III.E.

B. High-Z hydrogenic ions

The result in Sec. III.A can be easily generalized to hydrogenic ions (with one electron and nuclear charge Z). The adiabatic approximation (where the electron lies in the ground Landau level) holds when $\rho_0\ll a_0/Z$, or

$$b\gg Z^2. \tag{3.11}$$

TABLE I. Energy releases (in eV) in various atomic and molecular processes in a strong magnetic field; the values of Q's give the relative binding energies of different forms of hydrogen in the ground state. Here $B_{12}=B/(10^{12}\ \mathrm{G})$. The zero-point energies of the protons have been ignored in calculating the Q's for molecules. For H_2, the two columns give $Q_2^{(\infty)}$ (with infinite proton mass) and Q_2 [including zero-point energy correction; see Eq. (4.10)]; for H_∞, the two columns give $Q_\infty^{(\infty)}$ (with infinite proton mass) and Q_∞ [including zero-point energy correction; see Eq. (5.21)]. Note that for $B_{12}\lesssim 0.25$, the lowest energy state of H_2 corresponds to the weakly bound state, while for $B_{12}\gtrsim 0.25$, the tightly bound state is the ground state (see Sec. IV.C). The results are obtained using the numerical methods described by Lai *et al.* (1992) and Lai and Salpeter (1996). The numbers are generally accurate to within 10%.

	$e+p=\mathrm{H}$	$\mathrm{H}+e=\mathrm{H}^-$	$\mathrm{H}+p=\mathrm{H}_2^+$	$\mathrm{H}+\mathrm{H}=\mathrm{H}_2$		$\mathrm{H}_\infty+\mathrm{H}=\mathrm{H}_{\infty+1}$	
B_{12}	Q_1	$Q(H^-)$	$Q(H_2^+)$	$Q_2^{(\infty)}$	Q_2	$Q_\infty^{(\infty)}$	Q_∞
0.1	76.4	6.9	23.6	14	(13)	3.8	(1.2)
0.5	130	11	51.8	31	(21)	16.3	(10)
1	161	13	70.5	46	(32)	29	(20)
5	257	20	136	109	(80)	91	(71)
10	310	24	176	150	(110)	141	(113)
50	460	37	308	294	(236)	366	(306)
100	541	42	380	378	(311)	520	(435)
500	763	57	599	615	(523)	1157	(964)
1000	871	64	722	740	(634)	1630	(1350)

For a tightly bound state, $(m,\nu)=(m,0)$, the transverse size is $L_\perp \sim \rho_m$, while the longitudinal size is

$$L_z \sim \left(Z \ln \frac{1}{Z\rho_m} \right)^{-1} \text{ a.u.} \tag{3.12}$$

The energy is given by

$$E_m \simeq -0.16\, A Z^2 \left[\ln \frac{1}{Z^2} \left(\frac{b}{2m+1} \right) \right]^2 \text{ a.u.} \tag{3.13}$$

for $b \gg (2m+1)Z^2$. Results for the weakly bound states ($\nu>0$) can be similarly generalized from Eqs. (3.9) and (3.10).

C. Heavy atoms

We can imagine constructing a multielectron atom by placing electrons at the lowest available energy levels of a hydrogenic ion. This picture also forms the basis for more detailed calculations of heavy atoms that include electron-electron interactions in a self-consistent manner.

1. Approximate scaling relations

The lowest levels to be filled are the tightly bound states with $\nu=0$. When $a_0/Z \gg \sqrt{2Z-1}\rho_0$, i.e.,

$$b \gg 2Z^3, \tag{3.14}$$

all electrons settle into the tightly bound levels with $m=0,1,2,\ldots,Z-1$. The energy of the atom is approximately given by the sum of all the eigenvalues of Eq. (3.13). Accordingly, we obtain an asymptotic expression for $Z \gg 1$ (Kadomtsev and Kudryavtsev, 1971),

$$E \sim -Z^3 l_Z^2 \text{ a.u.}, \tag{3.15}$$

where

$$l_Z = \ln \left(\frac{a_0}{Z\sqrt{2Z-1}\rho_0} \right) \simeq \ln \sqrt{\frac{b}{2Z^3}}. \tag{3.16}$$

The size of the atom is given by

$$L_\perp \sim (2Z-1)^{1/2}\rho_0, \quad L_z \sim \frac{a_0}{Z l_Z}. \tag{3.17}$$

For intermediate-strong fields (but still strong enough to ignore the Landau excitation),

$$Z^{4/3} \ll b \ll 2Z^3, \tag{3.18}$$

many $\nu>0$ states of the inner Landau orbitals (states with relatively small m) are populated by the electrons. In this regime a Thomas-Fermi-type model for the atom is appropriate (at least for the "core" electrons in small Landau orbitals), i.e., the electrons can be treated as a one-dimensional Fermi gas in a more or less spherical atomic cavity (Kadomtsev, 1970; Mueller *et al.*, 1971). The electrons occupy the ground Landau level, with the z momentum up to the Fermi momentum $p_F \sim n_e/b$, where n_e is the number density of electrons inside the atom (recall that the degeneracy of a Landau level is $eB/hc \sim b$). The kinetic energy of electrons per unit volume is $\varepsilon_k \sim b\, p_F^3 \sim n_e^3/b^2$, and the total kinetic energy is $E_k \sim R^3 n_e^3/b^2 \sim Z^3/b^2R^6$, where R is the radius of the atom. The potential energy is $E_p \sim -Z^2/R$. Therefore the total energy of the atom can be written as

$$E \sim \frac{Z^3}{b^2R^6} - \frac{Z^2}{R} \text{ a.u.} \tag{3.19}$$

Minimizing E with respect to R yields

$$R \sim Z^{1/5} b^{-2/5}, \quad E \sim -Z^{9/5} b^{2/5}. \tag{3.20}$$

For these relations to be valid, the electrons must stay in the ground Landau level; this requires $Z/R \ll \hbar\omega_{ce} = b$, which corresponds to $b \gg Z^{4/3}$. More elaborate Thomas-Fermi-type models have been developed for this regime, giving approximately the same scaling relations (see Appendix B).

We now consider multielectron negative ions. First imagine forming a H^- ion by attaching an extra electron to a H atom in the ground state (with $m=0$). The extra electron can only settle into the $m=1$ state, which, if we ignore the screening of the proton potential due the first ($m=0$) electron, has a binding energy of $|E_1|$ as in Eq. (3.5). The Coulomb repulsion between the two electrons reduces the binding of the $m=1$ electron. The repulsive energy is of order $(\ln\sqrt{b})/L_z$, which is of the same order as $|E_1|$. But the repulsive energy is smaller than $|E_1|$ because of the cylindrical charge distribution of both electrons. Therefore H^- is bound relative to $H+e$ and its ionization potential is proportional to $(\ln\sqrt{b})^2$.

Similar consideration can be applied to a Z ion (nuclear charge Z) with N electrons in the superstrong-field regime ($b \gg Z^3$) (Kadomtsev and Kudryavtsev, 1971). The sizes of the ion perpendicular and parallel to the field are, respectively,

$$R \sim \sqrt{\frac{2N-1}{b}} a_0, \quad L_z \sim \frac{1}{Zl} a_0, \quad \text{with } l = \ln \left(\frac{L_z}{R} \right). \tag{3.21}$$

The ground-state energy of the ion is

$$E \simeq -\frac{N}{8} l^2 (4Z-N+1)^2 \text{ a.u.} \tag{3.22}$$

Applying this result for hydrogen ions ($Z=1$), we see that the ionization potential of H^- to $H+e$ is about 1/10 of the binding energy of the H atom. We also see that, for $n>2$, the negative ion $H^{-(n-1)}$ is unbound. This estimate is confirmed by numerical calculations (Lai, Salpeter, and Shapiro, 1992).

2. Numerical calculations and results

Reliable values for the energy of a multielectron atom for $b \gg 1$ can be calculated using the Hartree-Fock method (Virtamo, 1976; Pröschel *et al.*, 1982; Neuhauser *et al.*, 1987). For an electron in the ground Landau level with spin aligned antiparallel to the magnetic field (the adiabatic approximation), the kinetic energy and spin energy add up to $(1/2m_e)p_z^2$. Thus the Hamiltonian for a neutral atom with Z electrons is

$$H=\sum_i \frac{1}{2m_e}p_{zi}^2-Ze^2\sum_i \frac{1}{r_i}+e^2\sum_{i<j}\frac{1}{r_{ij}}, \tag{3.23}$$

where i labels electrons. The basis one-electron wave functions are

$$\Phi_{m\nu}(\mathbf{r})=W_m(\rho,\phi)f_{m\nu}(z), \quad m,\nu=0,1,2,\ldots. \tag{3.24}$$

In the Hartree-Fock approximation, the Z-electron wave function is formed by the antisymmetrized product of Z one-electron basis functions. Averaging the Hamiltonian over the transverse Landau functions, we obtain

$$\langle H\rangle=\frac{\hbar^2}{2m_e\rho_0^2}\sum_{m\nu}\int dz\,|f'_{m,\nu}(z)|^2 - \frac{Ze^2}{\rho_0}\sum_{m\nu}\int dz\,|f_{m,\nu}(z)|^2V_m(z)+E_{\rm dir}+E_{\rm exch}, \tag{3.25}$$

where $V_m(z)$ is given by Eq. (3.2). The direct and exchange energies for electron-electron interaction are given by

$$E_{\rm dir}=\frac{e^2}{2\rho_0}\sum_{m\nu,m'\nu'}\int dz\,dz'\,D_{mm'}(z-z') \times|f_{m\nu}(z)|^2|f_{m'\nu'}(z')|^2, \tag{3.26}$$

$$E_{\rm exch}=-\frac{e^2}{2\rho_0}\sum_{m\nu,m'\nu'}\int dz\,dz'\,E_{mm'}(z-z') \times f_{m\nu}(z)f_{m'\nu'}(z')f^*_{m\nu}(z')f^*_{m'\nu'}(z), \tag{3.27}$$

where

$$D_{mm'}(z_1-z_2)=\int d^2\mathbf{r}_{1\perp}d^2\mathbf{r}_{2\perp}|W_m(\mathbf{r}_{1\perp})|^2 \times|W_{m'}(\mathbf{r}_{2\perp})|^2\frac{1}{r_{12}}, \tag{3.28}$$

$$E_{mm'}(z_1-z_2)=\int d^2\mathbf{r}_{1\perp}d^2\mathbf{r}_{2\perp}W_m(\mathbf{r}_{1\perp}) \times W_{m'}(\mathbf{r}_{2\perp})W^*_m(\mathbf{r}_{2\perp})W^*_{m'}(\mathbf{r}_{1\perp})\frac{1}{r_{12}}. \tag{3.29}$$

(Useful mathematical relations for evaluating $V_m, D_{mm'}, E_{mm'}$ are given, for example, by Sokolov and Ternov, 1968; Virtamo and Jauho, 1975; Pröschel *et al.*, 1982; Lai *et al.*, 1992.) Varying $\langle H\rangle$ with respect to $f_{m\nu}$'s, we obtain the Hartree-Fock equations

$$\left[-\frac{\hbar^2}{2m_e\rho_0^2}\frac{d^2}{dz^2}-\frac{Ze^2}{\rho_0}V_m(z)+\frac{e^2}{\rho_0}K_m(z)-\varepsilon_{m\nu}\right]f_{m\nu}(z) =\frac{e^2}{\rho_0}J_{m\nu}(z), \tag{3.30}$$

where the direct and exchange potentials are

$$K_m(z)=\sum_{m'\nu'}\int dz'|f_{m'\nu'}(z')|^2D_{mm'}(z-z'), \tag{3.31}$$

$$J_{m\nu}(z)=\sum_{m'\nu'}f_{m'\nu'}(z)\int dz'\,f^*_{m'\nu'}(z')f_{m\nu}(z') \times E_{mm'}(z-z'). \tag{3.32}$$

After iteratively solving Eqs. (3.30)–(3.32) for the eigenvalues $\varepsilon_{m\nu}$ and eigenfunction $f_{m\nu}$, the total energy of the atom can be obtained from

$$E=\sum_{m\nu}\varepsilon_{m\nu}-E_{\rm dir}-E_{\rm exch}. \tag{3.33}$$

Accurate energies of the He atom as a function of B in the adiabatic approximation (valid for $b\gg Z^2$) were obtained by Virtamo (1976) and Pröschel *et al.* (1982). This work was extended to Z up to 26 (Fe atom) by Neuhauser *et al.* (1987; see also Miller and Neuhauser, 1991). Numerical results can be found in these papers. Neuhauser *et al.* (1987) gave an approximate fitting formula

$$E\simeq -160\,Z^{9/5}B_{12}^{2/5}\ \text{eV} \tag{3.34}$$

for $0.5\lesssim B_{12}\lesssim 5$. (Comparing with the numerical results, the accuracy of the formula is about 1% for $Z\simeq 18$–26 and becomes 5% for $Z\sim 10$.) For the He atom, more accurate results (which relax the adiabatic approximation) are given by Ruder *et al.* (1994) and by Jones *et al.* (1999a; this paper also considers the effect of electron correlation).

The Hartree-Fock method is approximate because electron correlations are neglected. Due to their mutual repulsion, any pair of electrons tends to be more distant from each other than the Hartree-Fock wave function would indicate. In zero field, this correlation effect is especially pronounced for the spin-singlet states of electrons for which the spatial wave function is symmetrical. In strong magnetic fields, the electron spins are all aligned antiparallel to the magnetic field and the spatial wave function is antisymmetric with respect to the interchange of two electrons. Thus the error in the Hartree-Fock approach is expected to be significantly smaller than the 1% accuracy characteristic of zero-field Hartree-Fock calculations (Weissbluth, 1978; Neuhauser *et al.*, 1987; Schmelcher, Ivanov, and Becken, 1999).

Other calculations of heavy atoms in strong magnetic fields include Thomas-Fermi-type statistical models (see Fushiki *et al.*, 1992 for a review and Appendix B for a brief summary) and density-functional theory (Jones, 1985, 1986; Kössl *et al.*, 1988; Relovsky and Ruder, 1996). The Thomas-Fermi-type models are useful in establishing asymptotic scaling relations, but are not adequate for obtaining accurate binding energy and excitation energies. The density-functional theory can potentially give results as accurate as the Hartree-Fock method but, without calibration with other methods, it is difficult to establish its accuracy *a priori* (see Neuhauser *et al.*, 1987; Vignale and Rasolt, 1987, 1988). Lieb *et al.* (1992, 1994a, 1994b) have presented detailed discussions of the asymptotic behaviors of heavy atoms (as $Z\to\infty$) for five different magnetic-field regimes: $b\ll Z^{4/3}$, $b\sim Z^{4/3}$, $Z^{4/3}\ll b\ll Z^3$, $b\sim Z^3$, and $b\gg Z^3$ [see also Eqs.

(3.14)–(3.18)]. They showed that various density-functional-type theories become exact in these asymptotic limits: the Thomas-Fermi theory corresponds to the first three regimes and a "density-matrix-functional" theory can be applied to the fifth regime (see Johnsen and Yngvason, 1996 for numerical calculations of heavy atoms based on this theory).

D. Intermediate-magnetic-field regime

For $B\sim B_0\sim 10^9$ G, the adiabatic approximation is no longer valid, and electrons can occupy excited Landau levels. In this intermediate-field regime, neither Coulomb nor magnetic effects can be treated as a perturbation. Accurate energy levels of the H atom for arbitrary field strengths were first calculated by Rösner *et al.* (1984); the method involves expansion of the wave function in terms of either spherical harmonics or cylindrical Landau orbitals, and subsequent approximate solution of the system of coupled integral-differential equations (see Ruder *et al.*, 1994 for tabulated numerical results). Recent calculations of the H atom in magnetic fields include Goldman and Chen (1991), Chen and Goldman (1992—relativistic effects), Melezhik (1993), Fassbinder and Schweizer (1996a, 1996b—with magnetic and electric fields), Kravchenko *et al.* (1996—exact solution for nonrelativistic electron), and references therein. Ruder *et al.* (1994) presented (less accurate) results for He atoms calculated using a Hartree-Fock method similar to that of Rösner *et al.* (1984). Recent studies of multielectron atoms (including radiative transitions) for the intermediate-field regime have used more elaborate implementations of the Hartree-Fock method with different basis functions (see Jones *et al.*, 1996, 1999a; Ivanov and Schmelcher, 1998, 1999, 2000; Becken *et al.*, 1999; Becken and Schmelcher, 2000). Accurate calculation of the hydrogen negative ion (H^-) was presented by Al-Hujaj and Schmelcher (2000, and references therein). A quantum Monte Carlo method has also been developed to calculate the He atom (Jones *et al.*, 1997). Accurate energy levels for the He atom at $B\sim 10^9$ G are needed to interpret the spectrum of the magnetic white dwarf GD229 (see Jordan *et al.*, 1998; Jones *et al.*, 1999b).

E. Effect of center-of-mass motion

Our discussion so far has implicitly assumed infinite nuclear mass, i.e., we have been concerned with the energy levels of electrons in the static Coulomb potential of a fixed ion. It has long been recognized that in strong magnetic fields the effects of finite nuclear mass and center-of-mass motion on the atomic structure are nontrivial (see, for example, Gor'kov and Dzyaloshinskii, 1968; Avron *et al.*, 1978; Herold *et al.*, 1981; Baye and Vincke, 1990; Vincke *et al.*, 1992; Pavlov and Mészáros, 1993; Potekhin, 1994). Here we illustrate the key issues by considering the hydrogen atom in strong magnetic fields: general quantum-mechanical solutions for this two-body problem have been obtained only recently (Vincke *et al.*, 1992; Potekhin, 1994). Some aspects of the problem are also important for applications to molecules. A recent discussion on this subject can be found in Baye and Vincke (1998; see also Johnson *et al.*, 1983 for an earlier review on the general problem of center-of-mass motion of atoms and molecules in external fields).

A free electron confined to the ground Landau level, the usual case for $b\gg 1$, does not move perpendicular to the magnetic field. Such motion is necessarily accompanied by Landau excitations. When the electron combines with a proton, the mobility of the neutral atom across the field depends on the ratio of the atomic excitation energy ($\sim \ln b$) and the Landau excitation energy for the proton, $\hbar\omega_{cp}=\hbar eB/(m_pc)$. It is convenient to define a critical field strength $B_{\rm cm}$ via (Lai and Salpeter, 1995)

$$b_{\rm cm}\equiv \frac{m_p}{m_e}\ln b_{\rm cm}=1.80\times 10^4;$$
$$B_{\rm cm}=b_{\rm cm}B_0=4.23\times 10^{13}\ \text{G}. \tag{3.35}$$

Thus for $B\gtrsim B_{\rm cm}$, the deviation from the free center-of-mass motion of the atom is significant even for small transverse momentum [see Eq. (3.42) below].

Consider now the electron-proton system. It is easy to show that even including the Coulomb interaction, the total pseudomomentum,

$$\mathbf{K}=\mathbf{K}_e+\mathbf{K}_p, \tag{3.36}$$

is a constant of motion. Moreover, all components of $\mathbf{K}$ commute with each other. Thus it is natural to separate the center-of-mass motion from the internal degrees of freedom using $\mathbf{K}$ as an explicit constant of motion. From Eq. (2.3), we find that the separation between the guiding centers of the electron and the proton is directly related to $\mathbf{K}_\perp$:

$$\mathbf{R}_K=\mathbf{R}_{ce}-\mathbf{R}_{cp}=\frac{c\mathbf{B}\times\mathbf{K}}{eB^2}. \tag{3.37}$$

The two-body eigenfunction with a definite value of $\mathbf{K}$ can be written as

$$\Psi(\mathbf{R},\mathbf{r})=\exp\left[\frac{i}{\hbar}\left(\mathbf{K}+\frac{e}{2c}\mathbf{B}\times\mathbf{r}\right)\cdot\mathbf{R}\right]\phi(\mathbf{r}), \tag{3.38}$$

where $\mathbf{R}=(m_e\mathbf{r}_e+m_p\mathbf{r}_p)/M$ and $\mathbf{r}=\mathbf{r}_e-\mathbf{r}_p$ are the center-of-mass and relative coordinates, and $M=m_e+m_p$ is the total mass. The Schrödinger equation reduces to $H\phi(\mathbf{r})=\mathcal{E}\phi(\mathbf{r})$, with[2]

$$H=\frac{\mathbf{K}^2}{2M}+\frac{1}{2\mu}\left(\mathbf{p}+\frac{e}{2c}\mathbf{B}\times\mathbf{r}\right)^2-\frac{e}{m_pc}\mathbf{B}\cdot(\mathbf{r}\times\mathbf{p})$$
$$-\frac{e^2}{r}+\frac{e}{Mc}(\mathbf{K}\times\mathbf{B})\cdot\mathbf{r}, \tag{3.39}$$

[2]The spin terms of the electron and the proton are not explictly included. For the electron in the ground Landau level, the zero-point Landau energy $\hbar\omega_{ce}/2$ is exactly canceled by the spin energy. For sake of brevity, we drop the zero-point energy of the proton, $\hbar\omega_{cp}/2$, as well as the spin energy $\pm g_p\hbar\omega_{cp}/2$ (where $g_p=2.79$).

where $\mathbf{p}=-i\hbar\partial/\partial\mathbf{r}$ and $\mu=m_e m_p/M$ (see, for example, Lamb, 1952; Avron *et al.*, 1978; Herold *et al.*, 1981). Clearly, the center-of-mass motion is coupled to the internal motion through the last term in H, which has the form of an electrostatic potential produced by an electric field $(\mathbf{K}/M)\times\mathbf{B}$. This term represents the so-called "motional Stark effect" (although such a description is not exactly accurate, since $\mathbf{K}_\perp/M$ does not correspond to the center-of-mass velocity; see Johnson *et al.*, 1983). In the adiabatic approximation ($b\gg1$, with the electron in the ground Landau level), we write the total energy of the atom as

$$\mathcal{E}_{m\nu}(K_z,K_\perp)=\frac{K_z^2}{2M}+m\hbar\omega_{cp}+E_{m\nu}(K_\perp), \tag{3.40}$$

where the azimuthal quantum number m measures the relative electron-proton z angular momentum $J_z=\hat{\mathbf{B}}\cdot(\mathbf{r}\times\mathbf{p})=-m$ (clearly m is a good quantum number only when $K_\perp=0$, but we shall use it as a label of the state even when $K_\perp\neq0$), and ν enumerates the longitudinal excitations. The $m\hbar\omega_{cp}$ term in Eq. (3.40) represents the Landau energy excitations for the proton; this "coupling" between the electron quantum number m and the proton Landau excitation results from the conservation of $\mathbf{K}$. Clearly, for sufficiently high b, states with $m>0$ become unbound [i.e., $\mathcal{E}_{m\nu}(\mathbf{K}=0)=m\hbar\omega_{cp}+E_{m\nu}(0)>0$].

For small $K_\perp$, the motional Stark term in H can be treated as a perturbation (see, for example, Vincke and Baye, 1988; Pavlov and Mészros, 1993). For the tightly bound states ($\nu=0$), we have

$$E_{m0}(K_\perp)\simeq E_m+\frac{K_\perp^2}{2M_{\perp m}}\quad(\text{for } K_\perp\ll K_{\perp p}), \tag{3.41}$$

where E_m is the energy of a bound electron in the fixed Coulomb potential (the correction due to the reduced mass μ can be easily incorporated into E_m; this amounts to a small correction). The effective mass $M_{\perp m}$ for the transverse motion increases with increasing b. For the $m=0$ state,

$$M_\perp\equiv M_{\perp0}=M\left(1+\frac{\xi b}{M\ln b}\right)\simeq M\left(1+\frac{\xi b}{b_{\rm cm}}\right), \tag{3.42}$$

where ξ is a slowly varying function of b (e.g., $\xi\simeq2-3$ for $b=10^2-10^5$). Similar results can be obtained for the $m>0$ states: $M_{\perp m}\simeq M+\xi_m(2m+1)b/l_m$, where ξ_m is of the same order of magnitude as ξ, and $l_m=\ln[b/(2m+1)]$. A simple fitting formula for $M_{\perp m}$ is proposed by Potekhin (1998):

$$M_{\perp m}=M[1+(b/b_0)^{c_0}], \tag{3.43}$$

with $b_0=6150\,(1+0.0389\,m^{3/2})/(1+7.87\,m^{3/2})$ and $c_0=0.937+0.038\,m^{1.58}$. Equation (3.41) is valid only when $K_\perp$ is much less than the "perturbation limit" $K_{\perp p}$, given by (for $m=0$) $K_{\perp p}=b^{1/2}(1+M\ln b/\xi b)$, which corresponds to $K_{\perp p}^2/(2M_\perp)\simeq1.7(1+b_{\rm cm}/\xi b)$. Numerical calculations by Potekhin (1994) indicate that Eq. (3.41) is a good approximation for $K_\perp\lesssim K_{\perp c}$ (see Fig. 2), where

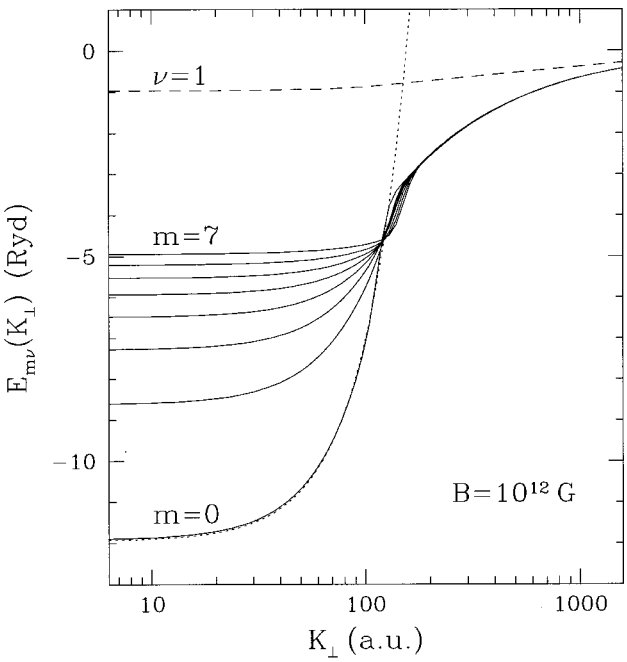

FIG. 2. Energy spectrum of a hydrogen atom moving across a magnetic field with $B=10^{12}$ G: solid lines, the tightly bound states ($\nu=0$) with $m=0,1,2,\ldots,7$; dashed line, weakly bound state with $\nu=1, m=0$; dotted line $E_{00}(K_\perp)=E_{00}(0)+K_\perp^2/(2M_\perp)$. The total energy of the atom is $\mathcal{E}_{m\nu}=K_z^2/(2M)+m\hbar\omega_{cp}+E_{m\nu}(K_\perp)$.

$$K_{\perp c}\simeq\sqrt{2M|E_m|}, \tag{3.44}$$

that is, $|E_{m0}(K_{\perp c})|\ll|E_m|$. The states with $K_\perp\lesssim K_{\perp c}$ are sometimes called *centered states*.

For $K_\perp\gtrsim K_{\perp c}$, the motional electric field [see Eq. (3.39)] induces a significant transverse separation (perpendicular to $\mathbf{K}$) between the electron and the proton. It is more convenient to use a new coordinate system to account for this effect. Since $\mathbf{K}_\perp$ measures the separation of the guiding centers of the electron and the proton, we can remove the "Stark term" in Eq. (3.39) by introducing a displaced coordinate $\mathbf{r}'=\mathbf{r}-\mathbf{R}_K$. After a gauge transformation with

$$\phi(\mathbf{r})\to\exp\left(\frac{i}{\hbar}\frac{m_p-m_e}{2M}\mathbf{K}_\perp\cdot\mathbf{r}\right)\phi(\mathbf{r}'), \tag{3.45}$$

we obtain $H'\phi(\mathbf{r}')=\mathcal{E}\phi(\mathbf{r}')$, with the Hamiltonian

$$H'=\frac{K_z^2}{2M}+\frac{1}{2\mu}\left(\mathbf{p}'+\frac{e}{2c}\mathbf{B}\times\mathbf{r}'\right)^2-\frac{e}{m_p c}\mathbf{B}\cdot(\mathbf{r}'\times\mathbf{p}')-\frac{e^2}{|\mathbf{r}'+\mathbf{R}_K|}, \tag{3.46}$$

where $\mathbf{p}'=-i\hbar\partial/\partial\mathbf{r}'$ (see Avron *et al.*, 1978; Herold *et al.*, 1981). We can estimate the size L_z of the atom along the z axis and the energy $E_{m\nu}(K_\perp)$ for two different regimes of R_K (see Lai and Salpeter, 1995): (i) For $R_K\lesssim L_z\lesssim1$ (but not necessarily $R_K<\rho_m$ or $K_\perp<\sqrt{mb}$), we have (for the $\nu=0$ states)

$$L_z \sim \left(\ln\frac{1}{\rho_m^2+R_K^2}\right)^{-1} a_0,$$

$$E_{m0}(K_\perp) \sim -0.16\left(\ln\frac{1}{\rho_m^2+R_K^2}\right)^2 \text{ a.u.} \quad (3.47)$$

Mixing between different m states is unimportant when $b \gg b_{\rm cm}$. (ii) For $R_K \gtrsim 1$, the electron-proton interaction does not contain the Coulomb logarithm, and the energy can be written as $E_{m0}(K_\perp) \sim L_z^{-2} - (L_z^2+R_K^2)^{-1/2}$. In the limit of $R_K \gg 1$, minimization of $\mathcal{E}_m$ with respect to L_z yields

$$L_z \sim R_K^{3/4} \ll R_K, \quad E_{m0}(K_\perp) \sim -\frac{1}{R_K} = -\frac{b}{K_\perp} \text{ a.u.} \quad (3.48)$$

independent of m (see, for example, Burkova *et al.*, 1976; Potekhin, 1994). The states with $K_\perp \gtrsim K_{\perp c}$ (which correspond to $R_K \gtrsim \rho_0$ for $b \gtrsim b_{\rm cm}$) are sometimes referred to as *decentered states* (Vincke *et al.*, 1992; Potekhin, 1994), but note that for a given $(m\nu)$ (defined at $K_\perp = 0$), there is a continuous energy $E_{m\nu}(K_\perp)$ that connects the centered state at small $K_\perp$ to the decentered state at large $K_\perp$.

To calculate the energy $E_{m\nu}(K_\perp)$ for general $K_\perp$, we must include mixing between different m orbitals. We may use $\phi(\mathbf{r}) = \Sigma_{m'} W_{m'}(\mathbf{r}_\perp) f_{m'}(z)$ in Eq. (3.39) and obtain a coupled set of equations for $f_{m'}(z)$; alternatively, for $K_\perp \gtrsim K_{\perp c}$, it is more convenient to use $\phi(\mathbf{r}') = \Sigma_{m'} W_{m'}(\mathbf{r}'_\perp) f_{m'}(z)$ in Eq. (3.46). Numerical results are presented by Potekhin (1994; see also Vincke *et al.*, 1992); analytical fitting formulas for the energies, atomic sizes, and oscillator strengths are given by Potekhin (1998). Figure 2 shows the energy $E_{m\nu}(K_\perp)$ (based on Potekhin's calculation) as a function of $K_\perp$ for several different states at $B_{12} = 1$. Note that the total energies of different states, $\mathcal{E}_{m\nu}(K_z, K_\perp)$, do not cross each other as $K_\perp$ increases.

While for neutral atoms the center-of-mass motion can be separated from the internal relative motion, this cannot be done for ions (Avron *et al.*, 1978). Ions undergo collective cyclotron motion which depends on the internal state. However, the existence of an approximate constant of motion allows an approximate pseudoseparation up to very high fields (see Bayes and Vincke, 1998 and references therein). Numerical results for He^+ moving in strong magnetic fields are obtained by Bezchastnov *et al.* (1998).

The effects of center-of-mass motion on multielectron systems (heavy atoms and molecules) in strong magnetic fields have not been studied numerically, although many theoretical issues are discussed by Johnson *et al.* (1983) and Schmelcher *et al.* (1988, 1994).

IV. MOLECULES

Most studies of molecules in strong magnetic fields have been restricted to hydrogen. We shall therefore focus on H to illustrate the basic magnetic effects and only briefly discuss molecules of heavier elements.

A. H_2: Basic mechanism of bonding

In a strong magnetic field, the mechanism of molecule formation is quite different from the zero-field case (see Ruderman, 1974; Lai *et al.*, 1992). The spins of the electrons in the atoms are aligned antiparallel to the magnetic field, and therefore two atoms in their ground states $(m=0)$ do not bind together according to the exclusion principle. Instead, one H atom has to be excited to the $m=1$ state. The two H atoms, one in the ground state $(m=0)$, another in the $m=1$ state, then form the ground state of the H_2 molecule by covalent bonding. Since the "activation energy" for exciting an electron in the H atom from the Landau orbital m to $(m+1)$ is small [see Eq. (3.5)], the resulting H_2 molecule is stable. The size of the H_2 molecule is comparable to that of the H atom. The interatomic separation $a_{\rm eq}$ and the dissociation energy D of the H_2 molecule scale approximately as

$$a_{\rm eq} \sim \frac{1}{\ln b} a_0, \quad D \sim (\ln b)^2 \text{ a.u.}, \quad (4.1)$$

although D is numerically smaller than the ionization energy of the H atom (see Table I).

Another mechanism for forming a H_2 molecule in a strong magnetic field is to let both electrons occupy the same $m=0$ Landau orbital, while one of them occupies the tightly bound $\nu=0$ state and the other the $\nu=1$ weakly bound state. This costs no activation energy. However, the resulting molecule tends to have a small dissociation energy, of the order of a Rydberg. We shall refer to this electronic state of the molecule as the weakly bound state and to the states formed by two electrons in the $\nu=0$ orbitals as the tightly bound states. As long as $\ln b \gg 1$, the weakly bound states constitute excited energy levels of the molecule.

B. Numerical calculations and results

In the Born-Oppenheimer approximation (see Schmelcher *et al.*, 1988, 1994 for a discussion on the validity of this approximation in strong magnetic fields), the interatomic potential $U(a,R_\perp)$ is given by the total electronic energy $E(a,R_\perp)$ of the system, where a is the proton separation along the magnetic field and $R_\perp$ is the separation perpendicular to the field. Once $E(a,R_\perp)$ is obtained, the electronic equilibrium state is determined by locating the minimum of the $E(a,R_\perp)$ surface. [For a given a, $E(a,R_\perp)$ is minimal at $R_\perp = 0$.]

The simplest system is the molecular ion H_2^+. For $b \gg 1$, the energy of H_2^+ can be easily calculated as in the case of the H atom (see, for instance, Wunner *et al.*, 1982; Khersonskii, 1984, 1985; Le Guillou and Zinn-Justin, 1984). When the molecular axis is aligned with the magnetic axis $(R_\perp = 0)$, we need only solve a Schrödinger equation similar to Eq. (3.1), except replacing $V_m(z)$ by

$$\tilde{V}_m(z) = V_m\left(z-\frac{a}{2}\right) + V_m\left(z+\frac{a}{2}\right). \quad (4.2)$$

The total electronic energy is simply $E(a,0)=\varepsilon_{m\nu}+e^2/a$. The ground state corresponds to $(m,\nu)=(0,0)$.

The Hartree-Fock calculation of H_2 is similar to the case of multielectron atoms. For the tightly bound states, the two electrons occupy the $(m,\nu)=(m_1,0),(m_2,0)$ orbitals (the ground state corresponds to $m_1=0,m_2=1$), with the wave function

$$\Psi(\mathbf{r}_1,\mathbf{r}_2)=\frac{1}{\sqrt{2}}[\Phi_{m_1 0}(\mathbf{r}_1)\Phi_{m_2 0}(\mathbf{r}_2) - \Phi_{m_1 0}(\mathbf{r}_2)\Phi_{m_2 0}(\mathbf{r}_1)]. \quad (4.3)$$

We obtain the same Hartree-Fock equation as (3.30) except that V_m is replaced by $\tilde{V}_m$ (for aligned configurations, $R_\perp=0$). The energy is given by

$$E(a,0)=\frac{e^2}{a}+\varepsilon_{m_1 0}+\varepsilon_{m_2 0}-\frac{e^2}{\rho_0}\int dz_1 dz_2 \times|f_{m_1 0}(z_1)|^2|f_{m_2 0}(z_2)|^2 D_{m_1 m_2}(z_1-z_2) + \frac{e^2}{\rho_0}\int dz_1 dz_2 f_{m_1 0}(z_1)f_{m_2 0}(z_2) \times f^*_{m_1 0}(z_2)f^*_{m_2 0}(z_1)E_{m_1 m_2}(z_1-z_2). \quad (4.4)$$

Although the Hartree-Fock method is adequate for small interatomic separations (a less than the equilibrium value, $a_{\rm eq}$), the resulting $E(a,0)$ becomes less reliable for large a: as $a\to\infty$, $E(a,0)$ does not approach the sum of the energies of two isolated atoms, one in the m_1 state, another in the m_2 state. The reason is that as a increases, another configuration of electron orbitals,

$$\Psi_2(\mathbf{r}_1,\mathbf{r}_2)=\frac{1}{\sqrt{2}}[\Phi_{m_1 1}(\mathbf{r}_1)\Phi_{m_2 1}(\mathbf{r}_2)-\Phi_{m_1 1}(\mathbf{r}_2)\Phi_{m_2 1}(\mathbf{r}_1)], \quad (4.5)$$

becomes more and more degenerate with the first configuration $\Psi_1=\Psi$ in Eq. (4.3), and there must be mixing of these two different configurations. Both Ψ_1 and Ψ_2 have the same symmetry with respect to the Hamiltonian: the total angular momentum along the z axis is $M_{Lz}=1$, the total electron spin is $M_{Sz}=-1$, and both Ψ_1 and Ψ_2 are even with respect to the operation $\mathbf{r}_i\to-\mathbf{r}_i$. To obtain a reliable $E(a,0)$ curve, the *configuration interaction* between Ψ_1 and Ψ_2 must be taken into account in the Hartree-Fock scheme (Lai *et al.*, 1992; see Slater, 1963 for a discussion of the zero-field case).

Molecular configurations with $R_\perp\neq0$ correspond to excited states of the molecules (see Sec. IV.C). To obtain $E(a,R_\perp)$, one needs to take into account the mixing of different m states in a single-electron orbital. Approximate energy surfaces $E(a,R_\perp)$ for both small $R_\perp$ and large $R_\perp$ have been computed by Lai and Salpeter (1996).

Numerical results of $E(a,0)$ (based on the Hartree-Fock method) for both tightly bound states and weakly bound states are given by Lai *et al.* (1992) and Lai and Salpeter (1996). Quantum Monte Carlo calculations have also been performed, confirming the validity of the method (Ortiz *et al.*, 1995). Figure 3 depicts some of the energy curves. The dissociation energy of H_2 in the ground state can be fitted by

$$Q_2^{(\infty)}\equiv 2|E(H)|-|E(H_2)| = 0.106[1+0.1\,l^{0.2}\ln(b/b_{\rm cm})]\,l^2 \quad (4.6)$$

(where $l=\ln b$), with an accuracy of $\lesssim5\%$ for $1\lesssim B_{12}\lesssim1000$, where $b_{\rm cm}=1.80\times10^4$ is defined in Eq. (3.35). [The superscript (∞) implies that the zero-point energy of the molecule is not included in $Q_2^{(\infty)}$; see Sec. IV.C below.] Thus $Q_2^{(\infty)}\simeq46$ eV for $B_{12}=1$ and $Q_2^{(\infty)}\simeq150$ eV for $B_{12}=10$ (see Table I). By contrast, the zero-field dissociation energy of H_2 is 4.75 eV.

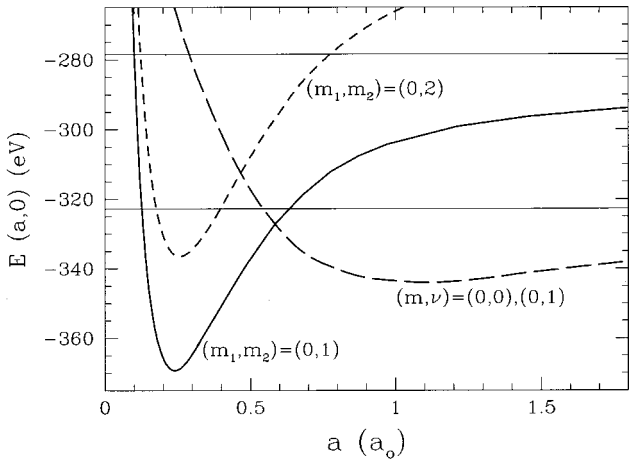

FIG. 3. The electronic-energy curves $E(a,0)$ of H_2 molecule at $B=10^{12}$ G when the molecular axis is aligned with the magnetic-field axis (a is the proton separation): solid curve, the electrons occupy the $m_1=0$ and $m_2=1$ orbitals (both with $\nu=0$); short-dashed curve, $(m_1,m_2)=(0,2)$; long-dashed curve, weakly bound state with $(m,\nu)=(0,0),(0,1)$. The solid horizontal lines correspond to $E=-323$ eV (the total energy of two isolated atoms in the ground state) and $E=-278$ eV [the total energy of two isolated atoms, one in the ground state (-161 eV), another in the first excited state (-117 eV)].

C. Molecular excitations

For the ground state of H_2, the molecular axis and the magnetic-field axis coincide, and the two electrons occupy the $m=0$ and $m=1$ orbitals, i.e., $(m_1,m_2)=(0,1)$. The molecule can have different types of excitation levels (Lai and Salpeter, 1996).

(i) *Electronic excitations*. The electrons occupy orbitals other than $(m_1,m_2)=(0,1)$, giving rise to electronic excitations. The energy difference between the excited state (m_1,m_2) (with $\nu_1=\nu_2=0$) and the ground state (0,1) is of order $\ln b$, as in the case for atoms. Typically, only the single-excitation levels (those with $m_1=0$ and $m_2>1$) are bound relative to two atoms in the ground states. Another type of electronic excitation is formed by two electrons in the $(m,\nu)=(0,0)$ and (0,1) orbitals. The dissociation energy of this weakly bound state is of the order of a Rydberg and does not depend sensitively on the magnetic-field strength (see Fig. 3). Note that,

since it does not cost any activation energy to form a H_2 in the weakly bound state, for relatively small magnetic field ($B_{12} \lesssim 0.25$), the weakly bound state actually has lower energy than the tightly bound state.

(ii) *Aligned vibrational excitations*. These result from the vibration of the protons about the equilibrium separation $a_{\rm eq}$ along the magnetic-field axis. To estimate the excitation energy, we need to consider the excess potential $\delta U(\delta a) = U(a_{\rm eq}+\delta a,0) - U(a_{\rm eq},0)$. Since $a_{\rm eq}$ is the equilibrium position, the sum of the first-order terms (proportional to δa) in δU, coming from proton-proton, electron-electron, proton-electron Coulomb energies and quantum-mechanical electron kinetic energy, must cancel, and $\delta U \propto (\delta a)^2$ for small δa. The dominant contribution to the energy of the molecule comes from the proton-electron Coulomb energy $\sim l/a$, in which the logarithmic factor $l \equiv \ln b \gg 1$ results from the Coulomb integral over the elongated electron distribution. The excess potential is of order $\delta U \sim l\,(\delta a)^2/a_{\rm eq}^3 \sim (\xi^{-3} l^4)\,(\delta a)^2$, where we have used $a_{\rm eq} = \xi/l$ (the dimensionless factor ξ decreases slowly with increasing b; e.g., $\xi \simeq 2$ for $B_{12}=0.1$ and $\xi = 0.75$ for $B_{12}=100$). Thus for small-amplitude oscillations around $a_{\rm eq}$, we obtain a harmonic oscillation spectrum with excitation energy quanta $\hbar\omega_\parallel \sim \xi^{-3/2} l^2 \mu^{-1/2}$, where $\mu = m_p/2m_e = 918$ is the reduced mass of the two protons in units of the electron mass. Numerical calculations yield a similar scaling relation. For the electronic ground state, the energy quanta can be approximated by

$$\hbar\omega_\parallel \simeq 0.13\,(\ln b)^{5/2}\mu^{-1/2}\ \text{a.u.} \simeq 0.12\,(\ln b)^{5/2}\ \text{eV}. \tag{4.7}$$

(This is accurate to within 10% for $40 \lesssim b \lesssim 10^4$.) Thus $\hbar\omega_\parallel \simeq 10$ eV at $B_{12}=1$ and $\hbar\omega_\parallel \simeq 23$ eV at $B_{12}=10$, in contrast to the vibrational energy quanta $\hbar\omega_{\rm vib} \simeq 0.52$ eV for the H_2 molecule at zero magnetic field.

(iii) *Transverse vibrational excitations*. The molecular axis can deviate from the magnetic-field direction, precessing and vibrating around the magnetic axis. Such an oscillation is the high-field analogy of the usual molecular rotation; the difference is that in strong magnetic fields, this "rotation" is constrained around the magnetic field line. To obtain the excitation energy, we need to estimate the excess potential $\delta U(R_\perp) \equiv U(a_{\rm eq},R_\perp) - U(a_{\rm eq},0)$. When the protons are displaced by $\sim R_\perp$ from the electron distribution axis, the proton-electron interaction is approximately given by $a_{\rm eq}^{-1} \ln[L_z/(\rho_0^2 + R_\perp^2)^{1/2}]$. Thus an order-of-magnitude expression for δU is $\delta U(R_\perp) \sim (1/2a_{\rm eq}) \ln(1+\rho_0^{-2}R_\perp^2) \sim \xi^{-1} l \ln(1+b\,R_\perp^2)$. This holds for any $R_\perp \ll a_{\rm eq} = \xi\, l^{-1}$. For small-amplitude transverse oscillations, with $R_\perp \lesssim \rho_0 = b^{-1/2} \ll a_{\rm eq}$, we have $\delta U \sim \xi^{-1} l\, b\, R_\perp^2$. The energy quantum is then $\hbar\omega_{\perp 0} \sim (\xi^{-1} l\, b)^{1/2} \mu^{-1/2}$, where the subscript 0 indicates that we are at the moment neglecting the magnetic forces on the protons that, in the absence of Coulomb forces, lead to proton cyclotron motions (see below). Numerical calculations give a similar scaling relation. For the electronic ground state, the excitation energy quanta $\hbar\omega_{\perp 0}$ can be approximated by

$$\hbar\omega_{\perp 0} \simeq 0.125\, b^{1/2} (\ln b)\, \mu^{-1/2}\ \text{a.u.} \simeq 0.11\, b^{1/2} (\ln b)\ \text{eV}. \tag{4.8}$$

(This is accurate to within 10% for $40 \lesssim b \lesssim 10^4$.) Thus $\hbar\omega_{\perp 0} \simeq 14$ eV at $B_{12}=1$ and $\hbar\omega_{\perp 0} = 65$ eV at $B_{12}=10$. (See Lai and Salpeter, 1996 for a discussion of large-amplitude oscillations.)

Note that in a strong magnetic field, the electronic and (aligned and transverse) vibrational excitations are all comparable, with $\hbar\omega_{\perp 0} \gtrsim \hbar\omega_\parallel$. This is in contrast to the zero-field case, where we have $\Delta\varepsilon_{\rm elec} \gg \hbar\omega_{\rm vib} \gg \hbar\omega_{\rm rot}$.

Equation (4.8) for the zero-point energy of the transverse oscillation includes only the contribution of the electronic restoring potential $\mu\omega_{\perp 0}^2 R_\perp^2/2$. Since the magnetic forces on the protons also induce a *magnetic restoring potential* $\mu\omega_{cp}^2 R_\perp^2/2$, where $\hbar\omega_{cp} = \hbar eB/(m_p c) \simeq 6.3\, B_{12}$ eV is the cyclotron energy of the proton, the zero-point energy of the transverse oscillation is

$$\hbar\omega_\perp = \hbar(\omega_{\perp 0}^2 + \omega_{cp}^2)^{1/2} - \hbar\omega_{cp}. \tag{4.9}$$

The dissociation energy of H_2, taking into account the zero-point energies of aligned and transverse vibrations, is then

$$Q_2 = Q_2^{(\infty)} - (\tfrac{1}{2}\hbar\omega_\parallel + \hbar\omega_\perp). \tag{4.10}$$

Some numerical values are given in Table I. Variation of Q_2 as a function of B is depicted in Fig. 1.

D. H_N molecules: Saturation

At zero magnetic field, two H atoms in their ground states with spins opposite to each other form a H_2 molecule by covalent bonding; adding more H atoms is not possible by the exclusion principle (unless one excites the third atom to an excited state; but the resulting H_3 is short-lived). In a strong magnetic field, the spins of the electrons in the atoms are all aligned antiparallel to the magnetic field, and because of the low excitation energy associated with $m \to m+1$, more atoms can be added to H_2 to form larger H_N molecules.

For a given magnetic-field strength, as the number of H atoms, N, increases, the electrons occupy more and more Landau orbitals (with $m = 0,1,2,\ldots,N-1$), and the transverse size of the molecule increases as $R \sim (N/b)^{1/2} a_0$. Let a be the atomic spacing and $L_z \sim Na$ the size of the molecule in the z direction. The energy per atom in the molecule can be written as $E \sim L_z^{-2} - l\,a^{-1}$, where $l = \ln(2a/R)$. Variation of E with respect to L_z gives

$$E \sim -N^2 l^2, \quad L_z \sim Na \sim (Nl)^{-1}. \tag{4.11}$$

This scaling behavior is valid for $1 \ll N \ll N_s$. The *critical saturation number* N_s is reached when $a \sim R$, or

$$N_s \sim [b/(\ln b)^2]^{1/5} \tag{4.12}$$

(Lai *et al.*, 1992). Beyond N_s, it becomes energetically more favorable for the electrons to settle into the inner Landau orbitals (with smaller m) with nodes in their longitudinal wave functions (i.e., $\nu \neq 0$). For $N \gtrsim N_s$, the

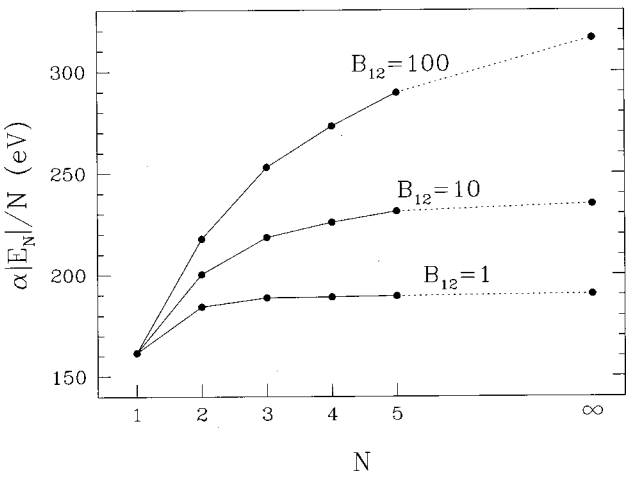

FIG. 4. Binding energy per atom, $|E_N|/N$, for H_N molecules in strong magnetic fields as a function of N. To facilitate plotting, the values of $|E_1|$ at different B_{12} are normalized to its value (161.5 eV) at $B_{12}=1$. This means $\alpha=1$ for $B_{12}=1$, $\alpha=161.5/309.6$ for $B_{12}=10$, and $\alpha=161.5/541$ for $B_{12}=100$.

energy per atom of the H_N molecule, $E=|E(H_N)|/N$, asymptotically approaches a value $\sim b^{2/5}$, and the size of the atom scales as $R\sim a\sim b^{-2/5}$, independent of N (see Sec. V.A). For the typical magnetic-field strength ($B_{12}=0.1-10^3$) of interest here, the energy saturation occurs at $N_s\sim 2-6$ (see Fig. 4).

E. Intermediate-magnetic-field regime

For intermediate magnetic-field strengths ($B\sim B_0\sim 10^9$ G), the only molecule that has been investigated in detail is the hydrogen molecular ion H_2^+; both parallel configurations (Le Guillou and Zinn-Justin, 1984; Vincke and Baye, 1985; Brigham and Wadehra, 1987; Kappes and Schmelcher, 1995; Kravchenko and Liberman, 1997; Lopez *et al.*, 1997) and nonparallel configurations (Larsen, 1982; Wille, 1987, 1988; Kappes and Schmelcher, 1996) have been studied using different variational methods. Other one-electron molecular ions such as H_3^{2+} and H_4^{3+} in strong magnetic fields have been studied by Lopez and Turbiner (2000, and references therein). For the H_2 molecule at intermediate fields, earlier studies (e.g., Turbiner, 1983; Basile *et al.*, 1987) are of qualitative character; quantitative calculations, for aligned configurations, have been attempted only recently (Detmer *et al.*, 1997, 1998; Kravchenko and Liberman, 1998; Schmelcher *et al.*, 2000).

An important issue concerns the nature of the ground electronic state of H_2 as a function of B. Starting from the strong-field regime (see Secs. IV.B and IV.C), we know that for $B_{12}\gtrsim 0.2$ ($b\gtrsim 100$), the ground state is the tightly bound state in which the electrons occupy the $(m,\nu)=(0,0)$ and (1,0) orbitals; this state corresponds to $^3\Pi_u$ in the standard spectroscopic notation. For $b\lesssim 100$ the lowest energy state becomes the weakly bound state in which the electron orbitals are (0,0) and (0,1); this corresponds to the $^3\Sigma_u$ state. Detmer *et al.* (1998) and Kravchenko and Liberman (1998) found that for $b\lesssim 0.18$, the ground state is the usual $^1\Sigma_g$; for $0.2\lesssim b\lesssim 12-14$, the ground state is $^3\Sigma_u$; for $b\gtrsim 12$, the ground state is $^3\Pi_u$. However, their $^3\Sigma_u$ state is predominantly repulsive except for a very shallow van der Waals (quadrupole-quadrupole interaction) minimum at large proton separation. The binding of the $^3\Sigma_u$ was not demonstrated in the calculations of Detmer *et al.* (1998) and Kravchenko and Liberman (1998). This is in contradiction to the $b\gg 1$ behavior of the weakly bound state found by Lai and Salpeter (1996). Obviously more work is needed to attain a clear picture of how the energies of different H_2 states behave as B increases from 0 to $b\gg 1$.

F. Molecules of heavy elements

Molecules of heavy elements (other than hydrogen) in strong magnetic fields have not been systematically investigated. There is motivation to study molecules of light elements such as He, since if the hydrogen on a neutron star surface is completely burnt out by nuclear reaction, helium will be the dominant species left in the atmosphere. There are also white dwarfs with pure He atmospheres. (Because of rapid gravitational separation of light and heavy elements in the gravitational field of a neutron star or white dwarf, the atmosphere is expected to contain pure elements.) For $b\gg 1$, the Hartree-Fock method discussed in Sec. IV.B can be generalized to the case of ion charge $Z>1$ (Lai *et al.*, 1992). Figure 5 shows the dissociation energy of the He_2 molecule as a function of B. In general, we expect that, as long as $a_0/Z\gg(2Z-1)^{1/2}\rho$, or $b\gg 2Z^3$, the electronic properties of the heavy molecule will be similar to those of H_2. When the condition $b\gg 2Z^3$ is not satisfied, the molecule should be quite different and may be unbound relative to individual atoms (e.g., Fe at $B=10^{12}$ G is unlikely to form a bound molecule). Some Hartree-Fock results on diatomic molecules (from H_2 up to C_2) at $b=1000$ are given by Demeur *et al.* (1994).

V. LINEAR CHAINS AND CONDENSED MATTER

As discussed in Sec. IV.D, in a strong magnetic field we can add more atoms to a diatomic molecule to form molecular chains. When the number of atoms exceeds the saturation number, the structure of the molecule is the same as that of an infinite chain. By placing a pile of parallel chains together, we can form three-dimensional condensed matter.

A. Basic scaling relations for linear chains

The simplest model for a linear chain is to treat it as a uniform cylinder of electrons, with ions aligned along the magnetic-field axis. After saturation, many electrons settle into the $\nu\neq 0$ states, and the electrons can be treated as a Fermi sea in the z direction. In order of magnitude, the electrons occupy states with $m=0,1,2,\ldots,N_s-1$ and $\nu=0,1,2,\ldots,N/N_s$. For $N\gg N_s$

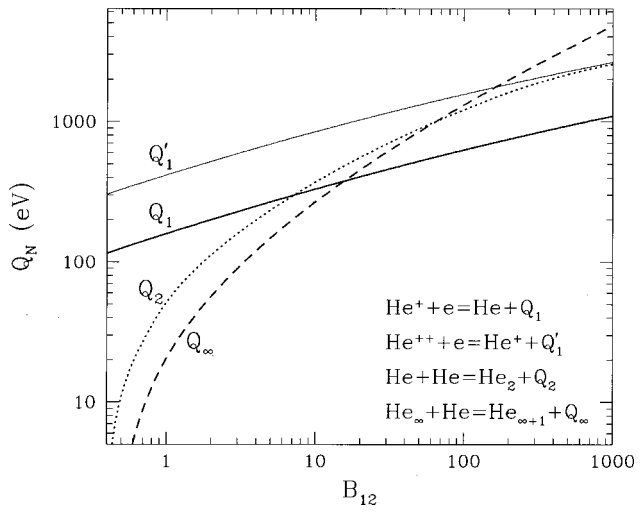

FIG. 5. Energy releases from several atomic and molecular processes as a function of the magnetic-field strength: solid line, ionization energy Q_1 of the He atom; dotted line, dissociation energy Q_2 of He_2; dashed line, cohesive energy Q_∞ of linear chain He_∞. The zero-point energy corrections are not included.

$\gg 1$, the uniform-cylinder approximation becomes increasingly valid because in the transverse direction the area covered by the m Landau orbitals scales as $(\sqrt{2m+1})^2 \propto m$; hence the volume increases with the number of interior electrons, giving a constant electron density. Let R be the radius of the cylinder and a be the atomic spacing a along the z axis. The energy per atom (unit cell) in the chain can be written as (Ruderman 1971, 1974; Chen, 1973)

$$E_\infty = \frac{2\pi^2 Z^3}{3b^2 R^4 a^2} - \frac{Z^2}{a}\left[\ln\frac{2a}{R} - \left(\gamma - \frac{5}{8}\right)\right], \tag{5.1}$$

where $\gamma = 0.5772\ldots$ is Euler's constant, and we have restored the dependence on the ion charge Z. In Eq. (5.1), the first term is the electron kinetic energy [see Eq. (A4)] and the second term is the (direct) Coulomb energy (the Madelung energy for the one-dimensional uniform lattice). Minimizing E_∞ with respect to R and a gives

$$\begin{aligned} &R = 1.65\, Z^{1/5} b^{-2/5} \text{ a.u.}, \quad a/R = 2.14, \\ &E_\infty = -0.354\, Z^{9/5} b^{2/5} \text{ a.u.} \end{aligned} \tag{5.2}$$

Not surprisingly, these scaling relations are the same as those for heavy atoms [see Eq. (3.20)].

B. Calculations of linear chains

While the uniform-cylinder model discussed above gives useful scaling relations for the structure and energy of a linear chain, it is not sufficiently accurate to determine the relative binding energy between the chain and the atom at $B_{12} \sim 0.1$–100. (The uniform-cylinder model becomes accurate only when $N_s \sim b^{1/5} \gg 1$.) More refined calculations are needed to obtain accurate energies for field strengths characteristic of neutron star surfaces. Glasser and Kaplan (1975) generalized the uniform-cylinder model by considering quantized electron charge distribution in the transverse direction. However, they assumed a uniform electron population in different Landau orbitals. The effect they treated amounts to only a small change in the value of the constant in the Madelung energy expression, and therefore it is still insufficient to account for the binding of linear chains. The next step in a more relaxed variational calculation is to treat the effect of the Coulomb potential on the population of electrons in different m orbitals (Flowers *et al.*, 1977; note that the calculation reported in this paper contained numerical errors and was corrected by Müller, 1984). This is clearly an important ingredient for calculating the binding energy of the chain, since it allows for more electrons in the inner orbitals (small m's), which increases the binding. A further improvement includes the nonuniform electron-density distribution in the z direction along the magnetic field (Neuhauser, Koonin, and Langanke, 1987). This effect is important for treating the bound electrons (i.e., the "electron core" in Flowers *et al.*, 1977) correctly for chains of heavy atoms like Fe.

The self-consistent Hartree-Fock method for linear chains is similar to that used for calculating multielectron atoms (see Sec. III.C.2; Neuhauser *et al.*, 1987). Consider a chain of length Na (where a is the ion spacing). The electron basis functions can be written as

$$\Phi_{m\nu k}(\mathbf{r}) = W_m(\mathbf{r}_\perp)\frac{1}{\sqrt{N}} f_{m\nu}(z)\exp(ikz), \tag{5.3}$$

where k is the Bloch wave number and $f_{m\nu}(z) = f_{m\nu}(z + a)$, normalized via $\int_{-a/2}^{a/2} |f_{m\nu}(z)|^2 dz = 1$. In each $(m\nu)$ band, the electrons occupy the k space up to $k_{m\nu}^F = \sigma_{m\nu}(\pi/a)$. Here $\sigma_{m\nu}$ is the number of electrons in the $(m\nu)$ orbital per unit cell in the chain, and satisfies the constraint

$$\sum_{m\nu} \sigma_{m\nu} = Z. \tag{5.4}$$

For each set of $\sigma_{m\nu}$, a coupled set of Hartree-Fock equations for $f_{m\nu}(z)$ can be derived and the energy of the system determined. One then varies $\sigma_{m\nu}$ and repeats the calculation until the energy minimum is attained.

For linear chains consisting of light atoms such as H and He (or in general, for sufficiently strong magnetic fields satisfying $b \gg 2Z^3$), the electron-density variation along the z axis is not significant, since all the electrons in the chain are "ionized" and are well approximated by plane waves. Thus a variational calculation that assumes uniform density in the z direction is adequate. This calculation is simpler than the full Hartree-Fock calculation, since the energy functional can be expressed in semianalytic form (Lai *et al.*, 1992). The basis electron wave functions are given by Eq. (5.3) with $f_{m\nu} = a^{-1/2}$. Electrons fill the mth orbital (band) up to a Fermi wave number given by $k_m^F = \sigma_m(\pi/a)$, where σ_m is the num-

ber of electrons in the mth orbital per cell, with $m=0,1,2,\ldots,m_0-1$. The energy per cell in a chain can be written as

$$E=\frac{\hbar^2}{2m_e}\sum_m \sigma_m\frac{1}{3}\left(\sigma_m\frac{\pi}{a}\right)^2+\frac{Z^2e^2}{a}\left[-\ln\left(\frac{2a}{\rho_0}\right)+\gamma\right.$$
$$\left.+\frac{1}{Z}\sum_m \sigma_m\psi(m+1)-\frac{1}{2Z^2}\sum_{mm'}\sigma_m\sigma_{m'}Y_{mm'}\right]$$
$$-\frac{e^2}{2a}\sum_{mm'}\sigma_m\sigma_{m'}\int_{-\infty}^{\infty}dz\,\frac{\sin(\sigma_m\pi z\rho_0/a)}{\sigma_m\pi z\rho_0/a}$$
$$\times\frac{\sin(\sigma_{m'}\pi z\rho_0/a)}{\sigma_{m'}\pi z\rho_0/a}E_{mm'}(z), \tag{5.5}$$

where the three terms represent the kinetic energy, the direct Colulomb energy, and the exchange energy. The digamma function ψ satisfies $\psi(m+1)=\psi(m)+(1/m)$, with $\psi(1)=-\gamma=-0.5772\ldots$; the coefficient $Y_{mm'}$ depends on m,m'; the function $E_{mm'}(z)$ is the same as defined in Eq. (3.29). For a given lattice spacing a, the occupation numbers σ_m $(m=0,1,2,\ldots,m_0-1)$ are varied to minimize the total energy E under the constraint of Eq. (5.4) (with ν suppressed). One can increase m_0 until further increase in m_0 results in no change in the distribution, i.e., $\sigma_{m_0-1}=0$. The constrained variation $\delta E-\varepsilon_F\delta\Sigma_{m=0}^{m_0-1}\sigma_m=0$ yields

$$\varepsilon_F=\frac{\hbar^2}{2m_e}\left(\frac{\pi\sigma_m}{a}\right)^2+\frac{Z^2e^2}{a}$$
$$\times\left[\frac{1}{Z}\psi(m+1)-\frac{1}{Z^2}\sum_{m'}\sigma_{m'}Y_{mm'}\right]$$
$$-\frac{e^2}{a}\sum_{m'}\int_{-\infty}^{\infty}dz\cos(\sigma_m\pi z\rho_0/a)$$
$$\times\frac{\sin(\sigma_{m'}\pi z\rho_0/a)}{\sigma_{m'}\pi z\rho_0/a}E_{mm'}(z). \tag{5.6}$$

Here ε_F is a constant Lagrange multiplier (Fermi energy) that must be determined self-consistently. The system (5.6) consists of m_0 equations for the m_0 unknown parameters σ_m plus the constant ε_F. They are solved together with Eq. (5.4) for these unknown quantities.

Density-functional theory has also been used to calculate the structure of linear chains in strong magnetic fields (Jones, 1985; Relovsky and Ruder, 1996). The problem with this approach is that the density-functional approximation has not been calibrated in strong magnetic fields, and therefore the accuracy of the approximation is not yet known. (For review of density-functional theory as applied to nonmagnetic terrestrial solids, see, for example, Callaway and March, 1984; Dreizler and Gross, 1990.) More accurate implementation of the density-functional theory in strong magnetic fields requires that the current–magnetic-field interaction be taken into account (Vignale and Rasolt, 1987, 1988) and that a better exchange-correlation functional be used.

C. Cohesive energy of linear chains

Selected numerical results of the linear chains for a number of elements (up to $Z=26$) have been obtained by Neuhauser *et al.* (1987) based on the Hartree-Fock method and by Jones (1985) based on density-functional theory, for a limited range of B's around 10^{12} G. The numerical results for the energy (per atom) of the hydrogen chain (Lai *et al.*, 1992) can be approximated (to within 2% accuracy for $1\lesssim B_{12}\lesssim 10^3$) by

$$E_\infty(\mathrm{H})=-0.76\,b^{0.37}\ \text{a.u.}=-194\,B_{12}^{0.37}\ \text{eV}. \tag{5.7}$$

This expression for E_∞ is a factor of 1.8 times that given in Eq. (5.2). The cohesive energy of the H chain (energy release in $\mathrm{H}+\mathrm{H}_\infty=\mathrm{H}_{\infty+1}$) is given (to $\lesssim 10\%$ accuracy) by

$$Q_\infty^{(\infty)}(\mathrm{H})=|E_\infty(\mathrm{H})|-|E(\mathrm{H})|$$
$$\simeq 0.76\,b^{0.37}-0.16\,(\ln b)^2\ \text{a.u.}, \tag{5.8}$$

where the superscript (∞) indicates that the proton has been treated as having infinite mass (see Sec. V.E). Figure 1 shows the cohesive energy of the H chain as a function of B, and Table I gives some numerical values. Figure 5 shows a similar result for a He chain. For these light elements, electron-density variation along the z axis can be safely ignored.

Numerical calculations carried out so far have indicated that for $B_{12}=1-10$, linear chains are unbound for large atomic numbers $Z\gtrsim 6$ (Jones, 1986; Neuhauser *et al.*, 1987). In particular, the Fe chain is unbound relative to the Fe atom; this is contrary to what some early calculations (e.g., Flowers *et al.*, 1977) indicated. Therefore the chain-chain interaction must play a crucial role in determining whether three-dimensional zero-pressure Fe condensed matter is bound or not (see Sec. V.E). The main difference between Fe and H is that for the Fe atom at $B_{12}\sim 1$, many electrons are populated in the $\nu\neq 1$ states, whereas for the H atom, as long as $b\gg 1$, the electron always settles down in the $\nu=0$ tightly bound state. Therefore the covalent bonding mechanism for forming molecules (see Sec. IV.A) is not effective for Fe at $B_{12}\sim 1$. However, for a sufficiently large B, when $a_0/Z\gg\sqrt{2Z+1}\rho_0$ or $B_{12}\gg 100(Z/26)^3$, we expect the Fe chain to be bound in a manner similar to the H chain or He chain.

D. 3D condensed matter: Uniform-electron-gas model and its extension

A linear chain naturally attracts neighboring chains through the quadrupole-quadrupole interaction. By placing parallel chains close together (with spacing of order $b^{-2/5}$), we obtain three-dimensional condensed matter (e.g., a body-centered tetragonal lattice; Ruderman, 1971).

The binding energy of magnetized condensed matter at zero pressure can be estimated using the uniform-electron-gas model (Kadomtsev, 1970). Consider a Wigner-Seitz cell with radius $r_i=Z^{1/3}r_s$, where r_s is the

mean electron spacing; the mean number density of electrons is $n_e = Z/(4\pi r_i^3/3)$. The electron Fermi momentum p_F is obtained from $n_e = (eB/hc)(2p_F/h)$. When the Fermi energy $p_F^2/(2m_e)$ is less than the cyclotron energy $\hbar\omega_{ce}$, or when the electron number density satisfies

$$n_e \leqslant n_B = \frac{1}{\sqrt{2}\pi^2\rho_0^3} = 0.0716\, b^{3/2} a_0^{-3} \tag{5.9}$$

(or $r_i \geqslant r_{iB} = 1.49\, Z^{1/3} b^{-1/2} a_0$), the electrons occupy only the ground Landau level. The energy per cell can be written as

$$E_s(r_i) = \frac{3\pi^2 Z^3}{8 b^2 r_i^6} - \frac{0.9 Z^2}{r_i}, \tag{5.10}$$

where the first term is the kinetic energy and the second term is the Coulomb energy. For zero-pressure condensed matter, we require $dE_s/dr_i = 0$, and the equilibrium r_i and energy are then given by

$$r_{i,0} \simeq 1.90\, Z^{1/5} b^{-2/5} a_0, \tag{5.11}$$

$$E_{s,0} \simeq -0.395\, Z^{9/5} b^{2/5} \text{ a.u.} \tag{5.12}$$

The corresponding zero-pressure condensation density is

$$\rho_{s,0} \simeq 561\, A\, Z^{-3/5} B_{12}^{6/5} \text{ g cm}^{-3}. \tag{5.13}$$

Note that, for $b \gg 1$, the zero-pressure density is much smaller than the magnetic density defined in Eq. (5.9), i.e., $\rho_{s,0}/\rho_B = (r_B/r_{i,0})^3 = 0.48\, Z^{2/5} b^{-3/10}$.

We now discuss several corrections to the uniform-electron-gas model.

(i) *Coulomb exchange interaction*. The exclusion principle for the electrons results in an exchange correction to the Coulomb energy. The Hartree-Fock exchange energy per Wigner-Seitz cell is given by

$$E_{ex} = -\frac{3Z}{4\, b\, r_s^3} F \text{ a.u.}, \tag{5.14}$$

where F is a function of the ratio $y \equiv n_e/n_B$ (see Appendix A)

$$F = 3 - \gamma - 2\ln(2y) - \tfrac{2}{3}[2\ln(2y) + \gamma - \tfrac{13}{6}]y^2 + \cdots \tag{5.15}$$

($\gamma = 0.577\,215\,7\ldots$ is Euler's constant). The effect of this (negative) exchange interaction is to increase $r_{i,0}$ and $|E_{s,0}|$.

(ii) *Relativistic effect*. As noted in Sec. II, the use of nonrelativistic quantum mechanics for the bound states is a good approximation even for $B \gtrsim B_{\rm rel} \simeq 137^2 B_0$. We can show that the density-induced relativistic effect is also small. The magnetic density n_B for onset of the Landau excitation is still given by Eq. (5.9). The relativistic parameter for the electron is $x_e \equiv p_F/(m_e c) = (n_e/n_B)(2B/B_{\rm rel})^{1/2}$. At the zero-pressure density as given by Eq. (5.13), we have $x_e \simeq 5\times 10^{-3} Z^{2/5} b^{1/5}$. Thus, near the zero-pressure density, the relativistic effect is negligible for the range of magnetic-field strengths of interest.

(iii) *Nonuniformity of the electron gas*. The Thomas-Fermi screening wave number $k_{\rm TF}$ is given by (Ashcroft and Mermin, 1976) $k_{\rm TF}^2 = 4\pi e^2 D(\varepsilon_F)$, where $D(\varepsilon_F) = \partial n_e/\partial \varepsilon_F$ is the density of states per unit volume at the Fermi surface $\varepsilon = \varepsilon_F = p_F^2/(2m_e)$. Since $n_e = (2eB/h^2c)p_F$, we have $D(\varepsilon_F) = n_e/2\varepsilon_F = (m_e/n_e)(2eB/h^2c)^2$, and

$$k_{\rm TF} = \left(\frac{4}{3\pi^2}\right)^{1/2} b\, r_s^{3/2} \text{ a.u.} \tag{5.16}$$

(More details on electron screening in strong magnetic fields, including anisotropic effects, can be found in Horing, 1969.) The gas is uniform when the screening length $k_{\rm TF}^{-1}$ is much longer than the particle spacing r_i, i.e., $k_{\rm TF} r_i \ll 1$. For a zero-pressure condensate with density parameter given by Eq. (5.11), we have $k_{\rm TF} r_i \simeq 1.83$, independent of B. Thus, even for $B \to \infty$, the nonuniformity of electron distribution must be considered for zero-pressure condensed matter. To leading order in $r_i \ll 1$, the energy correction (per cell) due to nonuniformity can be calculated using linear-response theory, which gives

$$E_{\rm TF} = -\frac{18}{175}(k_{\rm TF} r_i)^2 \frac{(Ze)^2}{r_i} \tag{5.17}$$

(see, for example, Lattimer *et al.*, 1985; Fushiki *et al.*, 1989). Using Eq. (5.16), we have

$$E_{\rm TF} = -0.0139\, Z\, b^2 r_i^4 \text{ a.u.} \tag{5.18}$$

Note that this expression is valid only for $k_{\rm TF} r_i \ll 1$. At lower densities, the nonuniformity effect can be studied only through detailed electronic (band) structure calculations. An approximate treatment relies on Thomas-Fermi-type statistical models, including the exchange-correlation and the Weizsäcker gradient corrections (see Appendix B).

E. Cohesive energy of 3D condensed matter

Although the simple uniform-electron-gas model and its Thomas-Fermi-type extensions give a reasonable estimate of the binding energy for the condensed state, they are not adequate for determining the *cohesive energy* of condensed matter. The cohesive energy Q_s is the difference between the atomic ground-state energy and the energy per atom of the condensed-matter ground state. One uncertainty concerns the lattice structure of the condensed state, since the Madelung energy can be very different from the Wigner-Seitz value [the second term in Eq. (5.10)] for a noncubic lattice. In principle, a three-dimensional electronic band-structure calculation is needed to solve this problem, as Jones (1986) has attempted for a few elements using density-functional theory. Jones adopted a local approximation in one angular variable in solving the electron eigenfunctions of the lattice Kohn-Sham potential; the validity of this approximation is not easy to justify (see discussion at the end of Sec. V.B).

The energy difference $\Delta E_s = |E_{s,0}| - |E_\infty|$ between 3D condensed matter and a 1D chain must be positive and can be estimated by calculating the interaction (mainly quadrupole-quadrupole) between the chains. Various considerations indicate that the difference is between 0.4% and 1% of $|E_\infty|$ (Lai and Salpeter, 1997). Therefore, for light elements such as hydrogen and helium, the binding of 3D condensed matter results mainly from the covalent bond along the magnetic-field axis, not from the chain-chain interaction. For convenience we shall write the cohesive energy Q_s of a 3D hydrogen condensate in terms of the cohesive energy (Q_∞) of the linear chain as

$$Q_s(\mathrm{H}) = Q_\infty(\mathrm{H}) + \Delta E_s = (1+\zeta) Q_\infty(\mathrm{H}), \tag{5.19}$$

with $\zeta \simeq 0.01-0.02$ for $B_{12} = 1-500$.

For hydrogen, the zero-point energy of the proton is not entirely negligible and can introduce a correction to the cohesive energy. The zero-point energy has not been rigorously calculated, but a reasonable estimate is as follows. Neglecting the magnetic force, the zero-point energy E_{zp} of a proton in the lattice is of order $\hbar\Omega_p$, where $\Omega_p = (4\pi e^2 n_e/m_p)^{1/2}$ is the proton plasma frequency. Using the mean electron density $n_e \simeq 0.035\, b^{6/5}$ as estimated from Eqs. (5.2) or (5.11), we find

$$E_{zp} \sim \hbar\Omega_p \simeq 0.015\, b^{3/5} \text{ a.u.} \tag{5.20}$$

This is much smaller than the total binding energy $|E_\infty|$ unless $B_{12} \gtrsim 10^5$. This means that, for the range of field strengths of interest, the zero-point oscillation amplitude is small compared to the lattice spacing. Thus quantum melting is not effective (see, for example, Ceperley and Alder, 1980; Jones and Ceperley, 1996), and the condensed matter is a solid at zero temperature. Accurate determination of E_{zp} requires a detailed understanding of the lattice phonon spectra. At zero field, Monte Carlo simulations give $E_{zp} \simeq 3\hbar\Omega_p\eta/2$, with $\eta \simeq 0.5$ (Hansen and Pollock, 1973). For definiteness, we shall adopt the same value for E_{zp} in a strong magnetic field. Taking into account the magnetic effect on the proton, the corrected cohesive energy of the H chain is expected to be

$$Q_\infty = Q_\infty^{(\infty)} - \tfrac{1}{2}[\hbar\Omega_p\eta + \hbar(\omega_{cp}^2 + 4\eta^2\Omega_p^2)^{1/2} - \hbar\omega_{cp}], \tag{5.21}$$

with $\eta \simeq 0.5$, where $\hbar\omega_{cp} = \hbar eB/(m_p c)$ is the cyclotron energy of the proton.

Figure 1 depicts the cohesive energy of H_∞ as a function of B; the energy releases Q_1 and Q_2 for $e+p=\mathrm{H}$ and $\mathrm{H}+\mathrm{H}=\mathrm{H}_2$ are also shown. Some numerical values are given in Table I. The zero-point energy corrections for Q_2 and Q_∞ have been included in the figure (if they are neglected, the curves are qualitatively similar, although the exact values of the energies are somewhat changed). Although $b \gg 1$ satisfies the nominal requirement for the strong-field regime, a more realistic expansion parameter for the stability of a condensed state over atoms and molecules is the ratio $b^{0.4}/(\ln b)^2$. This ratio exceeds 0.3 and increases rapidly with increasing field strength only for $b \gtrsim 10^4$. We see from Fig. 1 that $Q_1 > Q_2 > Q_\infty$ for $B_{12} \lesssim 10$, and $Q_1 > Q_\infty > Q_2$ for $10 \lesssim B_{12} \lesssim 100$, while $Q_\infty > Q_1 > Q_2$ for $B_{12} \gtrsim 100$. These inequalities have important consequences for the composition of the saturated vapor above the condensed phase for different magnetic fields (see Sec. VII.B). Figure 5 shows similar numerical results for He.

The cohesive properties of the condensed state of heavy elements such as Fe are different from those of hydrogen or helium. As discussed in Sec. V.C, a linear Fe chain is not bound relative to the Fe atom at $B_{12} = 1-10$ (although we expect the Fe chain to be bound for $B_{12} \gg 100$). Since chain-chain interactions only lower E_s relative to E_∞ by about 1% (see above), it is likely that the 3D condensed state is also unbound. Jones (1996) found a very small cohesive energy for 3D condensed iron, corresponding to about 0.5% of the atomic binding energy. In view of the uncertainties associated with the calculations, Jones's results should be considered as an upper limit, i.e.,

$$Q_s \lesssim 0.005\,|E_{\mathrm{atom}}| \sim Z^{9/5} B_{12}^{2/5} \text{ eV (for } Z \gtrsim 10), \tag{5.22}$$

where we have used Eq. (3.34) for $|E_{\mathrm{atom}}|$.

F. Shape and surface energy of condensed droplets

As we shall discuss in Sec. VII, for sufficiently strong magnetic fields and low temperatures, the condensed phase of hydrogen can be in pressure equilibrium with the vapor phase. The two phases have markedly different densities and one might have an "ocean/atmosphere interface." The question of droplets might have to be considered, and the shape and energy of a droplet is of interest (Lai and Salpeter, 1997).

For the phase equilibrium between a condensed state and the H_N molecules in a vapor, the most relevant quantity is the *surface energy* S_N, defined as the energy released in converting the 3D condensate $\mathrm{H}_{s,\infty}$ and a H_N molecule into $\mathrm{H}_{s,\infty+N}$. Clearly $S_1 = Q_s = (1+\zeta)Q_\infty$ is the cohesive energy defined in Sec. V.E. For a linear H_N molecule with energy (per atom) $E_N = E(\mathrm{H}_N)$, we have

$$S_N = N(E_N - E_s) = N\Delta E_s + N(E_N - E_\infty) = N\zeta Q_\infty + \xi Q_\infty, \tag{5.23}$$

where the first term on the right-hand side comes from cohesive binding between chains, and the second term is the *end energy* of the one-dimensional chain. Based on numerical results for H_2, H_3, H_4, and H_5 (see Fig. 4), we infer that the dimensionless factor ξ in Eq. (5.23) is of order unity. For $N \lesssim \xi/\zeta \sim 100$, the end energy dominates, while for $N \gtrsim 100$ the cohesion between chains becomes important. In the latter case, the configuration that minimizes the surface energy S_N is not the linear chain, but some highly elongated "cylindrical droplet" with $N_\perp$ parallel chains each containing $N_\parallel = N/N_\perp$ atoms. For such a droplet, the end energy is of order $N_\perp \xi Q_\infty$. On the other hand, there are $\sim N_\perp^{1/2}$ unpaired chains in such a droplet, each giving an energy $N_\parallel \zeta Q_\infty$. Thus the total surface energy is of order $[N_\perp \xi + \zeta(N/N_\perp)N_\perp^{1/2}]Q_\infty$. The minimum surface energy S_N of the droplet, for a fixed $N \gtrsim 2\xi/\zeta \equiv N_c$, is then obtained for $N_\perp \simeq (N/N_c)^{2/3}$, $N_\parallel \simeq N^{1/3} N_c^{2/3}$, and is of order

$$S_N \simeq 3\,\xi\left(\frac{N}{N_c}\right)^{2/3} Q_\infty \quad \text{for } N \gtrsim N_c \equiv \frac{2\xi}{\zeta} \sim 200. \tag{5.24}$$

Thus, although the optimal droplets are highly elongated, the surface energy still grows as $(N/200)^{2/3}$ for $N \gtrsim 200$.

VI. FREE-ELECTRON GAS IN STRONG MAGNETIC FIELDS

In Secs. III–V, we reviewed the electronic structure and binding energies of atoms, molecules, and condensed matter in strong magnetic fields. As discussed in Sec. I.A, one of the main motivations for studing matter in strong magnetic fields is to understand the neutron star surface layer, which directly mediates the thermal radiation from the star and acts as a boundary for the magnetosphere. Before discussing various properties of the neutron star envelope in Sec. VII, it is useful to summarize the basic thermodynamic properties of a free-electron gas in strong magnetic fields at finite temperature T.

The number density n_e of electrons is related to the chemical potential μ_e by

$$n_e = \frac{1}{(2\pi\rho_0)^2\hbar} \sum_{n_L=0}^{\infty} g_{n_L} \int_{-\infty}^{\infty} f\, dp_z, \tag{6.1}$$

where g_{n_L} is the spin degeneracy of the Landau level ($g_0=1$ and $g_{n_L}=2$ for $n_L \geq 1$) and f is the Fermi-Dirac distribution

$$f = \left[1+\exp\left(\frac{E-\mu_e}{kT}\right)\right]^{-1}, \tag{6.2}$$

with E given by Eq. (2.12). The electron pressure is given by

$$P_e = \frac{1}{(2\pi\rho_0)^2\hbar} \sum_{n_L=0}^{\infty} g_{n_L} \int_{-\infty}^{\infty} f \frac{p_z^2 c^2}{E}\, dp_z. \tag{6.3}$$

Note that the pressure is isotropic, contrary to what is stated by Canuto and Ventura (1977) and some earlier papers.[3] The grand thermodynamic potential is $\Omega = -P_e V$, from which all other thermodynamic quantities can be obtained. Note that for nonrelativistic electrons (valid for $E_F \ll m_e c^2$ and $kT \ll m_e c^2$), we use Eq. (2.10) for E, and the expressions for the density n_e and pressure P_e can be simplified to

$$n_e = \frac{1}{2\pi^{3/2}\rho_0^2 \lambda_{Te}} \sum_{n_L=0}^{\infty} g_{n_L} I_{-1/2}\left(\frac{\mu_e - n_L\hbar\omega_{ce}}{kT}\right), \tag{6.4}$$

$$P_e = \frac{kT}{\pi^{3/2}\rho_0^2 \lambda_{Te}} \sum_{n_L=0}^{\infty} g_{n_L} I_{1/2}\left(\frac{\mu_e - n_L\hbar\omega_{ce}}{kT}\right), \tag{6.5}$$

where $\lambda_{Te} \equiv (2\pi\hbar^2/m_e kT)^{1/2}$ is the thermal wavelength of the electron and I_η is the Fermi integral:

$$I_\eta(y) = \int_0^\infty \frac{x^\eta}{\exp(x-y)+1}\, dx. \tag{6.6}$$

Let us first consider the degenerate electron gas at zero temperature. The Fermi energy (excluding the electron rest mass) $E_F = \mu_e(T=0) - m_e c^2 = (m_e c^2)\epsilon_F$ is determined from

$$n_e = \frac{\beta}{2\pi^2 \lambda\!\!\!^{-3}_e} \sum_{n_L=0}^{n_{\max}} g_{n_L} x_F(n_L), \tag{6.7}$$

with

$$x_F(n_L) = \frac{p_F(n_L)}{m_e c} = [(1+\epsilon_F)^2 - (1+2n_L\beta)]^{1/2}, \tag{6.8}$$

where $\lambda\!\!\!^{-}_e = \hbar/(m_e c)$ is the electron Compton wavelength, $\beta = B/B_{\rm rel} = \alpha^2 b$, and $n_{\max}$ is set by the condition $(1+\epsilon_F)^2 \geq (1+2n_{\max}\beta)$. The electron pressure is given by

$$P_e = \frac{\beta m_e c^2}{2\pi^2 \lambda\!\!\!^{-3}_e} \sum_{n_L=0}^{n_{\max}} g_{n_L}(1+2n_L\beta)\,\Theta\left[\frac{x_F(n_L)}{(1+2n_L\beta)^{1/2}}\right], \tag{6.9}$$

where

$$\Theta(y) = \tfrac{1}{2}\, y\sqrt{1+y^2} - \tfrac{1}{2}\ln(y+\sqrt{1+y^2}) \to \tfrac{1}{3}\, y^3 \quad \text{for } y \ll 1. \tag{6.10}$$

The critical magnetic density below which only the ground Landau level is populated ($n_{\max}=0$) is determined by $(1+\epsilon_F)^2 = 1+2\beta$, which gives [see Eq. (5.9)]

$$\rho_B = 0.809\, Y_e^{-1} b^{3/2}\,\mathrm{g\,cm^{-3}} = 7.09\times 10^3\, Y_e^{-1} B_{12}^{3/2}\,\mathrm{g\,cm^{-3}}, \tag{6.11}$$

where $Y_e = Z/A$ is the number of electrons per baryon. Similarly, the critical density below which only the $n_L = 0,1$ levels are occupied ($n_{\max}=1$) is

$$\rho_{B1} = (2+\sqrt{2})\rho_B = 3.414\,\rho_B. \tag{6.12}$$

For $\rho < \rho_B$, Eq. (6.7) simplifies to

$$\rho = 3.32\times 10^4\, Y_e^{-1} B_{12}[(1+\epsilon_F)^2 - 1]^{1/2}\,\mathrm{g\,cm^{-3}}. \tag{6.13}$$

For nonrelativistic electrons ($\epsilon_F \ll 1$), the Fermi temperature $T_F = E_F/k = (m_e c^2/k)\epsilon_F$ is given by

$$T_F = \frac{E_F}{k} = 2.67\, B_{12}^{-2}(Y_e\rho)^2 \ \mathrm{K} \quad (\text{for } \rho < \rho_B), \tag{6.14}$$

where ρ is in units of $1\ \mathrm{g\,cm^{-3}}$. For $\rho \gg \rho_B$, many Landau levels are filled by the electrons, and Eqs. (6.1) and (6.3)

[3] The transverse kinetic pressure $P_{e\perp}$ is given by an expression similar to Eq. (6.3), except that $p_z^2 c^2$ is replaced by $\langle p_\perp^2 c^2\rangle = n_L\beta(m_e c^2)^2$. Thus the kinetic pressure is anisotropic, with $P_{e\parallel} = P_e = P_{e\perp} + \mathcal{M}B$, where $\mathcal{M}$ is the magnetization. When we compress the electron gas perpendicular to $\mathbf{B}$ we must also do work against the Lorentz force density $(\nabla\times\boldsymbol{\mathcal{M}})\times\mathbf{B}$ involving the magnetization curent. Thus there is a magnetic contribution to the perpendicular pressure of magnitude $\mathcal{M}B$. The composite pressure tensor is therefore isotropic, in agreement with the thermodynamic result $P_e = -\Omega/V$ (Blandford and Hernquist, 1982). For a nonuniform magnetic field, the net force (per unit volume) on the stellar matter is $-\nabla P_e - \nabla(B^2/8\pi) + (\mathbf{B}\cdot\nabla)\mathbf{B}/(4\pi)$.

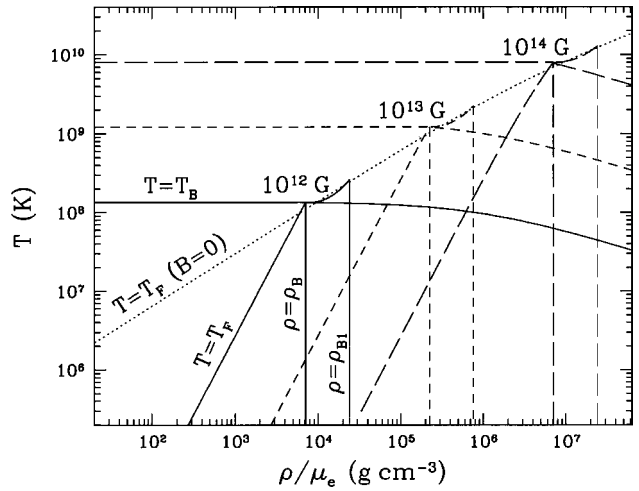

FIG. 6. Temperature-density diagram illustrating the different regimes of magnetic-field effects on the thermodynamic properties of a free-electron gas: solid lines, $B=10^{12}$ G: short-dashed lines, $B=10^{13}$ G; long-dashed lines, for $B=10^{14}$ G. For each value of B, the vertical lines correspond to $\rho=\rho_B$ (the density below which only the ground Landau level is occupied by the degenerate electrons) and $\rho=\rho_{B1}$ (the density below which only the $n_L=0,1$ levels are occupied); the Fermi temperature is shown for $\rho\leqslant\rho_B$ and for $\rho_B<\rho\leqslant\rho_{B1}$; the line marked $T=T_B$ [see Eq. (6.17)] corresponds to the temperature above which Landau-level effects are smeared out. The dotted line gives the Fermi temperature at $B=0$. The magnetic field is strongly quantizing when $\rho\leqslant\rho_B$ and $T\leqslant T_B$, weakly quantizing when $\rho\gtrsim\rho_B$ and $T\leqslant T_B$, and nonquantizing when $T\gg T_B$. See Sec. VI for details.

reduce to the zero-field expressions. In this limit, the Fermi momentum p_F is given by

$$x_F=\frac{p_F}{m_e c}=\frac{\hbar}{m_e c}(3\pi^2 n_e)^{1/3}=1.006\times10^{-2}(Y_e\rho)^{1/3}, \quad (B=0) \tag{6.15}$$

and the Fermi temperature is

$$T_F=\frac{m_e c^2}{k}(\sqrt{1+x_F^2}-1)\simeq 3.0\times10^5(Y_e\rho)^{2/3}\ \text{K}, \quad (B=0) \tag{6.16}$$

where the second equality applies to nonrelativistic electrons ($x_F\ll1$). Comparison of Eqs. (6.14) and (6.16) clearly shows that the magnetic field lifts the degeneracy of electrons even at relatively high density (see Fig. 6).

Finite temperature tends to smear out Landau levels. Let the energy difference between the $n_L=n_{\max}$ level and the $n_L=n_{\max}+1$ level be ΔE_B. We can define a *magnetic temperature*

$$T_B=\frac{\Delta E_B}{k}=\frac{m_e c^2}{k}(\sqrt{1+2n_{\max}\beta+2\beta}-\sqrt{1+2n_{\max}\beta}). \tag{6.17}$$

Clearly, $T_F=T_B$ at $\rho=\rho_B$ (see Fig. 6). The effects due to Landau quantization are diminished when $T\gtrsim T_B$. For $\rho\leqslant\rho_B$, we have $T_B=(\sqrt{1+2\beta}-1)(m_e c^2/k)$, which reduces to $T_B\simeq\hbar\omega_{ce}/k$ for $\beta=\alpha^2 b\ll1$. For $\rho\gg\rho_B$ (or $n_{\max}\gg1$), Eq. (6.17) becomes

$$T_B\simeq\frac{\hbar\omega_{ce}}{k}\left(\frac{m_e}{m_e^*}\right)=1.34\times10^8\,B_{12}(1+x_F^2)^{-1/2}\ \text{K}, \tag{6.18}$$

where $m_e^*=\sqrt{m_e^2+(p_F/c)^2}=m_e\sqrt{1+x_F^2}$, with x_F given by Eq. (6.15).

There are three regimes characterizing the effects of Landau quantization on the thermodynamic properties of the electron gas (Fig. 6; see also Yakovlev and Kaminker, 1994).

(i) $\rho\lesssim\rho_B$ and $T\lesssim T_B$: In this regime, the electrons populate mostly the ground Landau level, and the magnetic field modifies essentially all the properties of the gas. The field is sometimes termed "strongly quantizing." For example, for degenerate, nonrelativistic electrons ($\rho<\rho_B$ and $T\ll T_F\ll m_e c^2/k$), the internal energy density and pressure are

$$u_e=\tfrac{1}{3}n_e E_F, \tag{6.19}$$

$$P_e=2u_e=\tfrac{2}{3}n_e E_F\propto B^{-2}\rho^3. \tag{6.20}$$

These should be compared with the $B=0$ expression $P_e=2u_e/3\propto\rho^{5/3}$. Note that for nondegenerate electrons ($T\gg T_F$), the classical ideal gas equation of state,

$$P_e=n_e kT, \tag{6.21}$$

still holds in this "strongly quantizing" regime, although other thermodynamic quantities are significantly modified by the magnetic field.

(ii) $\rho\gtrsim\rho_B$ and $T\lesssim T_B$: In this regime, the electrons are degenerate (note that $T_F>T_B$ when $\rho>\rho_B$; see Fig. 6) and populate many Landau levels, but the level spacing exceeds kT. The magnetic field is termed "weakly quantizing." The bulk properties of the gas (e.g., pressure and chemical potential), which are determined by all the electrons in the Fermi sea, are only slightly affected by such magnetic fields. However, the quantities determined by thermal electrons near the Fermi surface show large oscillatory features as a function of density or magnetic-field strength. These de Haas–van Alphen-type oscillations arise as successive Landau levels are occupied with increasing density (or decreasing magnetic field). The oscillatory quantities are usually expressed as derivatives of the bulk quantities with respect to thermodynamic variables; examples include heat capacity, magnetization and magnetic susceptibility, adiabatic index ($\partial\ln P_e/\partial\ln\rho$), sound speed, and electron screening length of an electric charge in the plasma (see, for example, Ashcroft and Mermin, 1976; Blandford and Hernquist, 1982; Lai and Shapiro, 1991; Yakovlev and Kaminker, 1994). With increasing T, the oscillations become weaker because of the thermal broadening of the Landau levels; when $T\gtrsim T_B$, the oscillations are entirely smeared out, and the field-free results are recovered.

(iii) For $T\gg T_B$ (regardless of density): In this regime, many Landau levels are populated and the thermal widths of the Landau levels ($\sim kT$) are higher than the

level spacing. The magnetic field is termed "nonquantizing" and does not affect the thermodynamic properties of the gas.

VII. SURFACE LAYER OF A MAGNETIZED NEUTRON STAR

In this section we review the properties of the surface layer of a magnetized neutron star. We shall focus on the thermodynamic properties and phase diagram. We expect various forms of the magnetic bound states discussed in Secs. III–V to exist on the stellar envelope, depending on the field strength, temperature, and density.

The chemical composition of a neutron star surface is unknown. A neutron star is formed as a collapsed, hot ($kT \gtrsim 10\,\mathrm{MeV}$) core of a massive star in a supernova explosion. The neutron star matter may be assumed to be fully catalyzed and in the lowest energy state (see, for example, Salpeter, 1961; Baym, Pethick, and Sutherland, 1971). We therefore expect the neutron star surface to consist of iron (^{56}Fe) formed at the star's birth. This may be the case for young radio pulsars that have not accreted any gas. However, once the neutron star accretes material or has gone through a phase of accretion, either from the interstellar medium or from a binary companion, the surface (crust) composition can be quite different due to surface nuclear reactions and weak interactions during the accretion (see, for example, Blaes *et al.*, 1990; Haensel and Zdunik, 1990; Schatz *et al.*, 1999). Moreover, a hydrogen-helium envelope will form on the top of the surface unless it has completely burnt out. While a strong magnetic field and/or rapid stellar spin may prevent large-scale accretion, it should be noted that even with a low accretion rate of $10^{10}\,\mathrm{g\,s^{-1}}$ (typical of accretion from the interstellar medium) for one year, the accreted material will be more than enough to completely shield the original iron surface of the neutron star. The lightest elements, H and He, are likely to be the most important chemical species in the envelope due to their predominance in the accreting gas and also due to quick separation of light and heavy elements in the gravitational field of the neutron star (see Alcock and Illarionov, 1980 for a discussion of gravitational separation in white dwarfs; applied to neutron stars, we find that the settling time of C in a 10^6-K hydrogen photosphere is of the order of a second). If the present accretion rate is low, gravitational settling produces a pure H envelope. Alternatively, a pure He layer may result if the hydrogen has completely burnt out.

In this section, we shall mostly focus on the hydrogen envelope (Secs. VII.A and VII.B) both because of its predominance in the outer layer of the neutron star and because the properties of different phases of H are better understood. A pure He envelope would presumably have similiar properties to those of a H envelope. The iron surface layer and deeper crust will be discussed in Secs. VII.C and VII.E. We are interested only in the temperature regime $T \gtrsim 10^5\,\mathrm{K}$, since neutron stars with $T \lesssim 10^5\,\mathrm{K}$ are nearly impossible to observe.

A. Warm hydrogen atmosphere

We now consider the physical conditions and chemical equilibrium in a hydrogen atmosphere with photospheric temperature in the range $T_{\rm ph} \sim 10^5 - 10^{6.5}\,\mathrm{K}$ and magnetic field strength in the range $B_{12} \sim 0.1-20$. These conditions are likely to be satisfied by most observable neutron stars. For such relatively low field strengths, the atmosphere is largely nondegenerate and consists mainly of ionized hydrogen, H atoms, and small H_N molecules, and we can neglect the condensed phase in the photosphere. (In Sec. VII.B we shall consider the more extreme situation in which the nondegenerate atmosphere has negligible optical depth and the condensed phase becomes important.) Although the density scale height of the atmosphere is only $h \simeq kT_{\rm ph}/m_p g \simeq 0.08\, T_{\rm ph,5}\, g_{14}^{-1}\,\mathrm{cm}$, where $T_{\rm ph,5} = T_{\rm ph}/(10^5\,\mathrm{K})$, and $g = 10^{14}\, g_{14}\,\mathrm{cm\,s^{-2}}$ is the gravitational acceleration, the atmosphere has significant optical depth and therefore the atmospheric properties determine the thermal radiation spectrum from the neutron star (see Pavlov *et al.*, 1995 and references therein).

The photosphere of the neutron star is located at the characteristic photon optical depth $\tau = \int_{r_{\rm ph}}^{\infty} \rho\, \kappa_R\, dr = 2/3$, where κ_R (in units of $\mathrm{cm^2/g}$) is the Rosseland mean opacity; the photosphere pressure is $P_{\rm ph} \simeq 2g/(3\kappa_R)$. An accurate determination of the photosphere conditions requires a self-consistent solution of the atmospheric structure and radiative transport, but an order-of-magnitude estimate is as follows. In a strong magnetic field, the radiative opacity becomes anisotropic and depends on polarization (Canuto *et al.*, 1971; Lodenquai *et al.*, 1974; Pavlov and Panov, 1976; Ventura, 1979; Nagel and Ventura, 1980; see Mészáros, 1992 and references therein). For photons with polarization vector perpendicular to the magnetic field (the *extraordinary mode*), the free-free absorption and electron-scattering opacities are reduced below their zero-field values by a factor $(\omega/\omega_{ce})^2$, while for photons polarized along the magnetic field (the *ordinary mode*), the opacities are not affected. Pavlov and Yakovlev (1977) and Silant'ev and Yakovlev (1980) have calculated the appropriate averaged Rosseland mean free-free and scattering opacity; in the magnetic-field and temperature regime of interest, an approximate fitting formula is

$$\kappa_R(B) \simeq 400\, \eta \left(\frac{kT}{\hbar \omega_{ce}}\right)^2 \kappa_R(0), \tag{7.1}$$

where $\eta \simeq 1$ and $\kappa_R(0)$ is the zero-field opacity. Using the ideal-gas equation of state, $P_{\rm ph} \simeq \rho_{\rm ph} kT_{\rm ph}/m_p$, we obtain the photosphere density

$$\rho_{\rm ph} \simeq 0.5\, \eta^{-1/2}\, g_{14}^{1/2}\, T_{\rm ph,5}^{1/4}\, B_{12}\,\mathrm{g\,cm^{-3}}. \tag{7.2}$$

Note that for $\eta \sim 1/400$, this equation also approximately characterizes the density of the deeper layer where the extraordinary photons are emitted. Other sources of opacity such as bound-free and bound-bound absorptions will increase the opacity and reduce the photosphere density, but the above estimate defines the gen-

eral range of densities in the atmosphere if the $T_{\rm ph}$ is large enough for the neutral H abundance to be small. Clearly, a typical atmosphere satisfies $\rho \ll \rho_B$ and $T \ll T_B$, but $T \gg T_F$ (see Sec. VI and Fig. 6), i.e., the magnetic field is strongly quantizing in the atmosphere, but the electrons are nondegenerate.

An important issue for neutron star atmosphere modeling concerns the ionization equilibrium (or Saha equilibrium) of atoms in strong magnetic fields. Earlier treatments of this problem (e.g., Gnedin *et al.*, 1974; Khersonskii, 1987) assumed that the atom could move freely across the magnetic field; this is generally not valid for the strong-field regime of interest here (see Sec. III.E). Lai and Salpeter (1995) gave an approximate analytic solution for a limited temperature-density regime (see below). To date the most complete treatment of the problem is that of Potekhin *et al.* (1999), who used the numerical energy levels of a moving H atom as obtained by Potekhin (1994, 1998) and an approximate description of the nonideal-gas effect to derive the thermodynamic properties of a partially ionized hydrogen plasma in strong magnetic fields. Here we discuss the basic issues of ionization equilibrium in strong magnetic fields and refer the reader to Potekhin *et al.* (1999) for a more detailed treatment.

For nondegenerate electrons in a magnetic field, the partition function (in volume V) is

$$Z_e = \frac{V}{2\pi\rho_0^2} \sum_{n_L=0}^{\infty} g_{n_L} \exp\left(\frac{-n_L \hbar\omega_{ce}}{kT}\right) \int_{-\infty}^{\infty} \frac{dp_z}{h} \times \exp\left(\frac{-p_z^2}{2m_e kT}\right) = \frac{V}{2\pi\rho_0^2 \lambda_{Te}} \tanh^{-1}\left(\frac{\hbar\omega_{ce}}{2kT}\right) \simeq \frac{V}{2\pi\rho_0^2\lambda_{Te}}, \tag{7.3}$$

where $\lambda_{Te} = (2\pi\hbar^2/m_e kT)^{1/2}$ is the electron thermal wavelength and the last equality applies for $T \ll T_B$. For protons, we shall drop the zero-point energy and the spin energy in both free states and bound states [i.e., $E = n_L\hbar\omega_{cp} + p_z^2/(2m_p)$ for a free proton]. Treating the proton as a spinless particle ($g_{n_L}=1$), we find that the partition function of free protons is

$$Z_p = \frac{V}{2\pi\rho_0^2\lambda_{Tp}} \left[1 - \exp\left(-\frac{\hbar\omega_{cp}}{kT}\right)\right]^{-1}, \tag{7.4}$$

where $\lambda_{Tp} = (2\pi\hbar^2/m_p kT)^{1/2}$ is the proton thermal wavelength.

Using Eq. (3.40) for the energy of the H atom, we write the partition function for the bound states as

$$Z_H = \frac{V}{h^3} \sum_{m\nu} \int d^3K\, w_{m\nu}(K_\perp) \exp\left(-\frac{\mathcal{E}_{m\nu}}{kT}\right) = \frac{V}{\lambda_{TH}^3} Z_w, \tag{7.5}$$

where $\lambda_{TH} = (2\pi\hbar^2/MkT)^{1/2}$, and

$$Z_{m\nu} = \frac{\lambda_{TH}^2}{2\pi\hbar^2} \int dK_\perp\, K_\perp w_{m\nu}(K_\perp) \times \exp\left(-\frac{m\hbar\omega_{cp} + E_{m\nu}(K_\perp)}{kT}\right), \tag{7.6}$$

$$Z_w = \sum_{m\nu} Z_{m\nu}. \tag{7.7}$$

The Saha equation for the ionization equilibrium in strong magnetic fields then reads

$$\frac{n_H}{n_p n_e} = \frac{VZ_H}{Z_e Z_p} = \frac{\lambda_{Te}\lambda_{Tp}(2\pi\rho_0^2)^2}{\lambda_{TH}^3} \left[1 - \exp\left(-\frac{\hbar\omega_{cp}}{kT}\right)\right] Z_w. \tag{7.8}$$

In Eqs. (7.5) and (7.6), $w_{m\nu}(K_\perp)$ is the occupation probability of the hydrogen bound state characterized by $m, \nu, K_\perp$, and it measures deviation from the Maxwell-Boltzmann distribution due to the medium effect. Physically, it arises from the fact that an atom tends to be "destroyed" when another particle in the medium comes close to it. The atom-proton interaction introduces a correction to the chemical potential of the atomic gas,

$$\Delta\mu_H \simeq 2n_p kT \int d^3r\, [1 - \exp(-U_{12}/kT)] \tag{7.9}$$

(see, for example, Landau and Lifshitz, 1980), where U_{12} is the interaction potential. Similar expressions can be written for atom-electron and atom-atom interactions. For r much larger than the size of the elongated atom, the atom-proton potential U_{12} has the form $U_{12} \sim eQ(3\cos^2\theta - 1)/r^3$, where θ is the angle between the vector $\mathbf{r}$ and the z axis, and $Q \sim eL_z^2$ is the quadrupole moment of the atom; the atom-atom interaction potential has the form $U_{12} \sim Q^2(3 - 30\cos^2\theta + 35\cos^4\theta)/r^5$. Since the integration over the solid angle $\int d\Omega\, U_{12} = 0$ at large r, the contribution to $\Delta\mu(H)$ from large r is negligible. (An atom with $K_\perp \neq 0$ also acquires a dipole moment in the direction of $\mathbf{B}\times\mathbf{K}_\perp$; the resulting dipole interaction also satisfies $\int d^3r\, U_{12} = 0$.) Thus the main effect of particle interactions is the *excluded-volume effect*: Let $L_{m\nu}(K_\perp)$ be the characteristic size of the atom such that we can set $U_{12} \to \infty$ when $r \lesssim L_{m\nu}$. We then have $\Delta\mu_H \sim n_b kT(4\pi L_{m\nu}^3/3)$, where $n_b = n_H + n_p$ is the baryon number density. Therefore the occupation probability is of order

$$w_{m\nu}(K_\perp) \sim \exp\left[-\frac{4\pi}{3} n_b L_{m\nu}^3(K_\perp)\right]. \tag{7.10}$$

The size of the atom can be estimated as follows (see Secs. III.A and III.E): when $K_\perp = 0$, the tightly bound state ($\nu = 0$) has $L_z \sim l_m^{-1}, L_\perp \sim \rho_m$, while the $\nu > 0$ state has $L_z \sim \nu^2, L_\perp \sim \rho_m$; when $K_\perp \neq 0$, the electron and proton are displaced in the transverse direction by a distance $d \lesssim K_\perp/b$; thus we have $L_{m\nu}(K_\perp) \sim \max(L_z, L_\perp, K/b)$. A more accurate fitting formula for $L_{m\nu}(K_\perp)$ is given in Potekhin (1998).

More precise calculation of the occupation probability requires detailed treatment of interactions between various particles in the plasma. Even at zero magnetic field, the problem is challenging and uncertainties remain (see, for example, Hummer and Mihalas, 1988; Mihalas *et al.*, 1988; Saumon and Chabrier, 1991, 1992; Potekhin, 1996). In strong magnetic fields, additional complications arise from the nonspherical shape of the atom.

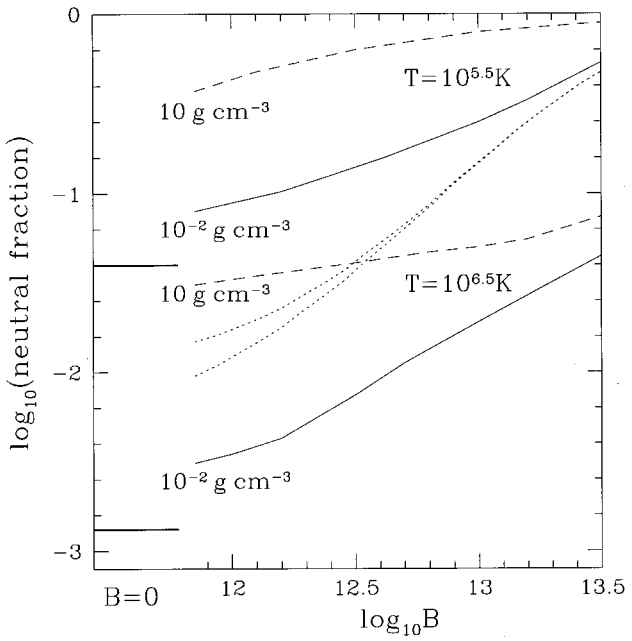

FIG. 7. Atomic hydrogen fraction n_H/n_b as a function of magnetic-field strength: solid lines, density $\rho=0.01\ \mathrm{g\,cm^{-3}}$ (for $T=10^{5.5}$ K and $T=10^{6.5}$ K) dashed lines, $\rho=10\ \mathrm{g\,cm^{-3}}$. These results are based on the calculations of Potekhin *et al.* (1999). The two dotted lines (for $T=10^{5.5}$ K, $\rho=0.01\ \mathrm{g\,cm^{-3}}$) correspond to the hydrogen fraction n_H'/n_b calculated ignoring the decentered states. The lower line includes only the $m=0$ state, while the upper line includes all m states. The two horizontal lines on the left correspond to zero-field results. For $\rho=0.01\ \mathrm{g\,cm^{-3}}$ and $T=10^{5.5}$ and $10^{6.5}$ K; for $\rho=10\ \mathrm{g\,cm^{-3}}$, all atoms are pressure ionized at zero field.

Nevertheless, using the hard-sphere approximation similar to the field-free situation, Potekhin *et al.* (1999) have constructed a free-energy model for partially ionized hydrogen, from which $w_{m\nu}(K_\perp)$ can be calculated along with other thermodynamic quantities. Figure 7 shows some numerical results based on the calculations of Potekhin *et al.* (1999). The general trend that the neutral fraction n_H/n_b increases with increasing B is the result of larger binding energy $|E_{m\nu}(K_\perp)|$ for larger B, although this trend is offset partially by the fact that the electron phase space also increases with B [see Eq. (7.3)]. For a given T and B, the neutral fraction increases with density until ρ reaches $\rho_c\sim 10$–$100\ \mathrm{g\,cm^{-3}}$ [for $B=10^{12}$–10^{13} G (see Potekhin *et al.*, 1999), ρ_c scales with b roughly as $(\ln b)^3$], above which the neutral fraction declines because of pressure ionization.

It is instructive to consider the relative importance of the centered states and the decentered states to the neutral hydrogen fraction. As discussed in Sec. III.E, the H energy can be approximated by $E_0(K_\perp)\simeq E_0+K_\perp^2/(2M_\perp)$ for $K_\perp\lesssim K_{\perp c}\sim\sqrt{2M|E_0|}$ (we consider only the $m=\nu=0$ state for simplicity). Setting $w_{00}(K_\perp)=1$ for low densities, the contribution of the $K_\perp\lesssim K_{\perp c}$ states to Z_w is given (in a.u.) by

$$Z_w^{(c)}\simeq\exp\left(-\frac{E_0}{T}\right)\left(\frac{M_\perp}{M}\right), \tag{7.11}$$

for $K_{\perp c}^2/(2M_\perp)\sim(M/M_\perp)|E_0|\gg T$. On the other hand, the contribution from the decentered states to Z_w can be estimated as

$$Z_w^{(d)}\simeq\frac{1}{MT}\int_{K_{\perp c}}^{K_{\max}}K_\perp\exp\left[-\frac{E_0(K_\perp)}{T}\right]dK_\perp, \tag{7.12}$$

where $K_{\max}$ is given by $(4\pi/3)(K_{\max}/b)^3 n_b\simeq 1$. Since $|E_0(K_\perp)|$ for $K\gtrsim K_{\perp c}$ is much less than $|E_0|$, we find

$$\frac{Z_w^{(c)}}{Z_w^{(d)}}\sim\frac{2M_\perp T}{K_{\max}^2}\exp\left(\frac{|E_0|}{T}\right)\sim\frac{5M_\perp T}{b^2}n_b^{2/3}\exp\left(\frac{|E_0|}{T}\right). \tag{7.13}$$

Thus for the centered states to dominate the atomic population, we require $|E_0|/T\gtrsim\ln(b^2/5M_\perp T n_b^{2/3})$; for example, at $T=10^{5.5}$ K, this corresponds to $B\gtrsim 10^{13.5}$ G, or $|E_0|/T\gtrsim 15$ (see the dotted lines in Fig. 7).

For sufficiently high B or sufficiently low T, we expect the atmosphere to have an appreciable abundance of H_2 molecules. Since there has been no detailed study of the effect of motion on H_2, only an approximate estimate is possible (Lai and Salpeter, 1997; Potekhin *et al.*, 1999). For example, at $B=10^{13}$ G there exists a large amount of H_2 in the photosphere ($\rho\sim 10$–$100\ \mathrm{g\,cm^{-3}}$) when $T\lesssim 10^{5.5}$ K. As we go deeper into the atmosphere, we expect larger molecules to appear; when the density approaches the internal density of the atom/molecule, the bound states lose their identities and we obtain a uniform, ionized plasma. With increasing density, the plasma becomes degenerate and gradually transforms into a condensed phase (Lai and Salpeter, 1997).

B. Surface hydrogen at ultrahigh fields: The condensed phase

We have seen in Sec. VII.A that, for sufficiently low field strengths and/or high temperatures, the outermost layer of the neutron star is nondegenerate, and the surface material gradually transforms into a degenerate Coulomb plasma as density increases. As discussed in Secs. III–V, the binding energy of the condensed hydrogen increases as a power-law function of B, while the binding energies of atoms and small molecules increase only logarithmically. We therefore expect that for sufficiently strong magnetic fields there exists a critical temperatire T_{crit}, below which a first-order phase transition occurs between the condensed hydrogen and the gaseous vapor; as the vapor density decreases with increasing B or decreasing T, the outermost stellar surface would be in the form of condensed hydrogen (Lai and Salpeter, 1997).

While a precise calculation of T_{crit} for the phase transition is not available at present, we can get an estimate by considering the equilibrium between the condensed hydrogen (labeled "s") and the gaseous phase (labeled "g") in the ultrahigh-field regime (where phase separation exists). The gaseous phase consists of a mixture of free electrons, protons, bound atoms, and molecules. Phase equilibrium requires the temperature, the pressure, and the chemical potentials of different species to satisfy the conditions

$$P_s = P_g = [2n_p + n(H) + n(H_2) + n(H_3) + \cdots]kT = P, \tag{7.14}$$

$$\mu_s = \mu_e + \mu_p = \mu(H) = \tfrac{1}{2}\mu(H_2) = \tfrac{1}{3}\mu(H_3) = \cdots. \tag{7.15}$$

For the condensed phase near zero pressure, the density is approximately

$$\rho_s \simeq 561 B_{12}^{6/5}\,\mathrm{g\,cm^{-3}}, \tag{7.16}$$

and the electron Fermi temperature is $T_F \simeq 0.236 b^{2/5} = 8.4\times 10^5 B_{12}^{2/5}$ K; thus, at a given temperature, the condensed hydrogen becomes more degenerate as B increases. Let the energy per Wigner-Seitz cell in the condensate be $E_s(r_s)$ [see Eq. (5.10) for an approximate expression; $r_s = r_i$ for hydrogen]. The pressure and chemical potential of the condensed phase are given by

$$P_s = -\frac{1}{4\pi r_s^2}\frac{dE_s}{dr_s}, \tag{7.17}$$

$$\mu_s = E_s(r_s) + P_s V_s \simeq E_{s,0} + P_s V_{s,0}, \tag{7.18}$$

where the subscript "0" indicates the zero-pressure values. We have assumed that the vapor pressure is sufficiently small so that the deviation from the zero-pressure state of the condensate is small, i.e., $\delta \equiv |(r_s - r_{s,0})/r_{s,0}| \ll 1$; this is justified when the saturation vapor pressure $P_{\rm sat}$ is much less than the critical pressure $P_{\rm crit}$ for phase separation, or when $T \ll T_{\rm crit}$. The finite temperature correction $\Delta\mu_s$ to the chemical potential of the condensed phase, as given by $\Delta\mu_s(T) \simeq \pi^2 T^2/(12T_F)$, is much smaller than the cohesive energy and can be neglected. Using the partition functions of free electrons, protons, and atoms as given in Sec. VII.A, we find that in the saturated vapor,

$$n_p = n_e \simeq \frac{bM^{1/4}T^{1/2}}{(2\pi)^{3/2}}\left[1 - \exp\left(-\frac{b}{MT}\right)\right]^{-1/2} \times \exp\left(-\frac{Q_1 + Q_s}{2T}\right), \tag{7.19}$$

$$n(\mathrm{H}) \simeq \left(\frac{MT}{2\pi}\right)^{3/2}\left(\frac{M'_\perp}{M}\right)\exp\left(-\frac{Q_s}{T}\right), \tag{7.20}$$

where $Q_s = |E_{s,0}| - |E(H)|$ is the cohesive energy of the condensed hydrogen (we have neglected $P_s V_{s,0}$ in comparison to Q_s), and $Q_1 = |E(H)|$ is the ionization energy of the hydrogen atom. In Eq. (7.20) we have included only the ground state ($m = \nu = 0$) of the H atom and have neglected the decentered states; this is valid for $T \lesssim Q_1/20$ (see Sec. VII.A). The equilibrium condition $N\mu_s = \mu_N$ for the process $\mathrm{H}_{s,\infty} + \mathrm{H}_N = \mathrm{H}_{s,\infty+N}$, where H_N represents a small molecular chain or a 3D droplet, yields

$$n(\mathrm{H}_N) \simeq N^{3/2}\left(\frac{MT}{2\pi}\right)^{3/2}\exp\left(-\frac{S_N}{T}\right), \tag{7.21}$$

where $S_N = NE_N - NE_s$ is the surface energy discussed in Sec. V.F. In Eq. (7.21), we have assumed that the H_N molecule (or 3D droplet) moves across the field freely; this should be an increasingly good approximation as N increases.

The critical temperature $T_{\rm crit}$, below which phase separation between the condensed hydrogen and the gaseous vapor occurs, is determined by the condition $n_s = n_g = n_p + n(\mathrm{H}) + 2n(\mathrm{H_2}) + 3n(\mathrm{H_3}) + \cdots$. Although Eqs. (7.19)–(7.21) are derived for $n_g \ll n_s$, we may still use them to obtain an estimate of $T_{\rm crit}$. Using the approximate surface energy S_N as discussed in Sec. V.F, we find

$$T_{\rm crit} \sim 0.1\, Q_s \simeq 0.1\, Q_\infty. \tag{7.22}$$

Thus $T_{\rm crit} \simeq 8\times 10^4$, 5×10^5, and 10^6 K for $B_{12} = 10$, 100, and 500, respectively. Figure 8 shows some examples of the saturation vapor density as a function of temperature for several values of B. It should be emphasized that the calculation is very uncertain around $T \sim T_{\rm crit}$. But when the temperature is below $T_{\rm crit}/2$ (for example), the vapor density becomes much less than the condensation density n_s and phase transition is unavoidable. When the temperature drops below a fraction of $T_{\rm crit}$, the vapor density becomes so low that the optical depth of the vapor is negligible and the outermost layer of the neutron star then consists of condensed hydrogen. The condensate will be in the liquid state when $\Gamma = e^2/(r_i kT) \lesssim 175$ (see Sec. VII.E), or when $T \gtrsim 1.3\times 10^3\,(\rho/1\,\mathrm{g\,cm^{-3}})^{1/3}$ K $\simeq 7\times 10^4 B_{14}^{2/5}$ K. The radiative properties of such a condensed phase are of interest to study (see Sec. VII.D).

The protons in the condensed hydrogen phase can undergo significant pycnonuclear reactions. Unlike the usual situation of pycnonuclear reactions (see Salpeter and Van Horn, 1969; Ichimaru, 1993), in which the high densities needed for the reactions at low temperatures are achieved through very high pressures, here the large densities (even at zero pressure) result from the strong magnetic field—this is truly a "zero-pressure cold fusion" (Lai and Salpeter, 1997). For slowly accreting neutron stars (so that the surface temperature is low enough for condensation to occur), the inflowing hydrogen can burn almost as soon as it has condensed into the liquid phase. It is not clear whether this burning proceeds smoothly or whether there is some kind of oscillatory relaxation (e.g., cooling leads to condensation, leading to hydrogen burning and heat release, followed by evaporation, which stops the burning and leads to further cooling; see Salpeter, 1998).

C. Iron surface layer

For a neutron star that has not accreted much gas, one might expect the surface to consist of iron formed at the neutron star's birth. As discussed in Sec. V.E, the cohesive energy of Fe is uncertain. If the condensed Fe is unbound with respect to the Fe atom ($Q_s = |E_s| - |E_{\rm atom}| < 0$), then the outermost Fe layer of the neutron star is characterized by a gradual transformation from a nondegenerate gas at low densities, which includes Fe atoms and ions, to a degenerate plasma as the pressure (or column density) increases. The radiative spectrum will be largely determined by the property of the nondegenerate layer. However, even a weak cohe-

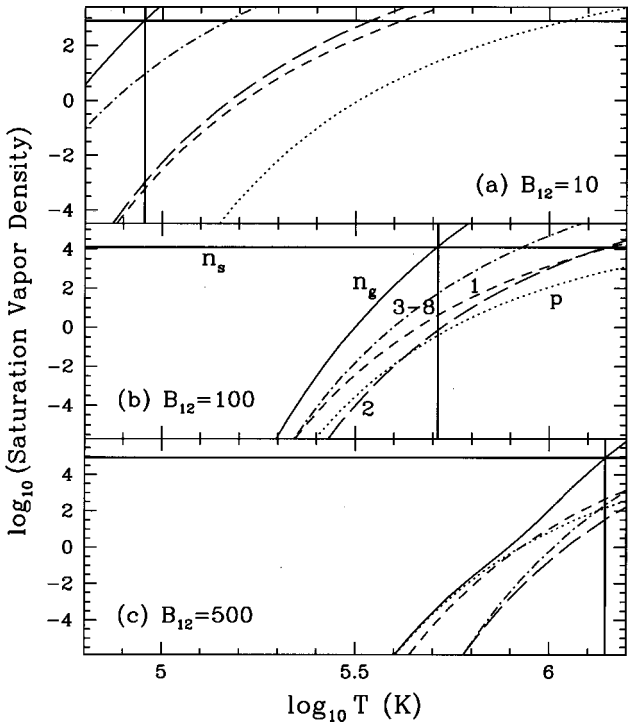

FIG. 8. The saturation vapor densities of various species (in the atomic units, a_0^{-3}) of condensed metallic hydrogen as a function of temperature for different magnetic field strengths: (a) $B_{12}=10$; (b) $B_{12}=100$; (c) $B_{12}=500$; dotted curves, n_p; short-dashed curves, $n(\mathrm{H})$; long-dashed curves, $n(\mathrm{H}_2)$; dot-dashed curves, $[3n(\mathrm{H}_3)+4n(\mathrm{H}_4)+\cdots+8n(\mathrm{H}_8)]$; solid curves, the total baryon number density in the vapor $n_g=n_p+n(\mathrm{H})+2n(\mathrm{H}_2)+\cdots$. The horizontal solid lines denote the condensation density $n_s\simeq 50\,B_{12}^{6/5}$ (a.u.), while the vertical solid lines correspond to the critical condensation temperature at which $n_g=n_s$. From Lai and Salpeter, 1997.

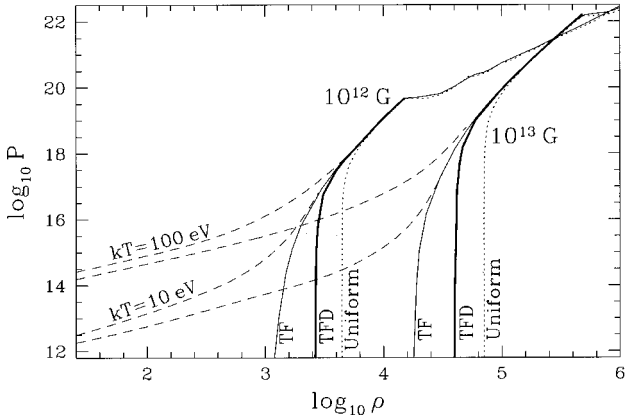

FIG. 9. Equation of state of Fe in strong magnetic fields ($B=10^{12}$ and 10^{13} G), based on Thomas-Fermi-type models: light solid lines, results of a Thomas-Fermi model allowing for many Landau levels (Rögnvaldsson *et al.*, 1993); heavy solid lines, results of a Thomas-Fermi-Dirac model allowing only for the ground Landau level (Fushiki *et al.*, 1989); dotted lines, results of the uniform-gas model as descibed by Eq. (7.25), all for zero temperature. The dashed lines are results of Thomas-Fermi models with $kT=10$ and 100 eV (Thorolfsson *et al.*, 1998).

sion of the Fe condensate ($Q_s>0$) can give rise to a phase transition at sufficiently low temperatures.[4] The number density of atomic Fe in the saturated vapor is of order

$$n_A\simeq\left(\frac{AMT}{2\pi}\right)^{3/2}\exp\left(-\frac{Q_s}{T}\right). \tag{7.23}$$

The gas density in the vapor is $\rho_g\gtrsim AMn_A$. The critical temperature for phase transition can be estimated from $\rho_g=\rho_s$. Using Eq. (5.13) as an estimate for the condensation density ρ_s, and using Eq. (5.22) as the upper limit of Q_s, we find

$$T_{\mathrm{crit}}\lesssim 0.1\,Q_s\lesssim 10^{5.5}\,B_{12}^{2/5}\ \mathrm{K}. \tag{7.24}$$

As in the case of hydrogen (see Sec. VII.B), we expect the vapor above the condensed iron surface to have negligible optical depth when $T\lesssim T_{\mathrm{crit}}/3$.

The iron surface layers of magnetic neutron stars have also been studied using Thomas-Fermi-type models (see, for example, Fushiki, Gudmundsson, and Pethick, 1989; Abrahams and Shapiro, 1991; Rögnvaldsson *et al.*, 1993; Thorolfsson *et al.*, 1998; see also Appendix B). While these models are too crude to determine the cohesive energy of the condensed matter, they provide a useful approximation to the gross properties of the neutron star surface layer. Figure 9 depicts the equation of state of iron at $B=10^{12}$ G and $B=10^{13}$ G based on Thomas-Fermi-type statistical models. At zero temperature, the pressure is zero at a finite density, which increases with increasing B. This feature is qualitatively the same as in the uniform-electron-gas model (Sec. V.D). Neglecting the exchange-correlation energy and the nonuniformity correction, we can write the pressure of a zero-temperature uniform electron gas as

$$P=P_e-\frac{3}{10}\left(\frac{4\pi}{3}\right)^{1/3}(Ze)^2\left(\frac{\rho}{Am_p}\right)^{4/3}, \tag{7.25}$$

where the first term is given by Eq. (6.9) [or by Eq. (6.20) in the strong-field, degenerate limit] and the second term results from the Coulomb interactions among the electrons and ions. Setting $P=0$ gives the condensation density $\rho_{s,0}$ as in Eq. (5.13). Note that near zero pressure, all these models are approximate (e.g., the calculated $\rho_{s,0}$ can differ from the true value by a factor of a few), and more detailed electronic-structure calculations are needed to obtain a reliable pressure-density relation. Figure 9 also shows the results of the finite-temperature Thomas-Fermi model (Thorolfsson *et al.*, 1998). Obviously, at finite temperatures, the pressure does not go to zero until $\rho\to 0$, i.e., an atmosphere is present. Note that the finite-temperature Thomas-Fermi model gives only a qualitative description of a dense atmosphere; important features such as atomic states and ionizations are not captured in this model.

[4]The condensation of Fe was first discussed by Ruderman and collaborators (see Ruderman, 1974; Flowers *et al.*, 1977), although these earlier calculations greatly overestimated the cohesive energy Q_s of Fe (see Secs. V.B and V.E).

D. Radiative transfer and opacities

As discussed in Sec. I.A, the surface thermal radiation detected from isolated neutron stars provides valuable information on the structure and evolution of neutron stars. To calculate the radiation spectrum from the neutron star surface, one needs to understand the radiative opacities and study radiative transport in the atmosphere. A thorough review of these subjects is beyond the scope of this paper. Here we briefly discuss what has been done and provide references to recent papers.

Nonmagnetic ($B=0$) neutron star atmosphere models were first constructed by Romani (1987). Further works (Rajagopal and Romani, 1996; Zavlin *et al.*, 1996) used improved opacity and equation-of-state data from the OPAL project (Iglesias and Rogers, 1996) for pure hydrogen, helium, and iron compositions. These works showed that the radiation spectra from light-element (hydrogen or helium) atmospheres deviate significantly from the blackbody spectrum. The zero-field models may be relevant for the low-field ($B\sim10^8$–10^9 G) recycled pulsars (e.g., PSR J0437-4715, from which thermal x rays have apparently been detected; see Zavlin and Pavlov, 1998), but it is possible that these intermediate magnetic fields can have non-negligible effects, at least for atmospheres of light elements. For example, even at $B\sim10^9$ G, the binding energies of light elements can differ significantly from the zero-field values, and at low temperatures the OPAL equation of state underestimates the abundance of the neutral species in the atmosphere.

The basic properties of radiation emerging from a completely ionized magnetic neutron star atmosphere (under the assumption of constant temperature gradient in the radiating layer) were considered by Pavlov and Shibanov (1978). Modeling of a magnetic neutron star atmosphere (which requires determining the temperature profile in the atmosphere as well as the radiation field self-consistently) was first attempted by Miller (1992), who adopted the polarization-averaged bound-free (photoionization) opacities calculated by Miller and Neuhauser (1991) while neglecting other radiative processes. However, separate transport of polarization modes, which have very different opacities, dramatically affects the emergent spectral flux. So far most studies of magnetic neutron star atmospheres have focused on hydrogen and moderate field strenghts of $B\sim10^{12}$–10^{13} G (e.g., Shibanov *et al.*, 1992; Pavlov *et al.*, 1994; Zavlin *et al.*, 1995; see Pavlov *et al.*, 1995 for a review). These models correctly take account of the transport of different photon modes through a mostly ionized medium in strong magnetic fields. The opacities adopted in the models include free-free transitions (bremsstrahlung absorption) and electron scattering, while bound-free (photoionization) opacities are treated in a highly approximate manner and bound-bound transitions are completely ignored. The models of Pavlov *et al.* are expected to be valid for relatively high temperatures ($T\gtrsim$ a few$\times10^6$ K) where hydrogen is almost completely ionized. As the magnetic field increases, we expect these models to break down at even higher temperatures as bound atoms, molecules, and condensate become increasingly important. The atmosphere models of Pavlov *et al.* have been used to compare the observed spectra of several radio pulsars and radio-quiet isolated neutron stars (see, for example, Pavlov *et al.*, 1996; Zavlin, Pavlov, and Trümper, 1998), and some useful constraints on neutron star properties have been obtained. Magnetic iron atmospheres (with $B\sim10^{12}$ G) were studied by Rajagopal *et al.* (1997). Because of the complexity in the atomic physics and radiative transport, these Fe models are necessarily crude. Most recently, neutron star atmosphere models in the superstrong field regime ($B\geqslant10^{14}$ G) have begun to be explored (Ho and Lai, 2001; Özel, 2001; Zane *et al.*, 2001). In addition to band species the effects of ion resonance and vacuum polarization are expected to play an important role in determining the radiative spectra of magnetars (see Sec. I.A).

As discussed in Sec. VII.A, a strong magnetic field increases the abundance of neutral atoms in a hydrogen atmosphere as compared to the zero-field case (see Fig. 7). Therefore one could in principle expect some atomic or molecular line features in the soft-x-ray or UV spectra. For example, the Lyman ionization edge is shifted to 160 eV at 10^{12} G and 310 eV at 10^{13} G. The free-free and bound-free (for a ground-state hydrogen atom at rest) cross sections for a photon in the extraordinary mode, with the photon electric field perpendicular to the magnetic field, are approximately given by (Gnedin, Pavlov, and Tsygan, 1974; Ventura *et al.*, 1992)[5]

$$\sigma_{\mathrm{ff}\perp}\simeq1.7\times10^3\rho T_5^{-1/2}\alpha^2a_0^2\omega^{-1}b^{-2}, \tag{7.26}$$

$$\sigma_{\mathrm{bf}\perp}\simeq4\pi\alpha a_0^2\left(\frac{Q_1}{\omega}\right)^{3/2}b^{-1}, \tag{7.27}$$

where $\alpha=1/137$ is the fine-structure constant, a_0 is the Bohr radius, ρ is the density in g cm^{-3}, ω is the photon energy in the atomic units, Q_1 is the ionization potential, and b is the dimensionless field strength defined in Eq. (1.3). Near the absorption edge, the ratio of the free-free and bound-free opacities is

$$\frac{\kappa_{\mathrm{ff}\perp}}{\kappa_{\mathrm{bf}\perp}}\sim10^{-4}\frac{\rho}{T_5^{1/2}B_{12}f_H}. \tag{7.28}$$

Thus, even for the relatively small neutral H fraction f_H, the discontinuity of the total opacity at the Lyman edge is pronounced and we expect the absorption feature to be prominent. Note that since the extraordinary mode has smaller opacity, most of the x-ray flux will come out in this mode. For photons in the ordinary mode, we have

$$\sigma_{\mathrm{ff}\parallel}\simeq1.65\times10^3\rho T_5^{-1/2}\alpha^2a_0^2\omega^{-3}, \tag{7.29}$$

$$\sigma_{\mathrm{bf}\parallel}\simeq10^2\pi\alpha a_0^2(Q_1/\omega)^{5/2}(\ln b)^{-2}, \tag{7.30}$$

[5]Note that Eqs. (7.27) and (7.30) are based on the Born approximation, which breaks down near the photoionization threshold. A more accurate fitting to σ_{bf}, valid for any tightly bound state and photon polarization, is given by Eqs. (39)–(43) of Potekhin and Pavlov (1993).

where $\sigma_{\rm ff\|}$ is the same as in zero field, which gives $\kappa_{\rm ff\|}/\kappa_{\rm bf\|}\sim 10^{-2}\rho T_5^{-1/2} f_H^{-1}$ for $B_{12}\sim 1$. Thus the absorption edge for the ordinary mode is less pronounced. Clearly, the position and the strength of the absorption edge can provide a useful diagnostic of the magnetic field at the neutron star surface.

A detailed review of electron scattering and free-free absorption opacities in a magnetized plasma is that of Mészáros (1992). Bound-bound transitions in strong magnetic fields have been thoroughly investigated for hydrogen and helium atoms at rest (see Ruder *et al.*, 1994 for review and tabulations of numerical results). Bound-free absorptions for hydrogen atoms at rest have also been extensively studied (see, for example, Gnedin *et al.*, 1974; Ventura *et al.*, 1992; Potekhin and Pavlov, 1993). Since the motion of an atom in a strong magnetic field modifies the atomic structure significantly (see Sec. III.E), the motional effects on opacities need to be included; see Pavlov and Potekhin, 1995 for bound-bound opacities and Potekhin and Pavlov, 1997 for bound-free opacities; see also Potekhin *et al.*, 1998 for total opacities. Some approximate results for radiative transitions in heavy atoms were presented by Miller and Neuhauser (1991).

In the regime in which the outermost layer of the neutron star is in the form of condensed matter, radiation directly emerges from the hot (but degenerate) condensed phase. The usual radiative transfer does not apply to this situation. Because of the high condensation density, the electron plasma frequency is larger than the frequency of a typical thermal photon. Thus the photons cannot be easily excited thermally inside the condensate. This implies that the neutron star surface has a high reflectivity. The spectral emissivity is determined by the bulk dielectric properties of the condensed phase (see Itoh, 1975; Brinkmann, 1980).

E. Magnetized neutron star crust

As discussed in Sec. VI, the effect of Landau quantization is important only for $\rho\lesssim\rho_B$ [see Eq. (6.11)]. Deeper in the neutron star envelope (and the interior), we expect the magnetic-field effect on the bulk equation of state to become negligible as more and more Landau levels are filled. In general, we can use the condition $\rho_B\gtrsim\rho$, or $B_{12}\gtrsim 27\,(Y_e\rho_6)^{2/3}$, to estimate the critical value of B above which Landau quantization will affect physics at density ρ. For example, at $B\gtrsim 10^{14}$ G, the neutronization transition from ^{56}Fe to ^{62}Ni (at $\rho=8.1\times 10^6\,{\rm g\,cm^{-3}}$ for $B=0$; Baym, Pethick, and Pines, 1971) in the crust can be significantly affected by the magnetic field (Lai and Shapiro, 1991).

The ions in the neutron star envelope form a one-component plasma and are characterized by the Coulomb coupling parameter

$$\Gamma=\frac{(Ze)^2}{r_i kT}=22.75\frac{Z^2}{T_6}\left(\frac{\rho_6}{A}\right)^{1/3}, \tag{7.31}$$

where $r_i=(3/4\pi n_i)^{1/3}$ is the Wigner-Seitz cell radius, $n_i=\rho/m_i=\rho/(Am_p)$ is the ion number density, $\rho_6=\rho/(10^6\,{\rm g\,cm^{-3}})$, and $T_6=T/(10^6\,{\rm K})$. For $\Gamma\ll 1$, the ions form a classical Boltzmann gas whose thermodynamic property is unaffected by the magnetic field. For $\Gamma\gtrsim 1$, the ions constitute a strongly coupled Coulomb liquid. The liquid freezes into a Coulomb crystal at $\Gamma=\Gamma_m\simeq 175$, corresponding to the classical melting temperature T_m (see, for example, Slattery *et al.*, 1980; Nagara *et al.*, 1987; Potekhin and Chabrier, 2000). The quantum effects of ion motions (zero-point vibrations) tend to increase Γ_m (Chabrier, Ashcroft, and DeWitt, 1992; Chabrier, 1993) or even suppress freezing (Ceperley and Alder, 1980; Jones and Ceperley, 1996). At zero field, the ion zero-point vibrations have a characteristic frequency of the order of the ion plasma frequency Ω_p, with

$$\hbar\Omega_p=\hbar\left(\frac{4\pi Z^2e^2n_i}{m_i}\right)^{1/2}=675\left(\frac{Z}{A}\right)\rho_6^{1/2}\ {\rm eV}. \tag{7.32}$$

For $T\ll T_{\rm Debye}\sim\hbar\Omega_p/k$, the ion vibrations are quantized. The effects of magnetic fields on strongly coupled Coulomb liquids and crystals have not been systematically studied (but see Usov *et al.*, 1980). The cyclotron frequency of the ion is given by

$$\hbar\omega_{ci}=\hbar\frac{ZeB}{Am_pc}=6.3\left(\frac{Z}{A}\right)B_{12}\ {\rm eV}. \tag{7.33}$$

The ion vibration frequency in a magnetic field may be estimated as $(\Omega_p^2+\omega_{ci}^2)^{1/2}$. Using Lindeman's rule, we obtain a modified melting criterion:

$$\Gamma\left(1+\frac{\omega_{ci}^2}{\Omega_p^2}\right)\simeq 175. \tag{7.34}$$

For $\omega_{ci}\ll\Omega_p$, or $B_{12}\ll 100\,\rho_6^{1/2}$, the magnetic field does not affect the melting criterion and other properties of ion vibrations.

Even in the regime in which magnetic quantization effects are small ($\rho\gg\rho_B$), the magnetic field can still strongly affect the transport properties (e.g., electric conductivity and heat conductivity) of a neutron star crust. This occurs when the effective gyrofrequency of the electron, $\omega_{ce}^*=eB/(m_e^*c)$, where $m_e^*=\sqrt{m_e^2+(p_F/c)^2}$, is much larger than the electron collision frequency, i.e.,

$$\omega_{ce}^*\tau_0\simeq 1.76\times 10^3\frac{m_e}{m_e^*}B_{12}\left(\frac{\tau_0}{10^{-16}\,{\rm s}}\right), \tag{7.35}$$

where τ_0 is the effective electron relaxation time (10^{-16} s is a typical value in the outer crust). For example, when $\omega_{ce}^*\tau_0\gg 1$, the electron heat conductivity perpendicular to the magnetic field is suppressed by a factor $(\omega_{ce}^*\tau_0)^{-2}$. A detailed review of the transport properties of a magnetized neutron star crust is given by Hernquist (1984) and Yakovlev and Kaminker (1994), where many earlier references can be found (see Potekhin, 1999 for a recent calculation). The thermal structure of a magnetized neutron star crust has been

studied by, for example, Van Riper (1988), Schaaf (1990), Hernquist (1985), Heyl and Hernquist (1998).

VIII. CONCLUDING REMARKS

The properties of matter in strong magnetic fields have always been an interesting subject for physicists. While early studies (e.g., Elliot and Loudon, 1960; Hasegawa and Howard, 1961) were mainly motivated by the fact that strong magnetic-field conditions can be mimicked in some semiconductors where a small effective electron mass and a large dielectric constant reduce the electric force relative to the magnetic force, recent work on this subject has been motivated by the huge magnetic field $\sim 10^{12}$ G known to exist in many neutron stars and the tentative evidence for fields as strong as 10^{15} G (see Sec. I.A). The study of matter in strong magnetic fields is obviously an important component of neutron star astrophysics research. In particular, interpretation of the ever-improving spectral data on neutron stars requires a detailed theoretical understanding of the physical properties of highly magnetized atoms, molecules, and condensed matter.

In this review, we have focused on the electronic structure and the bulk properties of matter in strong magnetic fields. We have only briefly discussed the issues of radiative opacities and conductivities in a magnetized medium (see Secs. VII.D and VII.E). There are other related problems that are not covered in this paper. For example, neutrino emissions in the neutron star crust and interior, which determine the cooling rate of the star, can be affected by strong magnetic fields (see, for example, Yakovlev and Kaminker, 1994; Baiko and Yakovlev, 1999; van Dalen *et al.*, 2000 and references therein). In proto-neutron stars, sufficiently strong magnetic fields ($B \gtrsim 10^{15}$ G) can induce asymmetric neutrino emission and impart a kick velocity to the star (see, for example, Dorofeev *et al.*, 1985; Vilenkin, 1995; Horowitz and Li, 1998; Lai and Qian, 1998a, 1998b; Arras and Lai 1999a, 1999b and references therein). We have not discussed magnetic-field effects on the nuclear matter equation of state (see, for instance, Chakrabarty *et al.*, 1997; Yuan and Zhang, 1999; Broderick *et al.*, 2000; Suh and Mathews, 2001), which are relevant for $B \gtrsim 10^{17}$–10^{18} G. Many other aspects of physics in strong magnetic fields are reviewed by Mészáros (1992).

The study of matter in strong magnetic fields spans a number of different subareas of physics, including astrophysics, atomic and molecular physics, condensed-matter physics, and plasma physics. As should be apparent from the preceding sections, although there has been steady progress over the years, many open problems remain to be studied in the future. Some of the problems should be easily solvable by specialists in their respective subareas. Since there is no recent review that covers this broad subject area, our emphasis has been on producing a self-contained account of the basic physical pictures, while referring the reader to the original literature for details (although we have also discussed aspects of calculational techniques). We hope that this review will make the original literature on matter in strong magnetic fields more easily accessible and stimulate more physicists to work on this problem.

ACKNOWLEDGMENTS

I am grateful to Edwin Salpeter for providing many insights on the subject of this paper and for his advice on writing this article. I also thank Wynn Ho, Edwin Salpeter, Ira Wasserman, and especially George Pavlov and Alexander Potekhin for commenting on early drafts of this paper, as well as Elliot Lieb, Peter Schmelcher, and Jokob Yngvason for useful comments and communications. This work has been supported in part by National Aeronautics and Space Administration grants NAG 5-8484 and NAG 5-8356, by National Science Foundation grant AST 9986740, and by a research fellowship from the Alfred P. Sloan Foundation.

APPENDIX A: JELLIUM MODEL OF ELECTRON GAS IN STRONG MAGNETIC FIELDS

Consider an electron gas in a uniform background of positive charges (the "jellium model"). The interelectronic spacing r_s is related to the electron number density n_e by $n_e^{-1} = 4\pi r_s^3/3$. At zero magnetic field, the energy per electron can be written as (Ashcroft and Mermin, 1976)

$$E = \frac{3}{5}\frac{\hbar^2 k_F^2}{2m_e} - \frac{3}{4}\frac{e^2 k_F}{\pi} + E_{\rm corr}$$
$$= \frac{2.21}{r_s^2} - \frac{0.916}{r_s} + 0.0622\ln(r_s) - 0.094\,({\rm Ry}). \qquad \text{(A1)}$$

The first term on the right-hand side is the kinetic energy, the second term is the (Hartree-Fock) exchange energy, and the remaining terms are the correlation energy. The expression for the correlation energy given here applies to the $r_s \ll 1$ limit; see Ceperley and Alder, 1980 for the full result.

Now consider the magnetic case. When the density is low (or the magnetic field high), so that only the ground Landau level is occupied, the Fermi wave number k_F can be calculated from

$$n_e = \frac{eB}{hc}\frac{1}{2\pi}\int_{-k_F}^{k_F} dk_z = \frac{2k_F}{(2\pi\rho_0)^2} \Rightarrow k_F = 2\pi^2\rho_0{}^2 n_e . \qquad \text{(A2)}$$

It is convenient to introduce two new parameters, the inverse Fermi wave number r_F and the filling factor for the lowest Landau level t,

$$r_F = \frac{1}{\pi k_F} = \frac{2}{3\pi^2}\frac{r_s^3}{\rho_0^2}, \quad t = \frac{\varepsilon_F}{\hbar\omega_{ce}} = \left(\frac{n_e}{n_B}\right)^2 = \frac{9\pi^2}{8}\left(\frac{\rho_0}{r_s}\right)^6, \qquad \text{(A3)}$$

where $\varepsilon_F=(\hbar k_F)^2/(2m_e)$ is the Fermi energy. For the electrons to occupy only the ground Landau level we require $t\leqslant 1$, or $n_e\leqslant n_B$ [see Eq. (5.9)]. The kinetic energy per electron is

$$\varepsilon_k=\frac{1}{n_e}\frac{1}{(2\pi\rho_0)^2}\int_{-k_F}^{k_F}\frac{\hbar^2k_z^2}{2m_e}dk_z=\frac{\hbar^2}{6\pi^2m_er_F^2}. \tag{A4}$$

The (Hartree-Fock) exchange energy can be written as (Danz and Glasser, 1971)

$$\varepsilon_{ex}=-\frac{F(t)e^2}{2\pi^2r_F}, \tag{A5}$$

where the dimensionless function $F(t)$ is

$$F(t)=4\int_0^\infty dx\left[\tan^{-1}\left(\frac{1}{x}\right)-\frac{x}{2}\ln\left(1+\frac{1}{x^2}\right)\right]e^{-4tx^2}. \tag{A6}$$

The function $F(t)$ can be expressed in terms of generalized hypergeometric functions; for small t, it can be expanded as (Fushiki *et al.*, 1989)

$$F(t)=3-\gamma-\ln(4t)+\frac{2t}{3}\left(\frac{13}{6}-\gamma-\ln 4t\right)+\frac{8t^2}{15}\left(\frac{67}{30}-\gamma-\ln 4t\right)+\mathcal{O}(t^3\ln t), \tag{A7}$$

where $\gamma=0.5772\ldots$ is Euler's constant. The expressions of exchange energy for higher Landau levels are given by Fushiki *et al.* (1992).

Correlation energy in strong magnetic fields has been calculated by Steinberg and Ortner (1998) in the limit of $r_F\ll 1$ and $t\ll 1$ in the random-phase approximation (see also Skudlarski and Vignale, 1993). The leading-order terms have the form

$$\varepsilon_{\rm corr}=D(t)\ln r_F+C(t), \tag{A8}$$

with $D(t)=(16\pi^2t)^{-1}$ (Horing *et al.*, 1972); the asymptotic ($t\ll 1$) expression for $C(t)$ is given by Steinberg and Ortner (1998). There are also some studies (e.g., Kleppmann and Elliot, 1975; Usov *et al.*, 1980; MacDonald and Bryant, 1987) for the very-low-density regime ($r_F\gg 1$, but $t<1$), where the electron gas is expected to form a Wigner crystal; a strong magnetic field tends to increase the density at which crystallization occurs. The low-density and high-density limits may be used to establish an interpolation formula for the correlation energy.

APPENDIX B: THOMAS-FERMI MODELS IN STRONG MAGNETIC FIELDS

Thomas-Fermi and related theories (e.g., Thomas-Fermi-Dirac theory, which includes the exchange energy of electrons) have been thoroughly studied as models of atoms and bulk matter in the case of zero magnetic field (see, for example, Lieb, 1981; Spruch, 1991). Since the early studies of Kadomtsev (1970) and Mueller, Rau, and Spruch (1971), there has been a long succession of papers on Thomas-Fermi-type models in strong magnetic fields. An excellent review on the subject is given by Fushiki *et al.* (1992); rigorous theorems concerning the validity of Thomas-Fermi theory in magnetic fields as an approximation of quantum mechanics are discussed by Yngvason (1991), Lieb *et al.* (1992, 1994a, 1994b), and references therein. Here we briefly summarize the basics of the theory.

The Thomas-Fermi-type theory is the simplest case of a density-functional theory. For a spherical atom (or a Wigner-Seitz cell of bulk matter), we write the energy as a functional of the local electron density $n(r)$:

$$\mathcal{E}[n(r)]=\int w_e[n(r)]\,d^3r-Ze^2\int\frac{n(r)}{r}d^3r+\frac{e^2}{2}\int\frac{n(r)n(r')}{|\mathbf{r}-\mathbf{r}'|}d^3rd^3r', \tag{B1}$$

where $w_e[n(r)]$ is the energy density of electrons at density $n(r)$, which includes kinetic, exchange, and correlation energy (see Appendix A). Minimizing $\mathcal{E}$ with respect to $n(r)$ yields the Thomas-Fermi equation:

$$\frac{dw_e}{dn}-e\Phi(r)=\mu_{\rm TF}, \tag{B2}$$

where $\Phi(r)$ is the total electrostatic potential and $\mu_{\rm TF}$ is a constant to be determined by the constraint $\int n(r)\,d^3r=Z$ (for a neutral system). Equation (B2) can be solved together with the Poisson equation,

$$\nabla^2\Phi=-4\pi Ze\,\delta(\mathbf{r})+4\pi en(r), \tag{B3}$$

to obtain $n(r)$ and $\Phi(r)$, and the energy $\mathcal{E}$ can then be evaluated. The pressure of bulk matter is then given by $P=-d\mathcal{E}/(4\pi r_i^2dr_i)$ and is equal to the pressure of a uniform electron gas at density $n(r_i)$, where r_i is the Wigner-Seitz radius.

Consider the Thomas-Fermi model, in which we include in $w_e[n(r)]$ only the kinetic energy of the electrons. We then have $dw_e/dn=\mu_e(r)=e\Phi(r)+\mu_{\rm TF}$. Using Eq. (6.4) (for nonrelativistic electrons) we can express the local electron density $n(r)$ in terms of $\Phi(r)$. At zero temperature, we have

$$n(r)=\frac{1}{\sqrt{2}\pi^2\rho_0^3}\sum_{n_L}^{n_{\rm max}}g_{n_L}\left[\frac{\mu_{\rm TF}+e\Phi(r)}{\hbar\omega_{ce}}-n_L\right]^{1/2}. \tag{B4}$$

This can be substituted into Eq. (B3) to solve for $\Phi(r)$.

Many Thomas-Fermi-type studies (e.g., Kadomtsev, 1970; Mueller, Rau, and Spruch, 1971; Banerjee *et al.*, 1974; Constantinescu and Rehák, 1976; Skjervold and Östgaard, 1984; Fushiki *et al.*, 1989; Abrahams and Shapiro, 1991) adopted the adiabatic approximation (only the ground Landau level is occupied, i.e., $n_{\rm max}=0$). Abrahams and Shapiro (1991) also considered the Weizsäcker gradient correction, in which a term of the form $(\hbar^2/m_e)(\nabla n)^2/n$ is included in $w_e[n]$, although the actual form of the Weizsäcker term in magnetic fields is uncertain (see Fushiki *et al.*, 1992 for a critical review). Tomishima and Yonei (1978), Gadiyak *et al.* (1981), Tomishima *et al.* (1982), and Rögnvaldsson *et al.* (1993) studied Thomas-Fermi models allowing for $n_{\rm max}>0$.

Constantinescu and Moruzzi (1978), Abrahams and Shapiro (1991, who restricted to $n_{\max}=0$), and Thorolfsson *et al.* (1998, allowing for $n_{\max}>0$) studied finite-temperature Thomas-Fermi models for condensed matter. Examples of Thomas-Fermi-type equations of state for iron are shown in Fig. 9.

As mentioned, the Thomas-Fermi model is too crude to determine the relative binding between atoms, molecules, and condensed matter. But the model becomes increasingly accurate in certain asymptotic limits (see Fushiki *et al.* 1992; Lieb *et al.*, 1992, 1994a, 1994b). In general, the validity of the Thomas-Fermi theory requires the local Fermi wavelength λ_F to be much less than the size of the atom (or Wigner-Seitz cell) r_i. For zero or weak magnetic fields ($n_{\max}\gg 1$), $\lambda_F \sim n_e^{-1/3} \sim r_i/Z^{1/3}$, the validity of Thomas-Fermi theory requires $Z^{1/3}\gg 1$. The size of the atom in weak fields is estimated from $\hbar^2/(m_e\lambda_F^2)\sim Ze^2/r_i$, which gives $r_i\sim Z^{-1/3}a_0$.

For atoms in strong magnetic fields ($n_{\max}=0$), we have $\lambda_F\sim r_i^2/(Z\rho_0^2)$, and the size is $r_i\sim Z^{1/5}b^{-2/5}a_0$. The condition $\lambda\ll r_i$ becomes $b\ll Z^3$. The Thomas-Fermi theory of the atom is exact when $Z,b\to\infty$, as long as $Z^3/b\to\infty$. To be in the strong-field regime requires the mean electron spacing in a nonmagnetic atom, $a_0/Z^{2/3}$, to be greater than ρ_0, i.e., $b>Z^{4/3}$. For bulk matter in strong magnetic fields ($n_{\max}=0$), the Thomas-Fermi model is valid when $\lambda_F\sim r_i^3/(Z\rho_0^2)\ll r_i$, i.e., $b\ll Zr_i^{-2}$ (at zero pressure, $r_i\sim Z^{1/5}b^{-2/5}$, this condition reduces to $b\ll Z^3$). The strong-field condition is $Z^{-1/3}r_i>\rho_0$, i.e., $b>Z^{2/3}r_i^{-2}$ (this reduces to $b>Z^{4/3}$ state at zero pressure density).

REFERENCES

Abrahams, A. M., and S. L. Shapiro, 1991, Astrophys. J. **374**, 652.

Al-Hujaj, O.-A., and P. Schmelcher, 2000, Phys. Rev. A **61**, 063413.

Alcock, C., and A. Illarinov, 1980, Astrophys. J. **235**, 534.

Angelie, C., and C. Deutch, 1978, Phys. Lett. **67A**, 353.

Arras, P., and D. Lai, 1999a, Astrophys. J. **519**, 745.

Arras, P., and D. Lai, 1999b, Phys. Rev. D **60**, 043001.

Ashcroft, N. W., and N. D. Mermin, 1976, *Solid State Physics* (Saunders College, Philadelphia).

Avron, J. E., I. B. Herbst, and B. Simon, 1978, Ann. Phys. (N.Y.) **114**, 431.

Bahcall, J. N., and R. A. Wolf, 1965, Phys. Rev. **140**, B1425.

Baiko, D. A., and D. G. Yakovlev, 1999, Astron. Astrophys. **342**, 192.

Banerjee, B., D. H. Constantinescu, and P. Rehák, 1974, Phys. Rev. D **10**, 2384.

Basile, S., F. Trombetta, and G. Ferrante, 1987, Nuovo Cimento D **9**, 457.

Baye, D., and M. Vincke, 1990, J. Phys. B **23**, 2467.

Baye, D., and M. Vincke, 1998, in *Atoms and Molecules in Strong Magnetic Fields*, edited by P. Schmelcher and W. Schweizer (Plenum, New York), p. 141.

Baym, G., C. Pethick, and P. Sutherland, 1971, Astrophys. J. **170**, 299.

Becken, W., and P. Schmelcher, 2000, J. Phys. B **33**, 545.

Becken, W., P. Schmelcher, and F. K. Diakonos, 1999, J. Phys. B **32**, 1557.

Becker, W., 2000, in *Highly Energetic Physical Processes and Mechanisms for Emission from Astrophysical Plasmas*, Proceedings of IAU Symposium No. 195 (ASP, San Francisco), p. 49.

Becker, W., and G. G. Pavlov, 2001, in *The Century of Space Science*, edited by J. Bleeker, J. Geiss, and M. Huber (Kluwer Academic, Dordrecht).

Becker, W., and J. Trümper, 1997, Astron. Astrophys. **326**, 682.

Bezchastnov, V. G., G. G. Pavlov, and J. Ventura, 1998, Phys. Rev. A **58**, 180.

Blaes, O., R. Blandford, P. Madau, and S. Koonin, 1990, Astrophys. J. **363**, 612.

Blaes, O., and P. Madau, 1993, Astrophys. J. **403**, 690.

Blandford, R. D., and L. Hernquist, 1982, J. Phys. C **15**, 6233.

Brigham, D. R., and J. M. Wadehra, 1987, Astrophys. J. **317**, 865.

Brinkmann, W., 1980, Astron. Astrophys. **82**, 352.

Broderick, A., M. Prakash, and J. M. Lattimer, 2000, Astrophys. J. **537**, 351.

Burkova, L. A., I. E. Dzyaloshinsky, G. P. Drukarev, and B. S. Monozon, 1976, Sov. Phys. JETP **44**, 276.

Callaway, J., and N. H. March, 1984, Solid State Phys. **38**, 135.

Canuto, V., and D. C. Kelley, 1972, Astrophys. Space Sci. **17**, 277.

Canuto, V., J. Lodenquai, and M. Ruderman, 1971, Phys. Rev. D **3**, 2303.

Canuto, V., and J. Ventura, 1977, Fundam. Cosm. Phys. **2**, 203.

Caraveo, P. A., G. F. Bignami, and J. Trümper, 1996, Astron. Astrophys. Rev. **7**, 209.

Caraveo, P. A., R. P. Mignani, G. G. Pavlov, and G. F. Bignami, 2000, in *A Decade of HST Science*, Proceedings, Baltimore; e-print astro-ph/0008523.

Ceperley, D., and B. Alder, 1980, Phys. Rev. Lett. **45**, 566.

Chabrier, G., 1993, Astrophys. J. **414**, 695.

Chabrier, G., N. W. Ashcroft, and H. E. DeWitt, 1992, Nature (London) **360**, 6399.

Chakrabarty, S., D. Bandyopadhyay, and S. Pal, 1997, Phys. Rev. Lett. **78**, 2898.

Chandrasekhar, S., and E. Fermi, 1953, Astrophys. J. **118**, 116.

Chen, H.-H., 1973, Ph.D. thesis (Columbia University).

Chen, Z., and S. P. Goldman, 1992, Phys. Rev. A **45**, 1722.

Chiu, H. Y., and E. E. Salpeter, 1964, Phys. Rev. Lett. **12**, 413.

Constantinescu, D. H., and G. Moruzzi, 1978, Phys. Rev. D **18**, 1820.

Constantinescu, D. H., and P. Rehák, 1976, Nuovo Cimento **32**, 177.

Crow, J. E., J. R. Sabin, and N. S. Sullivan, 1998, in *Atoms and Molecules in Strong Magnetic Fields*, edited by P. Schmelcher and W. Schweizer (Plenum, New York), p. 77 (see also http://www.magnet.fsu.edu/).

Danz, R. W., and M. L. Glasser, 1971, Phys. Rev. B **4**, 94.

Demeur, M., P.-H. Heenen, and M. Godefroid, 1994, Phys. Rev. A **49**, 176.

Detmer, T., P. Schmelcher, and L. S. Cederbaum, 1998, Phys. Rev. A **57**, 1767.

Detmer, T., P. Schmelcher, F. K. Diakonos, and L. S. Cederbaum, 1997, Phys. Rev. A **56**, 1825.

Dorofeev, O. F., D. N. Rodionov, and I. M. Ternov, 1985, Pis'ma Astron. Zh, **11** 302 [Sov. Astron. Lett. **11**, 123 (1985)].

Dreizler, R. M., and E. K. U. Gross, 1990, *Density Functional Theory: An Approach to the Many-Body Problem* (Springer-Verlag, Berlin).
Duncan, R. C., and C. Thompson, 1992, Astrophys. J. Lett. **392**, L9.
Edelstein, J., R. S. Foster, and S. Bowyer, 1995, Astrophys. J. **454**, 442.
Elliot, R. J., and R. Loudon, 1960, J. Phys. Chem. Solids **15**, 196.
Fassbinder, P., and W. Schweizer, 1996a, Phys. Rev. A **53**, 2135.
Fassbinder, P., and W. Schweizer, 1996b, Astron. Astrophys. **314**, 700.
Flowers, E. G., J. F. Lee, M. A. Ruderman, P. G. Sutherland, W. Hillebrandt, and E. Müller, 1977, Astrophys. J. **215**, 291.
Fushiki, I., E. H. Gudmundsson, and C. J. Pethick, 1989, Astrophys. J. **342**, 958.
Fushiki, I., E. H. Gudmundsson, C. J. Pethick, and J. Yngvason, 1992, Ann. Phys. (N.Y.) **216**, 29.
Gadiyak, G. V., M. S. Obrecht, and N. N. Yanenko, 1981, Astrofizica **17**, 765 [Astrophys. **17**, 416 (1982)].
Garstang, R. H., 1977, Rep. Prog. Phys. **40**, 105.
Glasser, M. L., and J. I. Kaplan, 1975, Astrophys. J. **199**, 208.
Gnedin, Yu. N., G. G. Pavlov, and A. I. Tsygan, 1974, Sov. Phys. JETP **39**, 201.
Goldman, S. P., and Z. Chen, 1991, Phys. Rev. Lett. **67**, 1403.
Gor'kov, L. P., and I. E. Dzyaloshinskii, 1968, Sov. Phys. JETP **26**, 449.
Haensel, P., and J. L. Zdunik, 1990, Astron. Astrophys. **222**, 353.
Haines, L. K., and D. H. Roberts, 1969, Am. J. Phys. **37**, 1145.
Hansen, J. P., and E. L. Pollock, 1973, Phys. Rev. A **8**, 3110.
Hasegawa, H., and R. E. Howard, 1961, J. Phys. Chem. Solids **21**, 179.
Hernquist, L., 1984, Astrophys. J., Suppl. Ser. **56**, 325.
Hernquist, L., 1985, Mon. Not. R. Astron. Soc. **213**, 313.
Herold, H., H. Ruder, and J. Wunner, 1981, J. Phys. B **14**, 751.
Heyl, J. S., and L. Herquist, 1998, Mon. Not. R. Astron. Soc. **300**, 599.
Ho, W. C. G., and D. Lai, 2001, Mon. Not. R. Astron. Soc (in press); e-print astro-ph/0104199.
Horing, N. J., 1969, Ann. Phys. (N.Y.) **54**, 405.
Horing, N. J., R. W. Danz, and M. L. Glasser, 1972, Phys. Rev. A **6**, 2391.
Horowitz, C. J., and G. Li, 1998, Phys. Rev. Lett. **80**, 3694.
Hummer, D. G., and D. Mihalas, 1988, Astrophys. J. **331**, 794.
Hurley, K., *et al.*, 1999, Nature (London) **397**, 41.
Ichimaru, S., 1993, Rev. Mod. Phys. **65**, 255.
Iglesias, C. A., and F. J. Rogers, 1996, Astrophys. J. **464**, 943.
Itoh, N., 1975, Mon. Not. R. Astron. Soc. **173**, 1P.
Ivanov, M. V., and P. Schmelcher, 1998, Phys. Rev. A **57**, 3793.
Ivanov, M. V., and P. Schmelcher, 1999, Phys. Rev. A **60**, 3558.
Ivanov, M. V., and P. Schmelcher, 2000, Phys. Rev. A **61**, 2505.
Johnsen, K., and J. Yngvason, 1996, Phys. Rev. A **54**, 1936.
Johnson, B. R., J. O. Hirschfelder, and K.-H. Yang, 1983, Rev. Mod. Phys. **55**, 109.
Johnson, M. H., and B. A. Lippmann, 1949, Phys. Rev. **76**, 828.
Jones, M. D., and D. M. Ceperley, 1996, Phys. Rev. Lett. **76**, 4572.
Jones, M. D., G. Ortiz, and D. M. Ceperley, 1996, Phys. Rev. A **54**, 219.
Jones, M. D., G. Ortiz, and D. M. Ceperley, 1997, Phys. Rev. E **55**, 6202.
Jones, M. D., G. Ortiz, and D. M. Ceperley, 1999a, Phys. Rev. A **59**, 2875.
Jones, M. D., G. Ortiz, and D. M. Ceperley, 1999b, Astron. Astrophys. **343**, L91.
Jones, P. B., 1985, Mon. Not. R. Astron. Soc. **216**, 503.
Jones, P. B., 1986, Mon. Not. R. Astron. Soc. **218**, 477.
Jordan, S., 1998, in *Atoms and Molecules in Strong Magnetic Fields*, edited by P. Schmelcher and W. Schweizer (Plenum, New York), p. 9.
Jordan, S., P. Schmelcher, W. Becken, and W. Schweizer, 1998, Astron. Astrophys. **336**, L33.
Kadomtsev, B. B., 1970, Zh. Éksp. Teor. Fiz, **58**, 1765 [Sov. Phys. JETP **31**, 945].
Kadomtsev, B. B., and V. S. Kudryavtsev, 1971, Pis'ma Zh. Éksp. Teor. Fiz, **13**, 61 [JETP Lett. **13**, 42].
Kappes, U., and P. Schmelcher, 1995, Phys. Rev. A **51**, 4542.
Kappes, U., and P. Schmelcher, 1996, Phys. Rev. A **53**, 3869.
Kaspi, V. M., D. Chakrabarty, and J. Steinberger, 1999, Astrophys. J. **525**, L33.
Kastner, M. A., 1992, Rev. Mod. Phys. **64**, 849.
Khersonskii, V. K., 1984, Astrophys. Space Sci. **98**, 255.
Khersonskii, V. K., 1985, Astrophys. Space Sci. **117**, 47.
Khersonskii, V. K., 1987, Sov. Astron. **31**, 225.
Klaassen, T. O., J. L. Dunn, and C. A. Bates, 1998, in *Atoms and Molecules in Strong Magnetic Fields*, edited by P. Schmelcher and W. Schweizer (Plenum, New York), p. 291.
Kleppmann, W. G., and R. J. Elliot, 1975, J. Phys. C **8**, 2729.
Koester, D., and G. Chanmugan, 1990, Rep. Prog. Phys. **53**, 837.
Korpela, E. J., and S. Bowyer, 1998, Astron. J. **115**, 2551.
Kössl, D., R. G. Wolff, E. Müller, and W. Hillebrandt, 1988, Astron. Astrophys. **205**, 347.
Kouveliotou, C., *et al.*, 1998, Nature (London) **393**, 235.
Kouveliotou, C., T. Strohmayer, K. Hurley, J. van Paradijs, M. H. Finger, S. Dieters, P. Woods, C. Thompson, and R. C. Duncan, 1999, Astrophys. J. Lett. **510**, L115.
Kravchenko, Yu. P., and M. A. Liberman, 1997, Phys. Rev. A **55**, 2701.
Kravchenko, Yu. P., and M. A. Liberman, 1998, Phys. Rev. A **57**, 3403.
Kravchenko, Yu. P., M. A. Liberman, and B. Johansson 1996, Phys. Rev. A **54**, 287.
Lai, D., and Y.-Z. Qian, 1998a, Astrophys. J. Lett. **495**, L103; **501**, L155(E).
Lai, D., and Y.-Z. Qian, 1998b, Astrophys. J. **505**, 844.
Lai, D., and E. E. Salpeter, 1995, Phys. Rev. A **52**, 2611.
Lai, D., and E. E. Salpeter, 1996, Phys. Rev. A **53**, 152.
Lai, D., and E. E. Salpeter, 1997, Astrophys. J. **491**, 270.
Lai, D., E. E. Salpeter, and S. L. Shapiro, 1992, Phys. Rev. A **45**, 4832.
Lai, D., and S. L. Shapiro, 1991, Astrophys. J. **383**, 745.
Lamb, Jr., W. E., 1952, Phys. Rev. **85**, 259.
Landau, L. D., and E. M. Lifshitz, 1977, *Quantum Mechanics*, 3rd ed. (Pergamon, Oxford).
Landau, L.D., and E.M. Lifshitz, 1980, *Statistical Physics*, Part 1, 3rd ed. (Pergamon, Oxford).
Larsen, D. M., 1982, Phys. Rev. A **25**, 1295.
Lattimer, J. M., C. J. Pethick, D. G. Ravenhall, and D. Q. Lamb, 1985, Nucl. Phys. A **432**, 646.
Le Guillou, J. C., and J. Zinn-Justin, 1984, Ann. Phys. (N.Y.) **154**, 440.
Lewin, W. H. G., J. van Paradijs, and E. P. J. van den Heuvel, 1995, *X-Ray Binaries* (Cambridge University, Cambridge).

Lieb, E. H., 1981, Rev. Mod. Phys. **53**, 603; **54**, 311(E).
Lieb, E. H., J. P. Solovej, and J. Yngvason, 1992, Phys. Rev. Lett. **69**, 749.
Lieb, E. H., J. P. Solovej, and J. Yngvason, 1994a, Commun. Pure Appl. Math. **47**, 513.
Lieb, E. H., J. P. Solovej, and J. Yngvason, 1994b, Commun. Math. Phys. **161**, 77.
Lieb, E. H., J. P. Solovej, and J. Yngvason, 1995, Phys. Rev. B **51**, 10 646.
Lodenquai, J., V. Canuto, M. Ruderman, and S. Tsuruta, 1974, Astrophys. J. **190**, 141.
Lopez, J. C., P. Hess, and A. Turbiner, 1997, Phys. Rev. A **56**, 4496.
Lopez, J. C., and A. Turbiner, 2000, Phys. Rev. A **62**, 022510.
Lyne, A. G., and F. Graham-Smith, 1998, *Pulsar Astronomy* (Cambridge University, Cambridge).
MacDonald, A. H., and G. W. Bryant, 1986, Phys. Rev. Lett. **58**, 515.
Melezhik, V. S., 1993, Phys. Rev. A **48**, 4528.
Mereghetti, S., 2000, in "The Neutron Star–Black Hole Connection" (NATO Advanced Study Institute); e-print astro-ph/9911252.
Mészáros, P., 1992, *High Energy Radiation from Magnetized Neutron Stars* (University of Chicago, Chicago).
Michel, F. C., 1991, *Theory of Neutron Star Magnetospheres* (University of Chicago, Chicago).
Mihalas, D., W. Däppen, and D. G. Hummer, 1988, Astrophys. J. **331**, 815.
Miller, M. C., 1992, Mon. Not. R. Astron. Soc. **255**, 129.
Miller, M. C., and D. Neuhauser, 1991, Mon. Not. R. Astron. Soc. **253**, 107.
Müller, E., 1984, Astron. Astrophys. **130**, 415.
Mueller, R. O., A. R. P. Rau, and L. Spruch, 1971, Phys. Rev. Lett. **26**, 1136.
Nagara, H., Y. Nagata, and T. Nakamura, 1987, Phys. Rev. A **36**, 1859.
Nagel, W., and J. Ventura, 1980, Astron. Astrophys. **118**, 66.
Nelson, R. W., E. E. Salpeter, and I. Wasserman, 1993, Astrophys. J. **418**, 874.
Neuhauser, D., S. E. Koonin, and K. Langanke, 1987, Phys. Rev. A **36**, 4163.
Ortiz, G., M. D. Jones, and D. M. Ceperley, 1995, Phys. Rev. A **52**, R3405.
Özel, F., 2001, Astrophys. J. (in press); e-print astro-ph/0103227.
Paczyński, B., 1992, Acta Astron. **42**, 145.
Page, D., 1998, in *Many Faces of Neutron Stars*, edited by R. Buccheri, J. van Paradijs, and M. A. Alpar (Kluwer Academic, Dordrecht), p. 539.
Pavlov, G. G., and P. Mészáros, 1993, Astrophys. J. Lett. **416**, 75.
Pavlov, G. G., and A. N. Panov, 1976, Sov. Phys. JETP **44**, 300.
Pavlov, G. G., and A. Y. Potekhin, 1995, Astrophys. J. **450**, 883.
Pavlov, G. G., and Y. A. Shibanov, 1978, Astron. Zh. [Sov. Astron.] **55**, 373.
Pavlov, G. G., Y. A. Shibanov, J. Ventura, and V. E. Zavlin, 1994, Astron. Astrophys. **289**, 837.
Pavlov, G. G., Y. A. Shibanov, V. E. Zavlin, and R. D. Meyer, 1995, in *The Lives of the Neutron Stars*, edited by A. Alpar, U. Kiziloglu, and J. van Paradijs (Kluwer Academic, Dordrecht), p. 71.
Pavlov, G. G., A. D. Welty, and F. A. Cordova, 1997, Astrophys. J. **489**, L75.
Pavlov, G. G., and D. G. Yakovlev, 1977, Astrofizika [Astrophys.] **13**, 173.
Pavlov, G. G., V. E. Zavlin, J. Trümper, and R. Neuhäuser, 1996, Astrophys. J. **472**, L33.
Pethick, C. J., 1992, Rev. Mod. Phys. **64**, 1133.
Potekhin, A. Y., 1994, J. Phys. B **27**, 1073.
Potekhin, A. Y., 1996, Phys. Plasmas **3**, 4156.
Potekhin, A. Y., 1998, J. Phys. B **31**, 49.
Potekhin, A. Y., 1999, Astron. Astrophys. **351**, 787.
Potekhin, A. Y., and G. Chabrier, 2000, Phys. Rev. E **62**, 8554.
Potekhin, A. Y., G. Chabrier, and Y. A. Shibanov, 1999, Phys. Rev. E **60**, 2193.
Potekhin, A. Y., and G. G. Pavlov, 1993, Astrophys. J. **407**, 330.
Potekhin, A. Y., and G. G. Pavlov, 1997, Astrophys. J. **483**, 414.
Potekhin, A. Y., Yu. A., Shibanov, and J. Ventura, 1998, in *Neutron Stars and Pulsars*, edited by N. Shibazaki *et al.* (University Academy Press, Tokyo), p. 161.
Prakash, M., J. M. Lattimer, J. A. Pons, A. W. Steiner, and S. Reddy, 2000 in *Physics of Neutron Star Interiors*, edited by D. Blaschke, N. K. Glendenning, and A. Sedrakian (Springer, Berlin/New York); e-print astro-ph/0012136.
Pröschel, P., W. Rösner, G. Wunner, H. Ruder, and H. Herold, 1982, J. Phys. B **15**, 1959.
Rajagopal, M., and R. W. Romani, 1996, Astrophys. J. **461**, 327.
Rajagopal, M., R. W. Romani, and M. C. Miller, 1997, Astrophys. J. **479**, 347.
Relovsky, B. M., and H. Ruder, 1996, Phys. Rev. A **53**, 4068.
Rögnvaldsson, Ö. E., I. Fushiki, E. H. Gudmundsson, C. J. Pethick, and J. Yngvason, 1993, Astrophys. J. **416**, 276.
Rösner, W., G. Wunner, H. Herold, and H. Ruder, 1984, J. Phys. B **17**, 29.
Romani, R. W., 1987, Astrophys. J. **313**, 718.
Ruder, H., G. Wunner, H. Herold, and F. Geyer, 1994, *Atoms in Strong Magnetic Fields* (Springer-Verlag, Berlin).
Ruderman, M., 1971, Phys. Rev. Lett. **27**, 1306.
Ruderman, M., 1974, in *Physics of Dense Matter*, I. A. U. Symposium No. 53, edited by C. J. Hansen (Dordrecht-Holland, Boston), p. 117.
Ruderman, M., and P. G. Sutherland, 1975, Astrophys. J. **196**, 51.
Salpeter, E. E., 1961, Astrophys. J. **134**, 669.
Salpeter, E. E., 1998, J. Phys.: Condens. Matter **10**, 11 285.
Salpeter, E. E., and H. M. van Horn, 1969, Astrophys. J. **155**, 183.
Saumon, D., and G. Chabrier, 1991, Phys. Rev. A **44**, 5122.
Saumon, D., and G. Chabrier, 1992, Phys. Rev. A **46**, 2084.
Schaaf, M. E., 1990, Astron. Astrophys. **227**, 61.
Schatz, H., L. Bildsten, A. Cumming, and M. Wiescher, 1999, Astrophys. J. **524**, 1014.
Schmelcher, P., L. S. Cederbaum, and U. Kappers, 1994, in *Conceptual Trends in Quantum Chemistry*, edited by E. S. Kryachko (Kluwer Academic, Dordrecht).
Schmelcher, P., L. S. Cederbaum, and H.-D. Meyer, 1988, Phys. Rev. A **38**, 6066.
Schmelcher, P., T. Detmer, and L. S. Cederbaum, 2000, Phys. Rev. A **6104**, 3411.
Schmelcher, P., M. V. Ivanov, and W. Becken, 1999, Phys. Rev. A **59**, 3424.
Schmelcher, P., and W. Schweizer, 1998, Eds., *Atoms and Molecules in Strong External Fields* (Plenum, New York).
Schwinger, J., 1988, *Particles, Sources and Fields* (Addison-Wesley, Redwood City).

Shapiro, S. L., and S. A. Teukolsky, 1983, *Black Holes, White Dwarfs and Neutron Stars* (Wiley, New York).
Shibanov, Y. A., G. G. Pavlov, V. E. Zavlin, and J. Ventura, 1992, Astron. Astrophys. **266**, 313.
Silant'ev, N. A., and D. G. Yakovlev, 1980, Astrophys. Space Sci. **71**, 45.
Simola, J., and J. Virtamo, 1978, J. Phys. B **11**, 3309.
Skjervold, J. E., and E. Östgaard, 1984, Phys. Scr. **29**, 543.
Skudlarski, P., and G. Vignale, 1993, Phys. Rev. B **48**, 8547.
Slater, J. C., 1963, *Quantum Theory of Molecules and Solids*, Vol. 1 (McGraw-Hill, New York).
Slattery, W. L., G. D. Doolen, and H. E. DeWitt, 1980, Phys. Rev. A **21**, 2087.
Sokolov, A. A., and I. M. Ternov, 1968, *Synchrotron Radiation* (Pergamon, Oxford).
Spruch, L., 1991, Rev. Mod. Phys. **63**, 151.
Steinberg, M., and J. Ortner, 1998, Phys. Rev. B **58**, 15 460; **59**, 12 693(E).
Suh, I.-S., and G. J. Mathews, 2001, Astrophys. J. **546**, 1126.
Thompson, C., and R. C. Duncan, 1993, Astrophys. J. **408**, 194.
Thompson, C., and R. C. Duncan, 1995, Mon. Not. R. Astron. Soc. **275**, 255.
Thompson, C., and R. C. Duncan, 1996, Astrophys. J. **473**, 322.
Thorolfsson, A., Ö. E. Rögnvaldsson, J. Yngvason, and E. H. Gudmundsson, 1998, Astrophys. J. **502**, 847.
Timofeev, V. B., and A. V. Chernenko, 1995, Pis'ma Zh. Éksp. Teor, Fiz. **61**, 603 [JETP Lett. **61**, 617].
Tomishima, Y., K. Matsuno, and K. Yonei, 1982, J. Phys. B **15**, 2837.
Tomishima, Y., and K. Yonei, 1978, Prog. Theor. Phys. **59**, 683.
Treves, A., and M. Colpi, 1991, Astron. Astrophys. **241**, 107.
Treves, A., R. Turolla, S. Zane, and M. Colpi, 2000, Publ. Astron. Soc. Pac. **112**, 297.
Tsuruta, S., 1964, Ph.D. thesis (Columbia University).
Tsuruta, S., 1998, Phys. Rep. **292**, 1.
Turbiner, A. V., 1983, Pis'ma Zh. Éksp. Teor. Fiz, **38**, 510 [JETP Lett. **38**, 618].
Usov, N. A., Yu. B. Grebenshchikov, and F. R. Ulinich, 1980, Sov. Phys. JETP **51**, 148.
Usov, V. V., and D. B. Melrose, 1996, Astrophys. J. **464**, 306.
van Dalen, E. N. E., A. E. L. Dieperink, A. Sedrakian, and R. G. E. Timmermans, 2000, Astron. Astrophys. **360**, 549.
Van Riper, K.A., 1988, Astrophys. J. **329**, 339.
Vasisht, G., and E. V. Gotthelf, 1997, Astrophys. J. , L129.
Ventura, J., 1979, Phys. Rev. D **19**, 1684.
Ventura, J., H. Herold, and N. Kopidakis, 1994, in *Lives of Neutron Stars*, edited by A. Alpar, U. Kiziloglu, and J. van Paradijs (Kluwer, Dordrecht), p. 97.
Ventura, J., H. Herold, H. Ruder, and F. Geyer, 1992, Astron. Astrophys. **261**, 235.
Vignale, G., and M. Rasolt, 1987, Phys. Rev. Lett. **59**, 2360.
Vignale, G., and M. Rasolt, 1988, Phys. Rev. B **37**, 10 685.
Vilenkin, A., 1995 Astrophys. J. **451**, 700.
Vincke, M., and D. Baye, 1985, J. Phys. B **18**, 167.
Vincke, M., and D. Baye, 1988, J. Phys. B **21**, 2407.
Vincke, M., M. Le Dourneuf, and D. Baye, 1992, J. Phys. B **25**, 2787.
Virtamo, J., 1976, J. Phys. B **9**, 751.
Virtamo, J., and P. Jauho, 1975, Nuovo Cimento Soc. Ital. Fis., B **26B**, 537.
Walter, F. M., and L. D. Matthews, 1997, Nature (London) **389**, 358.
Walter, F. M., S. J. Wolk, and R. Neuhäuser, 1996, Nature (London) **379**, 233.
Weissbluth, M., 1978, *Atoms and Molecules* (Academic, New York), p. 400.
Wickramasinghe, D. T., and L. Ferrario, 2000, Publ. Astron. Soc. Pac. **112**, 873.
Wille, U., 1987, J. Phys. B **20**, L417.
Wille, U., 1988, Phys. Rev. A **38**, 3210.
Wunner, G., H. Herold, and H. Ruder, 1982, Phys. Lett. **88A**, 344.
Yakovlev, D. G., and A. D. Kaminker, 1994, in *The Equation of State in Astrophysics*, edited by G. Chabrier and E. Schatzman (Cambridge University, Cambridge), p. 214.
Yakovlev, D. G., A. D. Kaminker, O. Y. Gnedin, and P. Haensel, 2001, Phys. Rep. (in press); e-print astro-ph/0012122.
Yngvason, J., 1991, Lett. Math. Phys. **22**, 107.
Yuan, Y. F., and J. L. Zhang, 1999, Astrophys. J. **525**, 950.
Zane, S., R. Turolla, L. Stella, and A. Treves, 2001, Astrophys J. (in press); e-print astro-ph/0103316.
Zavlin, V. E., G. G. Pavlov, and Y. A. Shibanov, 1996, Astron. Astrophys. **315**, 141.
Zavlin, V. E., and G. G. Pavlov, 1998, Astron. Astrophys. **329**, 583.
Zavlin, V. E., G. G. Pavlov, Y. A. Shibanov, and J. Ventura, 1995, Astron. Astrophys. **297**, 441.
Zhang, B., and A. K. Harding, 2000, Astrophys. J. **535**, L51.